Bioactive Materials 27 (2023) 15–57

Contents lists available at ScienceDirect

Bioactive Materials

journal homepage: www.keaipublishing.com/en/journals/bioactive-materials

Review article

Advanced surface engineering of titanium materials for biomedical applications: From static modification to dynamic responsive regulation

Pinliang Jiang [a,b], Yanmei Zhang [b], Ren Hu [b], Bin Shi [c], Lihai Zhang [c], Qiaoling Huang [d], Yun Yang [d], Peifu Tang [c,**], Changjian Lin [b,*]

[a] South China Advanced Institute for Soft Matter Science and Technology, School of Emergent Soft Matter, Guangdong Provincial Key Laboratory of Functional and Intelligent Hybrid Materials and Devices, South China University of Technology, Guangzhou, 510640, China
[b] State Key Lab of Physical Chemistry of Solid Surfaces, Department of Chemistry, College of Chemistry and Chemical Engineering, Xiamen University, Xiamen, 361005, China
[c] Department of Orthopaedics, General Hospital of Chinese PLA, Beijing, 100853, China
[d] Research Institute for Biomimetics and Soft Matter, Fujian Provincial Key Laboratory for Soft Functional Materials Research, College of Physical Science and Technology, Xiamen University, Xiamen, 361005, China

ARTICLE INFO

Keywords:
Titanium materials
Orthopedic implants
Bioactivity
Static modification
Dynamic responsive regulation

ABSTRACT

Titanium (Ti) and its alloys have been widely used as orthopedic implants, because of their favorable mechanical properties, corrosion resistance and biocompatibility. Despite their significant success in various clinical applications, the probability of failure, degradation and revision is undesirably high, especially for the patients with low bone density, insufficient quantity of bone or osteoporosis, which renders the studies on surface modification of Ti still active to further improve clinical results. It is discerned that surface physicochemical properties directly influence and even control the dynamic interaction that subsequently determines the success or rejection of orthopedic implants. Therefore, it is crucial to endow bulk materials with specific surface properties of high bioactivity that can be performed by surface modification to realize the osseointegration. This article first reviews surface characteristics of Ti materials and various conventional surface modification techniques involving mechanical, physical and chemical treatments based on the formation mechanism of the modified coatings. Such conventional methods are able to improve bioactivity of Ti implants, but the surfaces with static state cannot respond to the dynamic biological cascades from the living cells and tissues. Hence, beyond traditional static design, dynamic responsive avenues are then emerging. The dynamic stimuli sources for surface functionalization can originate from environmental triggers or physiological triggers. In short, this review surveys recent developments in the surface engineering of Ti materials, with a specific emphasis on advances in static to dynamic functionality, which provides perspectives for improving bioactivity and biocompatibility of Ti implants.

1. Introduction

Biomaterials commonly refers to materials that have been engineered to direct the course of any diagnostic or therapeutic procedure by regulation of interactions with components of living systems [1]. Biomaterials can be well classified into various types according to multiple principles. For instance, according to the material sources, biomaterials include synthetic, nature-derived and semi-synthetic or hybrid materials, where synthetic biomaterials show a big market share [2]. Further, synthetic biomaterials can be divided into the following types: metals, ceramics, polymers and composites [2]. Amongst all these, metal-based materials are widely used as orthopedic replacements because of the superior tolerance, stability and load-bearing properties, whose application as dental, spinal, hip and knee implants is extremely high. It is reported that more than 70% of implant devices—even including about 95% of orthopedic devices—are still comprised of metals [3]. The orthopedic implants and devices already shared the biggest amount in the global implants market in 2015, and the size continued to rapidly grow because of the increased number of the injured, aging and overweight groups, which is estimated to reach $116 billion by 2022 [4]. There is

Peer review under responsibility of KeAi Communications Co., Ltd.
* Corresponding author.
** Corresponding author.
E-mail addresses: pftang301@163.com (P. Tang), cjlin@xmu.edu.cn (C. Lin).

https://doi.org/10.1016/j.bioactmat.2023.03.006
Received 24 November 2022; Received in revised form 10 March 2023; Accepted 10 March 2023

tremendous growth in the demand for long-lasting implants, as the example collected from the total joint replacements surgery. It is reported that primary total hip arthroplasty (THA) and primary total knee arthroplasty (TKA) in the United States will increase by 71% (up to 0.635 million procedures) and 85% (up to 1.26 million procedures) in 2030 according to basis of 2000-to-2014 data, respectively [5]. Besides the replacement surgeries have increased, the revision surgeries have also greatly increased, which induce great pain for the patient. The main reasons for the revision surgeries are related to several factors, such as debris generation and metal ions release caused by wear or corrosion, mismatch in modulus between bone and implants, low fatigue strength and lack of biocompatibility [6]. In addition, the increased life expectancy is another factor that requires a longer useable lifetime of implants. Hence, orthopedic replacements especially for load-bearing applications tend to require appropriate mechanical properties, high corrosion and wear resistance, excellent osseointegration to extend useable lifetime and avoid revision surgeries.

Presently, 316L stainless steel, cobalt-chromium alloys and Ti and its alloys still constitute the main materials for orthopedic applications. Amongst these, Ti and its alloys are the first choice for the majority of implants, because of the high fatigue strength, high corrosion resistance, low modulus and density, and favorable biocompatibility. The mechanical properties and corrosion resistance of Ti-based materials combine to provide implants with high damage tolerance; the low modulus reduces bone resorption; the biocompatibility benefits bone integration. Since 1950s, Ti and its alloys have been widely used in orthopedic applications. Besides the well-known use as hip and knee prostheses, Ti-based materials are also applied as trauma plates, dental implants and bone screws. It is reported that more than 1000 tonnes of Ti-based materials are implanted in human body worldwide every year, and its amount is expected to increase gradually [7]. Although it is a type of traditional biomaterials, the advances in surface engineering may allow for the further development of Ti-based materials as bioactive implants. This paper first provides an overview of physicochemical properties and biocompatibility of Ti-based materials, and then presents various surface modification methods from both conventional and dynamic responsive aspects.

1.1. Physicochemical and mechanical properties

Ti and its alloys are encapsulated by an oxide layer of 3–10 nm on the surface, which typically contains three different oxide layers, with TiO (inner layer), Ti_2O_3 (intermediate layer) and TiO_2 (outer layer) [8]. The superior chemical inertness, corrosion resistance and even biocompatibility of Ti and its alloys are mostly related to the chemical stability and structure of such a native oxide layer, because the repassivation can occur immediately in 30 ms even the oxide layer is destroyed [9]. The suboxides, including TiO and Ti_2O_3, are easily turned into TiO_2 when Ti is immersed into an oxidizing medium, and the native layered structure composed of TiO (inner layer), Ti_2O_3 (intermediate layer) and TiO_2 (outer layer) is reestablished. The oxidation process obviously increases the amount of TiO_2 even the underlying suboxides cannot be detected, but the layered organization is not changed.

The mechanical properties greatly determine the type of materials selected for a specific application in the living organism. In case of orthopedic implants, the tolerance to repeated cyclic loads and strains in the long term is of prime importance. The materials used as ideal bone replacements are expected to show a modulus equivalent to that of bone. The mismatch in modulus between bone and implants usually leads to bone resorption and subsequent implant loosening. The modulus of natural bone generally ranges from 4 to 30 GPa based on the bone types and the measurement direction [10]. The current implants with much higher modulus than bone prevent appropriate stress being transferred to surrounding bone, and thus cause the death of bone cells and bone resorption, which is also known as “stress shielding effect” [10]. Amongst all the metals, Ti and its alloys are the preference for orthopedic implants, because their elastic moduli ranging from 48 to 112 GPa are much lower compared with 316L stainless steel of 210 GPa and cobalt-chromium alloys of 240 GPa, as shown in Fig. 1 [10]. The more similar modulus to bone would significantly reduce loosening of implants and prolong the lifetime to avoid revision surgery. In addition, all metal-based implants undergo various corrosion reactions once after implantation because the body environment involves salt solution (e.g., Na^+, K^+, Cl^- and PO_4^{3-}) and proteins [11,12], including pitting corrosion, crevice corrosion, fatigue corrosion and fretting corrosion [10,11]. As to the long-term usage, the corrosion resistance of Ti implants also influences its lifetime in human body. For instance, the wear ions and particles from Ti-based joints have disseminated to the liver and spleen via blood circulation, with induced inflammatory responses [13,14]. Therefore, it is noteworthy to improve the thickness and stability of passive oxide layers by various means to prevent the release of metal ions and particles, which would reduce the inflammation and osteolysis.

1.2. Biocompatibility and clinical challenges

1.2.1. Biocompatibility

Biocompatibility as the most important characteristic of biomaterials generally applies to the ability of a material to fulfill its desired function with an appropriate host response [15]. For orthopedic implants, biocompatibility is mostly related to biotolerability, which indicates the ability of a material to reside in the living body for long periods of time with relatively low degrees of inflammatory response [16]. Compared with stainless steel and Co-Cr alloys, Ti and its alloys display superior biocompatibility, which is mostly determined by the surface properties. Ti and its alloys form a stable passive oxide layer (mainly TiO_2) on its surface and the immediate repassivation would happen even if the passive layer is destroyed, to protect the underlying metal from corrosion [17]. As a result, the physicochemical characteristics of surface oxide layer, such as crystallinity, impurity segregation and stoichiometry of oxide, markedly influence the biocompatibility and stability. Upon implantation, a cascade of biological reactions would occur between Ti surface and bone tissue. The first step is that proteins from body fluids would rapidly adsorb on Ti surfaces to minimize the interface free energy, whose inner hydrophobic regions and hydrophilic domains are exposed to the surface and aqueous medium, respectively [18]. The initially adsorbed proteins may aggregate with or be replaced by proteins approaching later, forming a hydrated layer of various composition and conformation. Such a hydrated surface would trigger the attachment of different types of cells (e.g., macrophases, bone marrow cells and osteoblasts) and subsequent tissue responses that include foreign body reaction and fibrous capsule formation around the implants [19]. Fibrous capsules generally are formed on large impervious implant surfaces, including breast prostheses and bulk bionert materials. Hence,

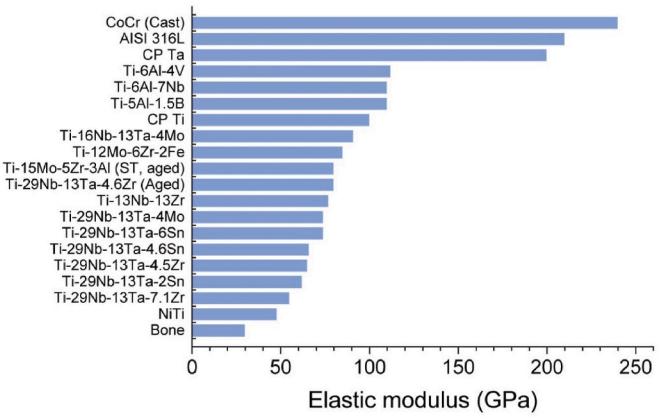

Fig. 1. Elastic moduli of biomedical metals and bone [10]. Reprinted with permission from Ref. [10].

it is clear that a critical factor modulating the appropriate tissue response is the characteristics of implant surface, where the first body contact occurs [20].

Ti and its alloys present well tolerated, but they are bioinert because the passive oxide layer shows unreactive on both the cellular and tissular levels. The smooth Ti surface lacks osseointegration with bones, with an intervening fibrous or connective layer between them that tends to induce implantation failure and caused great pain to the patients [21]. In orthopedic surgery, the higher the level of osseointegration, the better mechanical stability and the longer useable lifetime are exhibited. To achieve this, specific biomolecular adsorption and osteogenesis-related cell regulation are of great importance, whereas fibroblast adhesion and micromotions at the early stage should be avoided. It is commonly noted that the initial interface developed between the Ti surface and the attached tissue rules the ultimate success or failure of implants. The formation of required interface is influenced both by the nature of implant surfaces and the response of living body, between which the former is regulated in a much controllable way. Hence, in order to improve the interface interaction, surface modification is the most efficient way to modulate the biocompatibility.

1.2.2. Clinical challenges

Orthopedic implants have demonstrated great successful application in vivo, but most artificial implants show a life expectancy of 10–15 years [22]. For instance, Ti dental implants present a success rate of greater than 90%, whereas a cumulative complication rate of about 33.6% after 5 years has been observed according to both mechanical and biological complications [23]. The reasons for implant failure mainly result from aseptic loosening and infection [24]. Aseptic loosening is caused by various reasons, such as micromotion between the implant and the surrounding bone during loading, production of wear particles from implants, stress shielding from mechanical mismatching between implant and bone, and insufficient osseointegration of the interface between the implant and the bone [24,25]. The occurrence of micromotion during a postoperative stage may jeopardize the long-term stability that hampers healing process and results in callus/fibrous tissue formation, while it also endangers the stable osseointegrated implants that may induce fibrocartilage or fibrous tissue encapsulation in some areas [25]. Wear particles can induce macrophage to secrete cytokines (TNF-α, IL-1 and IL-6 etc.) that activate osteoclasts, and thus initiate bone resorption and inflammation [26]. Stress shielding mainly caused by the elastic mismatching can transfer inappropriate stress from the implant to surrounding bone, and generally lead to less bone mineralization adjacent to the implant [10]. Insufficient integration between the implant and the bone may result from the poor design of the functional interface and poor patient health besides the above factors. For instance, age-related diseases or disorders for the aging patients, including osteoporosis, diabetes and rheumatoid arthritis, complicate bone's capacity for self-healing and compromise the healing outcomes [27]. In short, aseptic loosening generally is the consequence of a combination of several factors once established.

Implant infection is another substantial cause of morbidity in clinic. It is reported that the values of infection rate for hip and knee arthroplasty are 0.4–2.4% and 1–2%, respectively, whereas the value is 2.4–8.9% for ankle arthroplasty because of the delayed wound healing [28]. The infection risk becomes much higher in revision cases. For instance, the values can reach up to 12% and 22% for revision hip and knee arthroplasty, respectively [28]. These statistics suggest that implant-related infections are a type of "chronic diseases" as a detrimental role in human health field. The contamination sources are various, including incomplete disinfection of surgical instruments, contamination from patient's soft tissues and poor hygiene after surgery etc [29]. Among all the pathogenic species, *S. aureus* and *S. epidermidis* are key pathogens to cause orthopedic prosthetic infections that account for 31–52% [30]. The adhesion of microbial cells to implant surfaces can accumulate to form biofilm that consists of a three-dimensional extracellular matrix and enmeshed organized microbial communities [31]. The formed biofilm benefits microbial adhesion and growth, and even protects them from antibacterial cleaning and host immune responses. Therefore, biofilm with multi-drug resistance characteristics makes implant infection as one of the most challenging problems to orthopedic doctors. How to endow implants with antibacterial property with the aims of preventing or treating bacterial colonization and biofilm formation, has attracted great considerations in biomedical field.

Aseptic loosening and implant infection seem to be mutually exclusive, however, the two problems about osseointegration and infection prevention are closely correlative. As suggested by Gristina et al., the phrase of "race for the surface" has been well introduced to describe the contest between host cells and bacteria to adhere, replicate and colonize the device surface [32]. If the host cells adhere and occupy the implant surface first, an interface integration will be established while a defensive barrier will also be obtained against bacterial adhesion and colonization. The rapid integration of biomaterials with host tissues is key for successful implantation, and the prompt osseointegration is crucial for inhibiting bacterial attachment as well [33]. Hence, strong osseointegration is the fundamental step to realize successful implant applications, and furthermore, there is an increasing need for multifunctional strategies to resolve the issues of osseointegration, implant infection and long-term mechanical and biological stability [22]. It is noteworthy that the balance between the different factors is challenging. Because some surface characteristics that benefit host cell adhesion and growth are also favorable to microbial cells and in turn, some surfaces with antibacterial property may hamper host cell activities [34]. Surface modification is the most effective strategy to achieve the above goals. In some cases, an optimal surface is able to bond directly with bone tissue [35]. Surface modification can alter one or more than one properties, including surface chemistry, wettability and topography, which greatly affect the implant performance both in vitro and in vivo [36]. For instance, implant surfaces with nanometer and micrometer scale features can achieve profound effects on bone integration [36]. The appropriate surface modification not only endows the implant with specific functions satisfying the requirements of osseointegration, but also preserves the superior characteristics of the underlying bulks, such as proper mechanical properties and corrosion resistance. In addition, the manufacturing process may introduce local contamination and defects, which may be stressed and plastically deformed. Such surfaces are unsuitable for the biomedical application, thus requiring for proper surface modification. In the following sections, various methods for improving bioactivity and biocompatibility of Ti implants are discussed in detail. Basically, the conventional modification strategies with static properties are grouped into three categories: mechanical, physical, and chemical methods. An overview about the conventional surface modification methods is listed as Table 1. In addition, because the cell and tissue require different signal cascades on demand at different time periods, dynamic responsive surfaces with stimuli regulation are discussed as well, with the signal originating from environmental triggers (e.g., light, X-ray, electrical field, piezoelectricity, ultrasound and magnetic/electromagnetic field) and physiological triggers (e.g., pH and enzyme).

2. Surface modification

2.1. Mechanical methods

Mechanical methods generally refer to treating, shaping or removal of the surface by use of physical forces performed via the action of another solid material. Such methods are to remove surface contamination and/or obtain specific surface topographies, which usually include machining, grinding, polishing, and grit blasting [17,37]. Amongst them, grit blasting is the most common approach used to form roughed topographies on Ti surfaces to improve the bioactivity. Hence, grit blasting is discussed in detail.

Table 1
An overview of conventional surface modification methods for Ti and its alloys.

Techniques	Advantages	Limitations
Grit blasting	Low-cost and simple operation	Blasting particle residues, hard to form nanoscale topography
Plasma spraying	Large-scale production, appropriate bioactivity	Low crystallinity, high tensile residual stress, hard to control composition and structure of the coatings
HVOF spraying	Large-scale production, appropriate bioactivity	Moderate crystallinity, moderate tensile residual stress, hard to control composition and structure of the coatings
Cold spraying	Improved bioactivity, suitable for oxygen- and heat-sensitive compounds.	Hard to form nanoscale topography, moderate adhesion of coatings to Ti substrates
PIII&D	Easy composition control, high bonding strength	Hard to form microscale topography, expensive machinery
Acid etching	Low-cost and easy operation	Hard to form nanoscale topography, poor uniformity
Alkali-heat treatment	Low-cost and easy operation, uniform distribution	Time consuming, easy loss of sodium ions under the moisture
Anodization	Uniform nanoscale topography with defined pore diameters	Hard to form microscale topography, moderate bonding strength
Micro-arc oxidation	High strength, micro-hardness and wear resistance	Hard to form nanoscale and suitable topography
Electrodeposition	Low-cost and easy operation, controllable thickness with broad range	Moderate bonding strength, limited coating diversity
Electrophoretic deposition	High deposition rate, controllable thickness with broad range	Uniformity limited by size of particles, hard to form nanoscale topography
Chemical covalent immobilization of biomolecules	Precise immobilization of various biomolecules	Complex operation in some cases, special storage conditions
Layer-by-layer assembly	Simple operation, controllable layered structures	Difficult-to-scale preparation, low bonding to substrates, special storage conditions

2.1.1. Grit blasting

Grit blasting that is also known as sandblasting is considered as the application of abrasive particles, like hard ceramic materials, against smooth surfaces by high pressure and compressed air [38]. The surface roughness and topography generated by such a crash depend on the shape and size of the grit particles, and the air pressure used. The grit particles should be chemically stable, biocompatible and should not hinder the osseointegration of Ti implants [39]. Generally, the particles, including Al_2O_3, TiO_2, SiC and hydroxyapatite (HA), are normally used for the blasting [17,36].

Some studies have used particles of different sizes to treat the surfaces, and the influence of surface roughness on the bone attachment was investigated. For instance, Wennerberg et al. have added four different values of roughness to the implant surfaces by using TiO_2 (25 μm) and Al_2O_3 (25, 75, and 250 μm) as the abrasive particles, with the Sa values ranging from 0.6 to 2.1 μm [40–42]. The strongest bone integration according to removal torque and bone-to-implant contact tests was detected for a blasted surface with a Sa value of 1.5 μm in rabbit bone after a follow-up time of 1 year, suggesting the moderate roughness benefitted implant bioactivity. Similar results were observed by Ronold et al. that the tensile strength in vivo of Ti implants showed a positive correlation with the increasing roughness produced by TiO_2 blasting, but the further increase in roughness was to decrease the effect [43]. The above results both provide the notion that a moderate roughed surface favors bone response. Blasting tends to introduce the contamination and alter the surface composition because of particle residues. For example, some previous studies have indicated that the presence of Al^{3+} inhibited the expression of the osteoblastic phenotype in vitro [44–46], and exerted an adverse effect on tissue reactions in vivo [47–49]. Therefore, to reduce the toxicity, some bioactive materials of bioceramics such as HA and biphasic calcium phosphate (BCP) have been used to blast the surfaces [50,51]. Grit blasting is more commonly combined with other methods to modify Ti surfaces, such as acid etching and anodization.

2.2. Physical methods

Physical methods generally refer to the layers directly formed on Ti surfaces almost without the occurrence of chemical reactions. In this case, the formation of layers are mainly driven by thermal, kinetic and electrical energy. Conventional physical methods include thermal spraying and plasma immersion ion implantation (PIII) and deposition (PIII&D).

2.2.1. Thermal spraying

Thermal spraying refers to a coating process that feedstock materials are loaded into a heating zone, accelerated and propelled from the torch towards the substrate in molten or semi-molten state by the high-temperature and high-velocity gas stream [52,53]. The feedstock includes metallic and nonmetallic materials in the form of powders, suspensions, rods, wires or liquids [53]. Thermal spraying technologies for medical coatings contain plasma spraying, high-velocity oxygen fuel (HVOF) spraying and cold spraying [53,54].

2.2.1.1. Plasma spraying. Plasma spraying has been introduced to treat the material surface for several decades [55,56]. This method utilizes plasma beam at a high temperature ranging from 6000 °C to 15,000 °C, to melt the supplied particles [54]. The melted powders then impinge onto the Ti substrates with a particle velocity ranging from 20 to 500 m/s where they are condensed and fused together with the kinetic energy turned into thermal and deformation energy [57], as shown in Fig. 2A [58]. The formed coating produced by plasma spraying tends to show a thickness varying from several micrometers to millimeters [59]. In general, to improve the bonding strength of the coating, the substrate surfaces are degreased and roughened in prior to plasma spraying. Plasma spraying contains atmospheric plasma spraying (APS), vacuum plasma spraying (VPS) and controlled atmospheric plasma spraying (CAPS) [56].

Since 1970s, a titanium plasma-spraying (TPS) technique was developed to treat titanium implants [60]. The titanium plasma by injecting the powder into a plasma torch was projected onto the implant surface where it formed a condensed coating of 30–50 μm thickness. The value of TPS-treated surface roughness can reach as high as 7 μm with extremely rough and irregular appearance, which is due to the existence of large areas of sheets, globular outcroppings, frequent fissures, deep pits and cracks [61,62], as shown in Fig. 2B [39]. In a clinical research, TPS-coated dental implants displayed a success rate of 86.7% of after the 5-year follow-up study, showing an acceptable success result [63]. However, some works have revealed the controversy on the binding strength and on granule release from TPS coatings into the host tissue, owing to the mechanical friction between the implant surface and the host bone. The detachment of metallic wear particles or the dissolution of metal ions arousing concern is because they may potentially induce local and systemic carcinogenic effects [64,65]. In order to reduce the dissolution and release of titanium particles, some post processing of the TPS surface is explored, including the introduction of another protective coatings. For instance, an additional coating of fluorohydroxyapatite (FHA) on the TPS surface can effectively reduce the detachment of titanium particles in the bone medullary spaces around the implants after

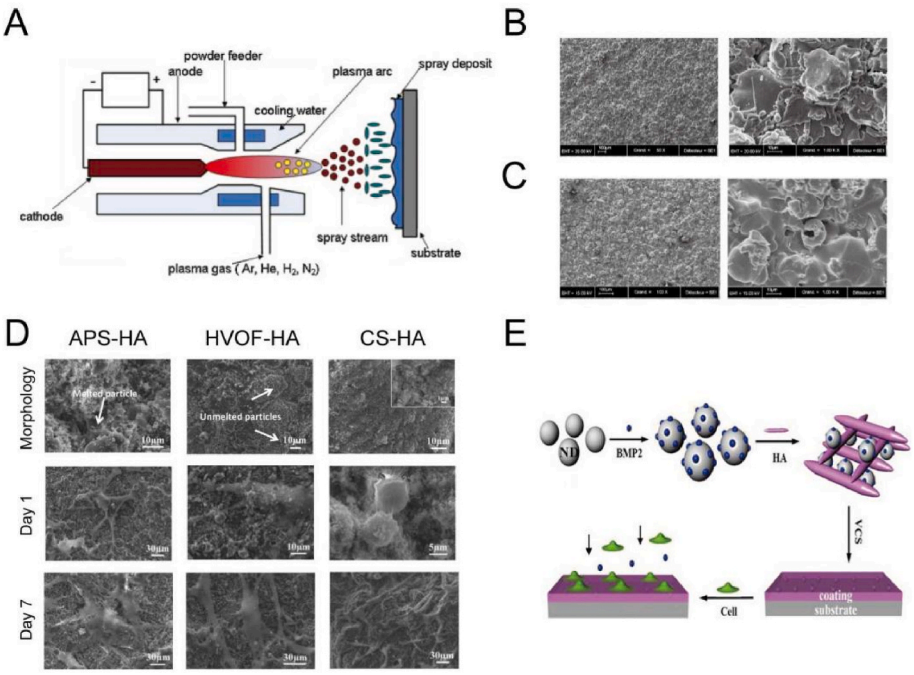

Fig. 2. (A) Schematic diagram of a non-transferred arc plasma setup [58]. Reprinted with permission from Ref. [58]. (B) SEM images of a titanium plasma-sprayed (TPS) surface (Courtesy of Cam Implants BV, The Netherlands) [39].
(C) SEM images of a plasma-sprayed hydroxyapatite (HA) coating surface (Courtesy of Cam Implants BV, The Netherlands) [39]. Reprinted with permission from Ref. [39].
(D) SEM images of surface morphology of APS, HVOF and CS HA coatings before and after cell culture for 1 and 7 days [86]. Reprinted with permission from Ref. [86]. (E) Schematic diagram of HA/nano-diamond/BMP-2 coating via vacuum CS [87]. Reprinted with permission from Ref. [87].

implantation in the femoral and tibial diaphysis of mongrel sheep for 12 weeks [66].

Some bioinert ceramic powders, such as Al_2O_3, ZrO_2 and TiO_2, have been widely used for the spraying because of favorable mechanical properties [67]. Although the wear resistance and corrosion resistance of Al_2O_3 and ZrO_2 are excellent, such coatings cannot directly bind to human bone tissues due to the bionert nature. Hence, bioactive HA is mostly chosen as a coating on metallic bulks to improve the osseointegration, because it constitutes the main inorganic component of bones. Plasma-sprayed HA coatings have been widely used in dental and orthopedic prostheses (e.g., hip and knee implants), whose typical morphology is as shown in Fig. 2C [39]. A lot of short-term and long-term investigations have been conducted on clinical behaviors of HA coatings [68–71]. For example, studies on the 15-years minimum follow-up of HA-coated fermoral componets (Ti alloy implant) by Capello et al. [70] and Epinette et al. [71], revealed (1) a high survival rate (over 99.20%), (2) a fast and painless bone ingrowth, and (3) superior bone tissue modelling and remodeling quality. However, the concerns on the durability, bonding strength and degradability of the HA coatings are still under discussion.

The structure, composition, crystallinity and bonding strength of HA coating strongly rely on the quality of HA powder and processing parameters of plasma spraying. The morphology, crystal structure and phase composition of plasma-sprayed HA coatings obviously differ from those of the original starting powders. This result arises because the plasma spraying process contains melting of particles that leads to thermal decomposition and phase changes of the individual particles.

Table 2
Thermal decomposition of HA. V represents a vacancy and $x < 1$ [72].

$Ca_{10}(PO_4)_6(OH)_2 \rightarrow Ca_{10}(PO_4)_6(OH)_{2\text{-}2x}O_xV_x + xH_2O$	(1)
Hydroxyapatite → Oxyhydroxyapatite (OHA)	
$Ca_{10}(PO_4)_6(OH)_{2\text{-}2x}O_xV_x \rightarrow Ca_{10}(PO_4)_6O_xV_x + (1\text{-}x)H_2O$	(2)
Oxyhydroxyapatite → Oxyapatite (OA)	
$Ca_{10}(PO_4)_6O_xV_x \rightarrow 2Ca_3(PO_4)_2 + Ca_4O(PO_4)_2$	(3)
Oxyapatite → Tricalcium phosphate (TCP) + Tetracalcium phosphate (TTCP)	
$Ca_3(PO_4)_2 \rightarrow 3CaO + P_2O_5$	(4a)
Tricalcium phosphate → Calcium oxide + Phosphorus pentoxide	
$Ca_4O(PO_4)_2 \rightarrow 4CaO + P_2O_5$	(4b)
Tetracalcium phosphate → Calcium oxide + Phosphorus pentoxide	

HA particles subjected to the high temperature within a plasma jet always undergo dehydroxylation and decomposition. Table 2 lists the main reactions that take place at the elevated temperature [72,73], and Table 3 gives out the reactions occurring as HA is heated from room temperature up to 1730 °C [73]. It is difficult to detect the accurate temperatures for those reactions because they arise over a wide temperature range that is influenced by factors related to the spraying environment and the HA composition. One major concern is about the effect of the crystallinity of HA on bioactivity. The existence of amorphous and metastable compounds in prepared HA coatings has both advantages and disadvantages. The advantage is that it accelerates fixation of the implant and promotes bone remodeling and attachment, because of its higher solubility than that of crystalline HA. The disadvantages is that the excessive dissolution would affect the long-term reliability and biocompatibility of the implants. From the viewpoint of long-term stability, a high crystallinity of HA coating is required. It is generally accepted that the minimum crystallinity of the HA coating for biomedical applications is 62% as described in the Food and Drug Administration (FDA) guidelines as well as in the International Organization for Standardization (ISO) standards [74]. Hence, to improve the crystallinity, some post processing has also been developed, such as furnace heating [75], and hydrothermal treatment [76]. In addition, another concern is about the influence of bonding strength and thickness of the HA coating on stability. The bonding strength between the HA

Table 3
Thermal effects of HA [73].

Temperature (°C)	Reactions
25–200	Evaporation of absorbed water
200–600	Evaporation of lattice water
600–800	Decarbonation
800–900	Dehydroxylation of HA to form partially or completely dehydroxylated oxyhydroxyapatite
1050–1400	HA decomposes into β-TCP and TTCP
<1120	β-TCP is stable
1120–1470	β-TCP is turned into α-TCP
1550	Melting temperature of HA
1630	Melting temperature of TTCP and leaving behand CaO
1730	Melting of TCP

coating and substrates is relatively poor which ranges from 5 to 35 MPa, because of the high residual stress gaining from the mismatch of coefficient of the thermal expansion between HA (13.3×10^{-6} K^{-1}) and titanium ($(8.4–8.8) \times 10^{-6}$ K^{-1}) [17]. In order to improve the bonding strength, some ceramic nanoparticles (e.g., ZrO_2 [77], TiO_2 [78] and $CaSiO_3$ [79]), were introduced to augment the HA properties. Such coatings exhibited enhanced cohesion as the existence of the particle reinforcement and the reduced residual stress state from the functional gradient coatings. The thickness of the HA coating also influences the resorption and mechanical properties. Although the value varies, a thickness ranging from 50 to 75 μm is commonly applied for orthopaedic implants by such technique [17]. Plasma spraying of HA is the only FDA-approved technique to coat implants in clinic, however, some disadvantages still exist, including thermal decomposition during spraying, the inability to modulate pore sizes and porosity as well as the difficulty to prepare coatings with less than 20 μm thickness [72]. Hence, the careful engineering of HA coatings via regulating plasma-spraying parameters is still under exploration to improve mechanical, microstructural and biological behaviors.

2.2.1.2. High-velocity oxygen fuel spraying. High-velocity oxygen fuel (HVOF) spraying ignites a mixed flow of oxygen and fuel gases inside a combustion chamber, producing a supersonic gas jet with a temperature up to 3000 °C and particle velocities up to 1000 m/s [53]. The high particle velocity at a moderate temperature makes coatings with low porosity, high bonding strength and high abrasive resistance, because of the short dwell time of particles during the spraying. Similar to plasma spraying, HA is still the predominant materials for coating Ti implants via HVOF technique. Luma et al. observed that the HVOF-HA coating on Ti6Al4V presented high crystallinity (84%), low porosity (1.4%), high bonding strength (24 MPa) and low degradation, because the HA particles flowing through the HVOF flame did not undergo phase transformations, whose average surface temperature was only 1826 ± 346 °C [80]. The high crystallinity, low degradation and dense coating benefit the long-term stability of Ti implants. A recent study conducted by Ghadami et al. revealed that HA coating prepared by HVOF method showed an enhanced crystallinity, hardness and elastic modulus than that of APS method [81]. However, the in vivo rabbit study presented no significant differences between the two methods even though the HVOF coating showed a slight higher values of pull-out force and bone-implant contact (BIC). Hence, it still needs more studies in the future to optimize the HVOF coatings. In addition, some ceramic-reinforced HA coatings, such as TiO_2/HA composite coating [82], can be facially prepared by this technique, which improves the mechanical properties but without compromising the bioactivity of HA composites.

2.2.1.3. Cold spraying. Cold spraying (CS) is a kinetic-spray and solid-state deposition process where particles are accelerated by a pre-heated gas with a low temperature (25–1100 °C) and propelled towards a substrate with supersonic velocities (300–1200 m/s) [83]. Cold spraying is suitable for depositing oxygen-sensitive metals, heat-sensitive organic compounds, because the temperature is generally lower than the thermal decomposition or melting point of the feedstock. Feedstock particles including metals, ceramics, composites and organic compounds have been successfully deposited on Ti surfaces, providing the coatings with various functionalities. Metallic particles, such as Ti [84] and Ta [85], that show exceptional corrosion resistance and non-toxic track record have been coated on Ti6Al4V implants to improve the chemical stability in physiological solution, in vitro biomineralization and osteoblast activities. However, metallic particles appear bioinert, and thus, bioactive HA and its composites attract great attention. For instance, Vilardell et al. prepared HA coatings on Ti6Al4V surfaces via APS, HVOF and cold spraying, respectively (Fig. 2D) [86]. It is found that the HA coatings with higher crystallinity by HVOF and CS methods presented higher proliferation and differentiation of human osteoblastic cells than that of lower crystallinity by APS method. Beyond conventional metal and ceramic particles, it is suitable to prepare HA composite coatings containing temperature-sensitive drugs and biomolecules, such as growth factors [87] and antibiotics [88], because feedstock particles can be sprayed at room temperature. For instance, Li et al. prepared the composite coating consisting of nano-diamond, BMP-2 and HA via vacuum cold spraying (Fig. 2E), [87]. The presence of nano-diamond and BMP-2 significantly improved the attachment and proliferation of human osteoblast cells compared with the pure HA coating. In short, cold spraying is one of the newest thermal techniques and more researches on the process are yet to be carried out.

2.2.2. Plasma immersion ion implantation and deposition (PIII&D)

Plasma immersion ion implantation and deposition (PIII&D) is a flexible technique that can perform multiple processes, including simultaneous and consecutive implantation, deposition and etching, because of its combining advantages of other conventional plasma and ion beam methods [89,90]. A PIII&D system contains a vacuum chamber with a workpiece stage, a high-voltage pulse modulator and a plasma source (Fig. 3A) [89]. During the processing, a workpiece is placed in plasma at a high bias voltage, repelling electrons away from the workpiece and driving the positive ions toward it, thus a plasma sheath formed around the workpiece [91]. Then ions bombard the sample surfaces provided that the dimensions of plasma sheath are small compared with the feature sizes of workpiece. The plasma sheath has a critical impact, because it determines the implantation operation and foresees the process parameters and results, such as implantation current and dose as well as impurities profile [89]. Many elements have been implanted into the titanium surface, including non-metallic element (e.g., N and O) and metallic elements (e.g., Ca, Ag and Zn) [92].

Non-metallic elements generally induce polar functional groups and change the physicochemical properties but without altering surface topography [92]. The implantation of N and O is able to improve the corrosion resistance, wear resistance and cell activities. Huang et al. used N-PIII treatment to add a TiN film (<1 μm in thickness) to improve the surface hardness and corrosion resistance of Ti6Al4V [93]. Together with the modified mechanical strength, the N-PIII-treated surface enhanced the adhesion, proliferation and mineralization of human bone marrow mesenchymal stem cells (hMSCs) but prevent the adhesion of *Streptococcus salivarius*. Similarly, two oxygen ions with low and high doses were implanted into the Ti surface to form compact oxide layers that higher oxygen ions dose obtained higher thickness and amount of rutile phase [94]. The high oxygen-treated surface enhanced differentiation of hMSCs and in vivo osseointegration. Additionally, the O-PIII-treated surface with a rutile phase can also enhance blood-clotting and platelet activation but reduce the adhesion of *Streptococcus mutans* [95]. Beyond N and O, non-metallic species including H_2O have been used to modify the hydroxyl groups on Ti surfaces to improve the adhesion, spreading and growth of human osteoblastic OPC-1 cells [96].

Metallic elements are generally implanted to the Ti surface to improve the osteogenesis and antibacterial activity [92]. Ca is generally ion-implanted to favor osteogenic response [97], while Ag and Zn are sources to reduce bacterial infection [98–100]. For instance, Cao et al. prepared Ti surface embedded with Ag nanoparticles (Ag NPs) by one-step silver plasma immersion ion implantation (Ag-PIII) (Fig. 3B–E) [98]. When placed in a physiological solution, a Ti-Ag micro-galvanic couple would appear, where α-Ti matrix and Ag NPs served as the anode and cathode, respectively. The cathodic reactions would generate a proton-depleted region between bacterial membrane and Ag-embedded Ti substrate, which may destroy the proton electrochemical gradient across the intermembrane space, interfere with the synthesis of adenosine triphosphate (ATP) and ultimately lead to bacteria death. However, the promoted proliferation of MG-63 cells may be due to the difference in structure and size between bacteria and osteoblast-like cells. MG-63 cells have a much more complex endomembrane system compared with

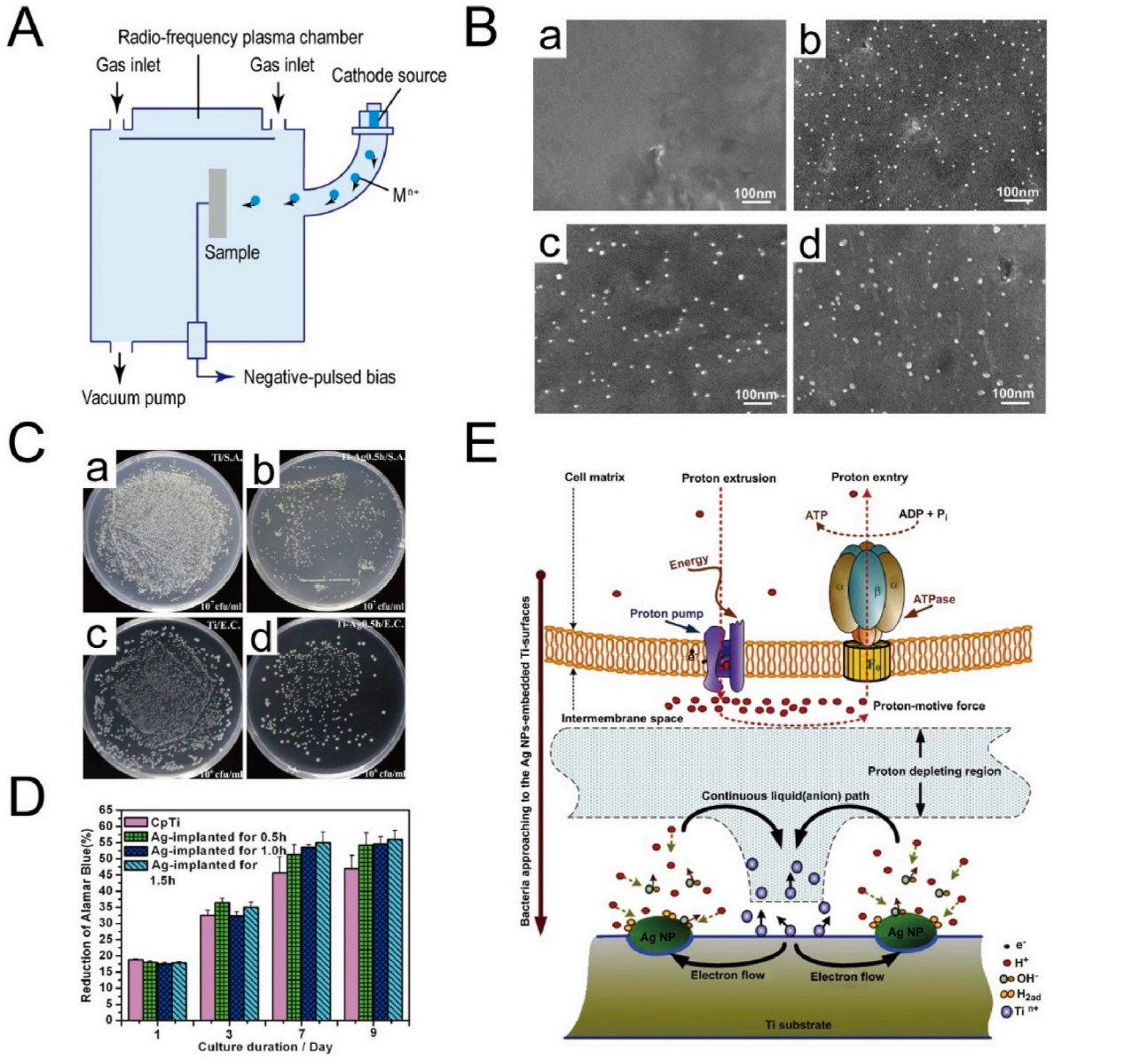

Fig. 3. (A) Schematic diagram of ion implantation and deposition setup [89]. Reprinted with permission from Ref. [89] with minor modification.
(B) SEM images of surface morphology of Ti surfaces after Ag-PIII: (a) Cp Ti, (b) 0.5 h-Ag-PIII, (c) 1.0 h-Ag-PIII, and (d) 1.5 h-Ag-PIII [98].
(C) Re-cultivated bacterial colonies on agar:*S. aureus* colonies are previous dissociated from (a) Cp Ti and (b) 0.5 h-Ag-PIII. The *E. coli*colonies are previous dissociated from (c) Cp Ti and (d) 0.5 h-Ag-PIII [98].
(D) The alamarBlue™ assay for MG63 cells on the various surfaces [98].
(E) Schematic diagram for the possible toxicity mechanism of the Ag NPs embedded surfaces [98]. Reprinted with permission from Ref. [98].

bacteria, making it unaffected but with enhanced energy-dependent proliferation. In addition to single metallic element, two types of elements can be co-implanted into Ti surfaces. Jin et al. modified Ti surfaces with Zn and Ag co-implantation by PIII&D [101]. The Zn/Ag co-implanted Ti surface not only significantly induced the proliferation, differentiation of rat bone mesenchymal stem cells (rBMSCs) and effectively killing bacteria in vitro, but also exhibited strong osteogenic activity and antibacterial ability in vivo. The excellent performance was related with the synergistic effects from the long-range and short-range interactions of the released Zn^{2+} and Ag NPs, respectively. Similarly, Ag and Ca were co-implanted into Ti surface to produce bifunctional galvanics, which synergistically hindered bacterial activity and enhanced osteoblastic differentiation [102]. Besides the treatment of smooth Ti surfaces after polishing, PIII&D can treat roughed Ti surfaces after other modification, including acid etching [103], anodization [104], plasma spraying [105] and acid etching/sandblasting [106].

2.3. Chemical methods

Chemical modification is mainly based on the occurrence of chemical reaction at the interface between Ti substrate and the immersed medium. Such kind of modification generally involves acid etching, alkali-heat treatment, electrochemical methods and biochemical methods.

2.3.1. Acid etching

Acid treatment is commonly used to remove surface oxide and contamination to clean and uniform surface finishes. Some strong corrosive acids, such as H_2SO_4, HCl, HNO_3 and HF, are adopted to roughen the Ti surface with a micro-scale feature, because H^+ ions attack TiO_2 and Ti with the production of soluble Ti compounds and hydrogen.

However, the adsorption of hydrogen generally forms titanium hydride, which may lead to hydrogen embrittlement [107,108]. Table 4 lists typical reactions of Ti substrates subjected to H_2SO_4 etching [109]. The micro-scale feature relies on acid concentration, solution temperature and etching time. The micropits created by acid etching varying from submicron to several microns tend to favor cell activities (red blood cells and osteoblasts) and bone integration [17,36,110]. Many studies have revealed the positive effect of the acid etching on bone regeneration. For instance, Lamolle et al. cultured MC3T3-E1 cells on the Ti surface that was treated with weak HF (0.2 vol%) solution, and observed the lower cytotoxicity level and better cell attachment compared with smooth control surface, as shown in Fig. 4A [111]. The reason may be due to the fact that the micro- and nano-level topography and the surface composition that included low hydrocarbon content and presence of fluoride, hydride and oxide, produced a favorable microenvironment together for cell growth with enhanced biocompatibility.

More commonly, acid etching is performed after a sandblasting step to remove blasting residues and to refine the surface morphology and roughness. Many studies have indicated that the combined treatment of sandblasting and acid etching (SLA) on Ti surfaces significantly improved osseointegration [112–115]. A typical morphology after SLA treatment is shown in Fig. 4B [115], with irregular micropits in a few microns. For instance, the TiO_2 grit-blasted surface after HF modification significantly promoted osteoblastic differentiation and interfacial bone formation, when compared with the TiO_2 grit-blasted surface (Fig. 4C) [112]. Therefore, acid etching provides an efficient way to improve the bioactivity of sand-blasted Ti surfaces. In a clinic study, a 10-year follow-up study of SLA dental implants has suggested the survival and success rate of 511 implants was 98.8% and 97.0%, respectively, and the prevalence of peri-implantitis was low with 1.8% [116].

2.3.2. Alkali-heat treatment

Since 1990s, alkali-heat treatment is used to modify Ti surface by immersing the substrate in 5–10 M NaOH or KOH solution at 60 °C for 24 h and subsequently heating treatment at 600 °C for 1 h [117–119]. The typical process of alkali-heat treatment is shown in Fig. 5A [120]. In the first step, the Ti substrate can react with the NaOH to form an alkalinic titanate hydrogel layer and the corresponding reactions are described in Table 5 [117]. After heat treatment, the hydrogel layer undergoes dehydration and densification to form a stable amorphous or crystalline sodium titanate layer, whose scratch resistance is increased from 5 to 50 mN [120,121]. Heat treatment significantly impoves the bioactivity of Ti substrates in vivo after alkali treatment [122,123]. The reason may be due to the unstable reactive and mechanically weak layer of the alkali-treated surface, while subsequent heat treatment reinforced the stability of the sodium titanate layer [122].

The sodium titanate layer undergoes ion exchange with H_3O^+ ions upon immersion in SBF to form a titania gel layer rich in Ti-OH groups, thus inducing apatite nucleation and deposition via alternative adsorption of positively charged calcium ions and negatively charged phosphate ions [118]. However, the apatite-forming ability of Ti surface with alkali-heat treatment tends to decrease when stored in a humid environment over a long time period, because the Na^+ ions can exchange with the H_3O^+ in the moisture. Hence, in some cases, the Na^+ ion is replaced by Ca^{2+} ion to strength the apatite-forming ability. Kizuki et al. immersed the alkali-treated Ti surface in a $CaCl_2$ solution for replacing Na^+ with Ca^{2+} to form calcium hydrogen titanate [124]. After heat treatment, the calcium hydrogen titanate was transformed into calcium titanate. Because of the tight structure, the release of Ca^{2+} from calcium titanate was slow and made it hardly to induce apatite formation in SBF. To enhance the mobility of Ca^{2+} ions, the calcium titanate layer was further subjected to hot-water treatment, and thus its apatite-forming ability was obviously restored (Fig. 5C), and strongly maintained even in the humid environment (Fig. 5D). Furthermore, Ti alloys after this treatment led to their direct bonding with bone without an intervening fibrous layer after implantation in rabbit tibia for 26 weeks [125,126]. Tian et al. also noted that the NaOH-$CaCl_2$-heat-water-treated surface showed a similar bone-bonding ability to the alkali-heated surface at 2 and 3 weeks after implantation in rabbit tibias, but it presented a greater bonding ability at 4 weeks [127]. Therefore, such a method enriches the originally-developed alkali-heat treatment to improve the bioactivity of Ti implants. Alternatively, other bioactive ions, such as Ag^+ [128] and Sr^{2+} [129], can be incorporated into the calcium-deficient calcium titanate layer by introducing them either into the $CaCl_2$ solution or into the hot water of the last step, and thus a multifunctional surface with bifunctional ions can be achieved to improve osteogenetic and antibacterial activity [128,129].

Since September 2000, a series of 70 artificial total hip joints with an alkali-heat treatment was carried out in clinical trials [130,131]. A titanium macroporous structure was generated on the surface of a Ti alloy as a proximal site stem, and on the entire surface of a Ti alloy covering a polyethylene cup, and then the joints underwent alkali-heat treatment [130], as shown in Fig. 5B [118]. Although a gap between the host tissue and the socket existed in over 70% cases, it disappeared and closed within one year [131]. During the average 4.8-year follow-up study, 68 hips (97%) were considered as bone ingrowth fixation and only two hips (3%) as stable fibrous ingrowth, indicating the good osteoconduction [131]. As the time prolonged to 10 years, the overall survival rate was 98% of the 67 hips (two patients were lost) [132]. No obvious signs appeared of osteolysis, loosening, or formation of a reactive line.

2.3.3. Electrochemical methods

2.3.3.1. Anodization. Anodization is a traditional method to form compact and protective oxide films on valve metals. In a typical procedure, the Ti serves as an anode and an inert materials as a counter electrode, such as graphite and platinum. In 2001, a well-aligned TiO_2 nanotube arrray was prepared on pure Ti sheet by anodization in HF solution [133]. Since then, the preparation and application of TiO_2 nanotubes have been extensively studied. The F^- ion is needed in nanotubular formation and the mechanism can be explained as follows, as shown in Table 6 [134,135]. Firstly, a compact oxide layer is formed with the reactions shown by Eqs (1-4). Secondly, F^- in the electrolyte can react with Ti^{4+} dissolved at the oxide-electrolyte interface and attack the formed TiO_2 to form irregular nanoscale pores with Eqs (5-6). Finally, the competition between oxidation and dissolution reaching steady leads to the formation of a regular nanopore or nanotube layer. The tube geometry, diameter and length of the nanotube array can be varied by regulating the anodization parameters, such as applied voltage, anodization time and electrolyte [134,136].

The biomedical application of TiO_2 nanotube array has been widely investigated. Park et al. cultured rat mesenchymal stem cells on TiO_2 nanotubes with defined diameters between 15 and 100 nm, as shown in Fig. 6A [137]. The best performance in cell adhesion, spreading, growth, and differentiation was obtained on the nanotube array with a diameter of 15 nm, because such a size effectively accelerated integrin assembly into focal contacts and therefore induced actin filament assembly and signaling conduction to the nucleus. However, tube size larger than 50 nm severely impaired cell activity, and the diameter of 100 nm almost completely hindered integrin clustering and focal adhesion formation, resulting in a high degree of anoikis that is the adhesion-dependent type of apoptosis. Oh et al. noted that the small nanotube array (~30 nm) enhanced the adhesion without noticeable differentiation of human mesenchymal stem cells (hMSCs), but larger nanotube array (70–100

Table 4
Ti substrates subjected to concentrated H_2SO_4 etching [109].

$TiO_2 + H_2SO_4 \rightarrow Ti(SO_4)_2 + 2H_2O$	(1)
$Ti + 2H_2SO_4 \rightarrow Ti(SO_4)_2 + 2H_2$	(2)
$Ti + H_2 \rightarrow TiH_2$	(3)

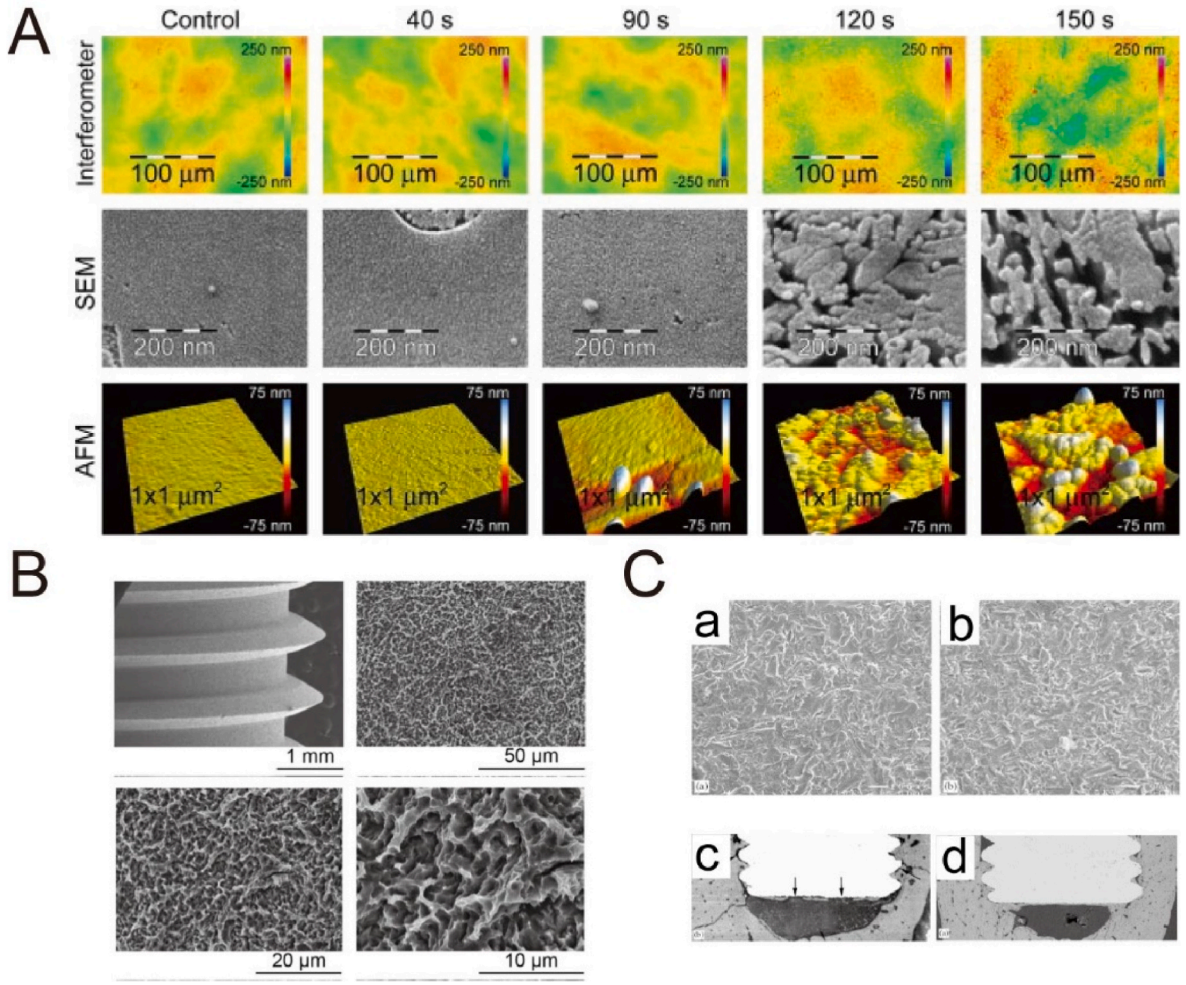

Fig. 4. (A) Blue light interferometer, SEM and AFM images of the modified Ti disks in 0.2 vol% HF [111]. Reprinted with permission from Ref. [111]. (B) SEM images of the untreated SLA implants at different magnifications [115]. Reprinted with permission from Ref. [115]. (C) SEM images of (a) TiO_2 grit-blasted Ti surface and (b) fluoride ion-modified TiO_2 grit-blasted Ti surface. Histological assessment of bone-to-implant contact of (c) TiO_2 grit-blasted implant surface and (d) fluoride ion-modified TiO_2 grit-blasted implant surface [112]. Reprinted with permission from Ref. [112].

nm) obviously accelerated cytoskeletal stress and differentiation into osteoblast-like cells [138]. The mechanism was related with the fact that small-diameter nanotubes induced protein aggregate adhesion configurations and thus caused adhesion and growth of hMSCs with minimal differentiation, while large-diameter nanotubes made cells elongate and stretch to seek protein aggregates and thus were forced to differentiate into osteoblasts. The inconsistent results are common of the effect of diameters on the osteoblast response [139–142]. The reason for the differences is associated with the processing parameters, surface chemistry, crystal phase of TiO_2 as well as cell origins [143]. As to in vivo studies, Ti implants with TiO_2 nanotube array positively induced molecular response and osseointegration at the bone-implant interface [144–147]. It is noted that the overexpression of purinergic receptor P2Y6 caused by TiO_2 nanotubes can increase osteogenic differentiation of bone marrow mesenchymal stem cells (BMSCs) through activating PKCα-ERK1/2 signal pathway, and thus enhance bone tissue deposition around the implant in vivo [147]. In addition, the crystalline phase of TiO_2 nanotubes strongly affects the cell activity. For instance, Yu et al. prepared the anatase and anatase/rutile TiO_2 nanotubes by annealing at 450 °C and 550 °C, respectively [148]. They observed the better proliferation and mineralization of MC3T3-E1 cells on anatase and anatase/rutile surfaces than on smooth and amorphous nanotube surfaces, and even the anatae/rutile surface showed slightly better performance compared with the anatase surface. However, in Park et al.'s study, adhesion and proliferation rates of rat bone marrow mesenchymal cells (MSCs) presented somewhat higher adhesion and proliferation rates on amorphous than on anatase nanotubes [149]. Hence, it is still necessary to investigate the influence of crystalline phase on cell behaviors and osseointegration in vivo, thus optimizing the bioactivity of Ti implants.

Because of the unique tubular structure, TiO_2 nanotube array is usually loaded with drug and biomolecules to strength bioactivity. Some model drugs, such as large-molecular proteins (e.g., BMP-2 [150], PDGF-BB [151] and FGF-2 [152]) and common small-molecular antibiotics (e.g., gentamicin [153] and sirolimus [154]), have been loaded into the nanotube array to enhance osteogenic response and antibacterial property. For instance, the nanotube array loaded with PDGF-BB that was released for at least 14 days, promoted adhesion, proliferation as well as differentiation of bone marrow stem cells (BMSCs) in vitro and induced fast new bone formation in vivo, as shown in Fig. 6B [151]. Although the nanotube structure provides a smart platform for the local drug release, unsatisfying results on the release kinetics still occur, including burst release, because the drug is usually immobilized by repeated lyophilization or vacuum extraction. Therefore, a barrier coating with degradation is exploited to improve the release kinetics. Biopolymers, such as poly(lactic-co-glycolic acid) (PLGA), have been applied to coat the TiO_2 nanotube after loading BMP-2 [155] or ciprofloxacin [156], respectively, to enhance the release patterns.

Besides in F^--containing solution, anodization can also be conducted

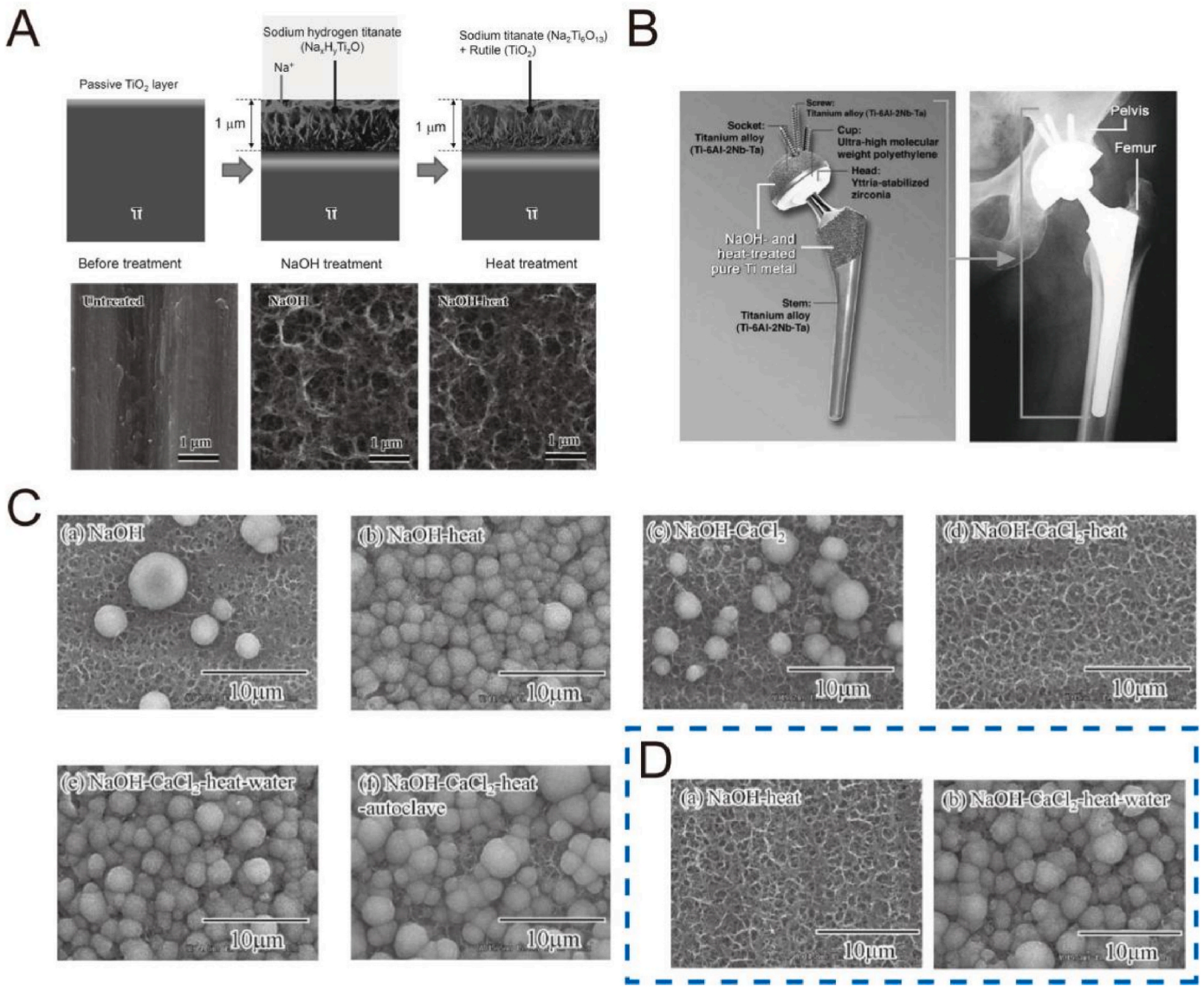

Fig. 5. (A) Structural change of the surface of Ti metal after NaOH and heat treatments [120]. Reprinted with permission from Ref. [120].
(B) A total hip joint system of Ti-6Al-2Nb-Ta alloys after NaOH and heat treatments (left), and its clinical application (right) [118]. Reprinted with permission from Ref. [118].
(C) SEM images of various Ti surfaces after immersion in SBF for 1 day [124].
(D) SEM images of the Ti surfaces soaked in SBF for 1 day after storage at 95% relative humidity for 1 week with NaOH-heat and NaOH-$CaCl_2$-heat-water treatments [124]. Reprinted with permission from Ref. [124].

Table 5
Ti substrates subjected to alkali treatment [117].

$TiO_2 + OH^- \rightarrow HTiO_3^-$	(1)
$Ti + 3OH^- \rightarrow Ti(OH)_3^+ + 4e^-$	(2)
$Ti(OH)_3^+ + e^- \rightarrow TiO_2{\cdot}H_2O + 0.5H_2$	(3)
$Ti(OH)_3^+ + OH^- \rightarrow Ti(OH)_4$	(4)
$TiO_2{\bullet}nH_2O + OH^- \leftrightarrow HTiO_3^-{\bullet}nH_2O$	(5)

Table 6
TiO_2 TNTs formation in fluoride-containing electrolyte [134,135].

$2H_2O \rightarrow O_2 + 4H^+ + 4e^-$	(1)
$Ti \rightarrow Ti^{4+} + 4e^-$	(2)
$H_2O \rightarrow O^{2-} + 2H^+$	(3)
$Ti^{4+} + 2O^{2-} \rightarrow TiO_2$	(4)
$Ti^{4+} + F^- \rightarrow [TiF_6]^{2-}$	(5)
$TiO_2 + 6F^- + 4H^+ \rightarrow [TiF_6]^{2-} + 2H_2O$	(6)

in NaOH solution to form nanostructures on Ti surfaces [157,158]. The nanonetwork-structured TiO_2 layers, with average lateral pore sizes of 70 ± 30 nm (~200 nm thickness) and 90 ± 50 nm (~300 nm thickness), were formed depending on the anodized current [158]. The nanonetwork-structured surfaces favored focal adhesion formation and signaling conduction via integrins and activated FAK and ERK1/2 pathways, and thus obviously improved the motility, spreading, proliferation as well as differentiation of human bone marrow mesenchymal stem cells (hBMSCs) (Fig. 6C) [158].

2.3.3.2. Micro-arc oxidation. The electrode process obeys Faraday's law and Ohm's law at relatively low voltages, however, increased gas evolution, sparks and micro arc discharges would appear when the voltages are beyond the dielectric breakdown limit of the grown oxide [159,160]. This kind of anodization is usually referred to micro-arc oxidation (MAO), anodic spark oxidation or plasma electrolytic oxidation (PEO). In MAO, the voltage usually varies in 150–1000 V and in 0–100 V in the

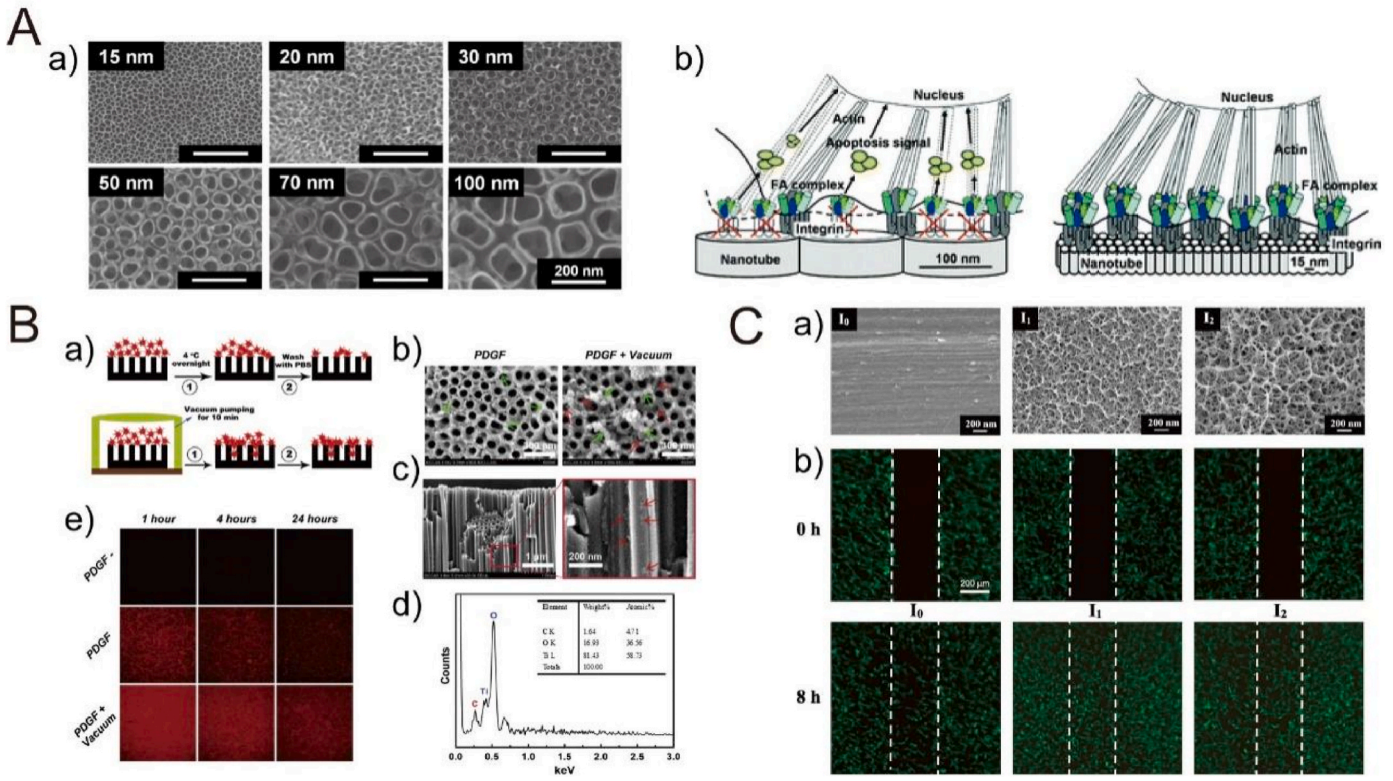

Fig. 6. (A) SEM images (a) of TiO_2 nanotubes with different diameters created by controlling potentials ranging from 1 to 20 V. (b) Schematic model showing the lateral spacing of focal contact formation on nanotubes of different diameters [137]. Reprinted with permission from Ref. [137]. (B) Immobilization and release of rhPDGF-BB: (a) schematic diagram of vacuum extraction, (b) SEM images of rhPDGF-BB-loaded nanotube surface, (c) cross-sectional SEM image of the protein particles loaded into the nanotubes in the PDGF + Vacuum group, (d) corresponding EDS of the rectangular region, and (e) the decrease trends of PDGF-BB fluorescence intensity on the Ti plates from 1 to 24 h after immersion in PBS [151]. Reprinted with permission from Ref. [151]. (C) SEM images (a) of the Ti surfaces with (I_1 and I_2) and without (I_0) electrochemical anodization treatment. (b) Cell (hBMSCs) motility by the wound healing assay on Ti surfaces with (I_1 and I_2) and without (I_0) anodization treatment [158]. Reprinted with permission from Ref. [158].

anodic and cathodic half circles, respectively [17]. The local temperature and pressure generated inside the discharge channel can reach up to 10^3-10^4 K and 10^2-10^3 MPa, respectively, which induces the plasma thermochemical reactions between the substrate and the electrolyte [161]. Interestingly, the porous surface morphology usually shows crater-like with holes at the center, whose size tends to be a few microns [135]. The quality and characteristics of MAO coating are associated with processing parameters, such as applied voltage, electrolyte composition, and anodization time.

Many studies have focused on the preparation of oxide coatings on Ti surfaces by MAO treatment with improved bioactivity, biocompatibility and antibacterial properties. The electrolyte formulation greatly affects the composition of surface oxide coatings, so some bio-functional elements, such as Ca, P, Mg and S, can be readily incorporated into the oxide layer by introducing their corresponding compounds to the electrolyte [135]. For instance, Fe^{3+}-incorporated TiO_2 film significantly enhanced proliferation, osteogenic differentiation and extracellular matrix mineralization of osteoblasts (hFOB1.19) [162]. Ca- and P-incorporated oxide layers showed an improved bone-implant contact and removal torques [163,164]. In order to reduce infection, some antibacterial elements, such as Ag [165], Zn [166], Cu [167] and Mn [168], can be incorporated into the oxide film to hinder bacterial adhesion and biofilm formation. In one case, the TiO_2-Ag coatings with different concentrations of Ag NPs (designated as TiO_2-0.3Ag and TiO_2-3.0Ag) showed an effective antibacterial activity against methicillin-resistant *Staphylococcus aureus* (MRSA), with percentage killing as high as 98.0 ± 2% for TiO_2-0.3Ag and 99.75 ± 0% for TiO_2-3.0Ag, respectively [165]. As to cell viability, the TiO_2-0.3Ag presented no obvious cytotoxicity to human osteoblastic cells (SV-HFO), but TiO_2-3.0Ag significantly inhibited cell adhesion and proliferation, because higher concentration of Ag NPs may disrupt normal cell behaviors. Because Ag as a strong bactericide may induce the cytotoxic risk, some mild bactericides, such as Zn and Cu, may be safer towards mammalian cells. For instance, Ye et al. prepared Zn-doped TiO_2 coatings with Zn existing in the form of weaken Zn-O bonds in the outer layer and Zn_2TiO_4 underneath, respectively, as shown in Fig. 7 [166]. The reactive oxide species (ROS) induced by the Zn^{2+} ions released from Zn-doped coatings can break the cell walls and plasma membranes, and further strength the intracellular ROS level of *S. aureus*, resulting in bacteria death. In contrast to the overdose of Zn-doped coating ($M_{Zn\text{-}530\ V}$), the moderate doses of Zn ions ($M_{Zn\text{-}300\ V}$ and $M_{Zn\text{-}400\ V}$) did not generate intracellular ROS and reduce viability of osteoblasts, but it inversely enhanced proliferation of osteoblasts and osseointegration in both *S. aureus*-uninfected and infected rat tibias.

Ti implants subjected to MAO treatment have been successfully applied in clinic. In a long-term study, 210 implants of TiUnite with a porous anodized surface were implanted in 59 patients [169]. During a 10-year follow-up study, 47 (22.38%) implants were lost because these patients refused to continue the study, and another 5 implants were lost. Based on the final follow-up, the cumulative survival rate of the implants placed in healed and postextractive sites were 98.05% and 96.52%, respectively, suggesting a positive result in terms of bone maintenance and integration.

2.3.3.3. Electrodeposition. Electrochemical deposition can be divided into electrodeposition (ED) and electrophoretic deposition (EPD). ED is an electrochemical reduction process of metallic ions hydrolyzed or metal complexes by cathodic reactions to generate dispersive particles

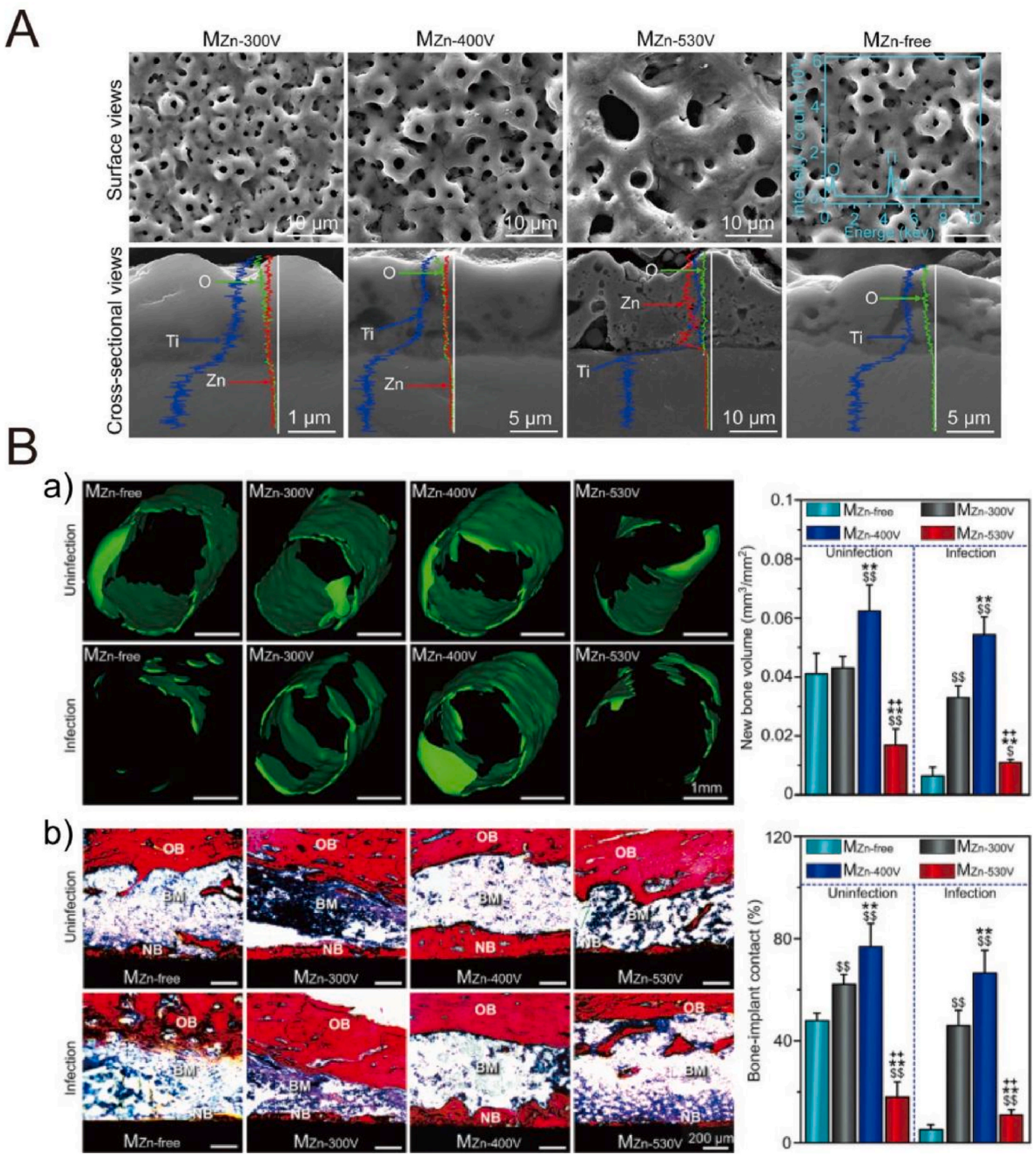

Fig. 7. (A) SEM images of $M_{Zn\text{-}300\ V}$, $M_{Zn\text{-}400\ V}$ and $M_{Zn\text{-}530\ V}$ and $M_{Zn\text{-}free}$ coatings prepared by micro-arc oxidation [166]. (B) Micro-CT (a) and histological analyses (b) of the coated pillars implanted in rat tibias under *S. aureus*-infected and uninfected conditions at week 4 of surgery. OB: original bone, NB: new bone and BM: bone marrow [166]. Reprinted with permission from Ref. [166].

or continuous film on the substrates, whereas EPD uses an electric field to drive the charged organic or inorganic particles in suspended solution towards the oppositely charged electrode to form thin and thick films [135]. Distinctions of such two techniques are displayed in Table 7 [135].

ED not only can fabricate various metallic coatings on the electrodes, but also is able to construct organic or inorganic films on the conductive materials by controlling electrochemical condition and electrode interfacial environment. As a powerful modification method, ED is widely used to deposit CaP-based coatings on Ti surfaces to improve the

Table 7
Distinctions of electrodeposition and electrophoretic deposition [135].

	Electrodeposition	Electrophoretic deposition
Medium	Solution	Suspension
Moving species	Ions or complexes	Particles
Electrode reaction	Reduction of metal ions or hydrolyzation by electrogenerated base	None
Preferred liquid bath	Mixed solvent (water-organic)	Organic solvent
Required conductivity	High	Low
Deposition rate	10^{-3} - 1 μm/min	1–10^{3} μm/min
Deposition thickness	10^{-3} - 10 μm	1–10^{3} μm
Deposition uniformity	On nanometer scale	Limited by size of particles

bioactivity under galvanostatic processing. The typical reactions of CaP deposition can be described as follows [170–173], as shown in Table 8. The cathodic polarization produces OH^- and H_2 (Eqs 1-5), and then the produced OH^- makes the local pH around the cathode increase to facilitate reactions (Eqs 6-7) and move the ionization equilibrium forward of $H_2PO_4^-$ and HPO_4^{2-} (Eqs 8-9), thus generating PO_4^{3-}. In addition, PO_4^{3-} can also be produced by reduction of $H_2PO_4^-$ (Eqs 10–11). The accumulated Ca^{2+}, HPO_4^{2-}, PO_4^{3-} and OH^- ions lead to local supersaturation and subsequent nucleation and growth of CaP based on the applied current density (Eqs 12). The composition, morphology, crystallinity and stability of CaP are associated with the deposition parameters, such as current density, deposition time and temperature, and electrolyte properties (e.g., pH, additives, ion concentrates) [135]. In some cases, low current density produces HA precursors, including $CaHPO_4{\cdot}2H_2O$ (DCPD) (Eqs 12a), $Ca_8H_2(PO_4)_6{\cdot}5H_2O$ (OCP) (Eqs 12b), and $Ca_2(PO_4)_3{\cdot}nH_2O$ (TCP) (Eqs 12c), high current density facilitates HA (Eqs 12d) formation [170,172].

The bioactivity of HA and other CaP-based coatings by ED has been widely investigated. HA-coated Ti surfaces significantly improve osteoblast adhesion, spreading and gene expression of ALP as well as osteocalcin related with differentiation in vitro [174–176]. The in vivo studies have also indicated the superior bone regeneration and apposition [177,178]. Chai et al. modified a three-dimensional porous Ti6Al4V scaffold with HA by perfusion electrodeposition with different current densities (1.54, 5, 10 and 20 mA/cm^2) [178]. After in vitro test, they implanted HA-Ti hybrids (5 and 10 mA/cm^2) seeded with human periosteum-derived cells on the backs of mice in the cervical region. The absolute volume and the percentage of bone formed on the hybrids produced at 10 mA/cm^2 were significantly higher than that of hybrids produced at 5 mA/cm^2. It was assumed that the osteoclastic resorption may occur earlier on the hybrids produced at 10 mA/cm^2, resulting in a faster initiation of ectopic bone formation. Because various elements exists as ionic substitutions in bone mineral, such as Na^+, Mg^{2+}, Sr^{2+}, Zn^{2+}, CO_3^{2-}, F^- and Cl^- [179,180], which obviously influence the biological activity of bone mineral, some ion-substituted HA materials are facilely prepared via adding corresponding ions into the electrolytes. Such ion-substituted HA significantly improves coating stability, cell activity, and antibacterial properties. For example, Sr-HA via addition of Sr^{2+} obviously enhanced cell adhesion, proliferation and differentiation in vitro, and induced superior new bone formation as well as bone-implant contact in vivo [181]. Similarly, Ag^+ [182], Cu^{2+} [183], Cu^{2+}/Zn^{2+} [184] and $Sr^{2+}/Mg^{2+}/Zn^{2+}$ [185], are introduced into the HA by single- or co-substitution to promote the osteoblast activity as well as to reduce bacterial infection [182–185]. In addition, some HA-based composite coatings have been obtained on Ti surfaces by ED to better mimic the inorganic/organic hierarchical structure and composition. For instance, after addition of collagen I into the electrolyte, the electrolyte viscosity was increased, which would benefit the stability of the H_2 bubbles on the interface as a dynamic porous template [186]. During the nucleation and growth, the collagen might act as a "glue" to chemically bond with HA and hinder the fast growth of HA, and thus produced a gel-crystal hybridized and micro-nano porous coating with fiber-like crystals orderly arranged together, as shown in Fig. 8A. Similarly, by introducing the soluble chemicals, such as chitosan [187], heparin [188] and amino acids [189], the corresponding HA-based composite coatings can be realized via the incorporation during the nucleation and growth, to construct a bioactive platform [187–189].

Besides HA-based coatings, some other CaP-based composites have been prepared as well. Some inorganic/organic hierarchical structures based on octacalcium phosphate (OCP) coatings have been obtained by assembling from fiber-like nanocrystals, such as OCP/collagen [190,191], OCP/silk fibroin (SF) [192,193]. For instance, the OCP/SF coating with a bioinspired nano-micro structure was formed because the produced hydrogen bubbles functioned as a template during ED process, as shown in Fig. 8B [192]. The OCP/SF coating improved adhesion, spreading and proliferation of MC3T3-E1 cells and human umbilical cord-derived mesenchymal stem cells (HUMSCs), because of the multiscale structure and proper chemical composition.

2.3.3.4. Electrophoretic deposition. Electrophoretic deposition (EPD) is a typical colloidal processing technique usually used in ceramic production with many advantages, such as short formation time and little restriction of the substrate shape [194]. The charged particles are first dispersed or suspended in a liquid medium, and then moved towards the electrode of opposite charge under an electric field to form a deposited film [195]. A major difference between the EPD and ED is that, the electrolyte of EPD is a suspension of particles in a solvent but the latter is a solution of salts (e.g., ionic species) [196]. The EPD is usually carried out in organic solvents with the advantages of low conductivity, favorable chemical stability of the suspension and absence of the electrolytic reactions, because water tends to cause the electrolysis and evolution of H_2 and O_2, resulting in formation of incompact coating [197]. Many factors influence the coating properties, such as particle size, dielectric constant of liquid, conductivity of suspension, Zeta potential, deposition time and applied voltage [198].

The EPD of HA or HA-based composited coating has been widely developed since 1986 [199]. Compared with other techniques, the advantage of EPD-prepared HA coating shows fine stoichiometry control, high purity of the deposited coating, and wide range of coating thickness varying from 0.1 μm to more than 100 μm [200]. The prepared HA coating obviously promoted cell adhesion, spreading, proliferation, differentiation and cytoskeleton organization [201,202], suggesting favorable cell-substrate interaction. In order to endow the coating with better bioactivity as well as antibacterial activity, some other one or two components (inorganics or organics) were incorporated to form HA-based composite coatings, such as polyetheretherketone/HA [203],

Table 8
Typical reactions of preparation of CaP coating by ED [170–173].

$2H_2O + O_2 + 4e^- \rightarrow 4OH^-$		(1)
$2H_2O + 2e^- \rightarrow H_2 + 2OH^-$		(2)
$2H^+ + 2e^- \rightarrow H_2$		(3)
$NO_3^- + H_2O + 2e^- \rightarrow NO^{2-} + 2OH^-$		(4)
$H_2PO_4^- + H_2O + 2e^- \rightarrow H_2PO_3^- + 2OH^-$		(5)
$H_2PO_4^- + OH^- \rightarrow HPO_4^{2-} + H_2O$		(6)
$HPO_4^{2-} + OH^- \rightarrow PO_4^{3-} + H_2O$		(7)
$H_2PO_4^- \leftrightarrow HPO_4^{2-} + H^+$		(8)
$HPO_4^{2-} \leftrightarrow PO_4^{3-} + H^+$		(9)
$2H_2PO_4^- + 2e^- \rightarrow 2HPO_4^{3-} + H_2$		(10)
$H_2PO_4^- + 2e^- \rightarrow PO_4^{3-} + H_2$		(11)
Overall reactions:		
$Ca^{2+} + HPO_4^{2-} + 2H_2O \rightarrow CaHPO_4{\cdot}2H_2O$	(DCPD)	(12a)
$8Ca^{2+} + 6HPO_4^{2-} + 5H_2O \rightarrow Ca_8H_2(PO_4)_6{\cdot}5H_2O$	(OCP)	(12b)
$3Ca^{2+} + 2PO_4^{2-} + nH_2O \rightarrow Ca_3(PO_4)\cdot nH_2O$	(TCP)	(12c)
$10Ca^{2+} + 6PO_4^{3-} + 2OH^- \rightarrow Ca_{10}(PO_4)_6(OH)_2$	(HA)	(12d)

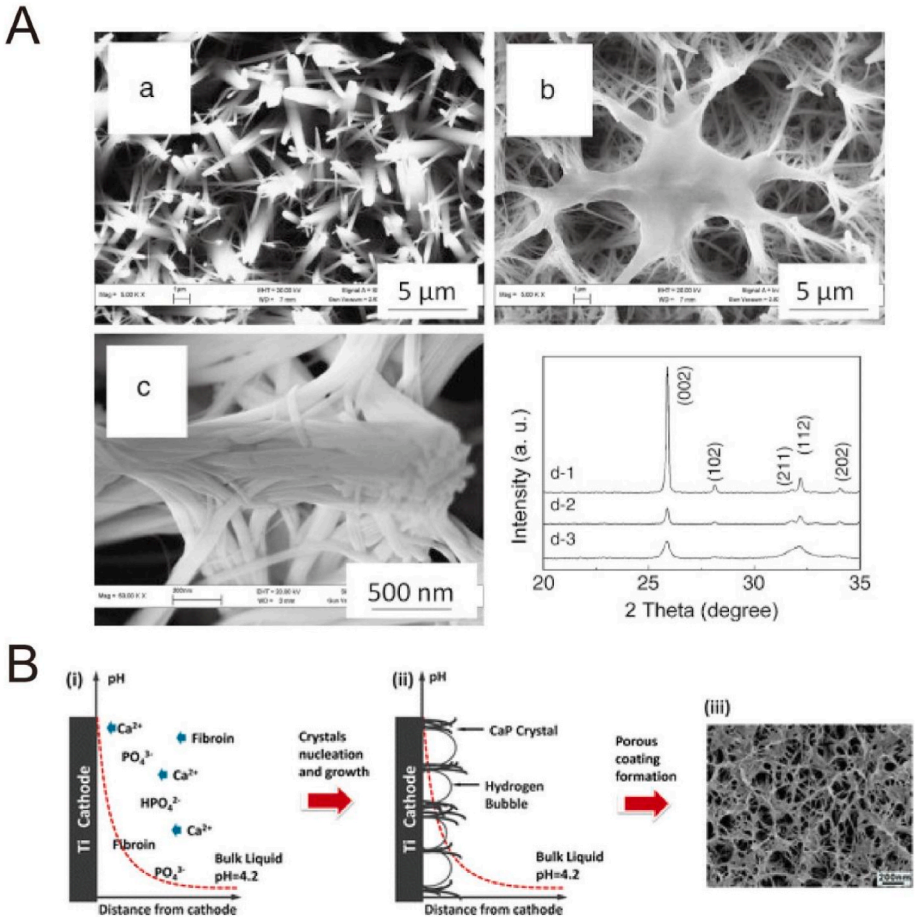

Fig. 8. (A) SEM images (a–c) of the hydroxyapatite coatings: (a) without collagen, and (b, c) with collagen prepared by electrodeposition method. (d) XRD patterns of (1) hydroxyapatite coating, (2) collagen-modified hydroxyapatite coating, and (3) bovine cortical bone [186]. Reprinted with permission from Ref. [186]. (B) Schematic diagram of mechanism in the formation of OCP/SF composite coatings [192]. Reprinted with permission from Ref. [192].

graphene oxide/HA [204], chitosan/HA [205], Ag/amorphous calcium phosphate/HA [206], Fe_3O_4/chitosan/HA [207] and poly-l-lysine/3, 4-dihydroxybenzylaldehyde/HA [208]. In one case, Suo et al. modified the Ti surface with a graphene oxide/chitosan/hydroxyapatite (GO/CS/HA) composite coating with a thickness of 10 μm by one-step EPD, as shown in Fig. 9A-B [209]. Such a crack-free GO/CS/HA composite displayed a bonding strength of 27.1 ± 1.2 MPa, much higher than that of HA, GO/HA, CS/HA coatings with a value of 16.8 ± 1.5 MPa, 24.5 ± 1.3 MPa and 17.3 ± 1.7 MPa, respectively. The GO/CS/HA coating significantly enhanced not only the extension, proliferation, ALP activity and mineralization of bone marrow stromal cells (BMSCs), but also the bone area ratio, bone-to-implant ratio and the biomechanical properties after implantation in rat tibia for 12 weeks. In addition, some drugs or proteins are easily incorporated into the coatings by EPD [210–214]. For instance, gentamicin was loaded to the chitosan/HA coating by dissolving it in the electrolyte, and such coating effectively inhibited growth of *Staphylococcus aureus* and *Escherichia coli*, without inducing obvious cytotoxicity towards fibroblast cells (L929 and MRC-5) [210].

Beyond CaP-based coatings, some polyelectrolyte components have been deposited on Ti surfaces as well. Chitosan/gelatin [215] and chitosan/silk fibroin [216], can form polyelectrolyte complex by electrostatic interaction in acidic aqueous solution. After the pH value around the cathode increased higher than chitosan's pK_a with the applied voltage, the amino groups of chitosan were deprotonated, leading to the decreased solubility and subsequent co-deposited coatings of the chitosan/gelatin [215] and chitosan/silk fibroin [216]. Similarly, Zhang et al. observed comparable and positive behaviors of MC3T3-E1 cells on the porous chitosan/gelatin coating with various surface porosity. The best cell response was observed in small pores with integral and continuous structure of G1 group, because of the synergistic effects of the porous structure and component, as shown in Fig. 9C [217]. Furthermore, some inorganic elements, such as Mg [218], Sr [219] and Zn [220], were able to incorporate into the chitosan/gelatin to form organic/inorganic composites, and the promoted cell proliferation and differentiation as well as antibacterial activity were obtained via the ion release. In addition to inorganic elements, drug-loaded nanoparticles can be co-deposited to realize the controlled release of functional molecules [221,222]. For instance, Cheng et al. loaded vancomycin into the silk fibroin (SF) nanospheres via electrostatic and hydrophobic interactions, and then deposited nanospheres on Ti surfaces by oxidation of water near the anode to neutralize the negatively charged SF nanospheres to induce irreversible aggregation and deposition, as shown in Fig. 9D [222]. The drug-loaded coating effectively inhibited *S. aureus* for at least 21 days, but it did not show cytotoxic to fibroblasts. In short, the EPD process has gained considerable interest for fabrication of functional coatings on Ti surfaces in 2-D and 3-D substrates, because of the simple and easy-to-use properties.

2.3.4. Biochemical methods

2.3.4.1. Chemical covalent immobilization of biomolecules. Chemical covalent immobilization of biomolecules usually binds selective biomolecules onto the surfaces by chemical grafting approach to realize specific cell or tissue response [18,36]. In contrast to the non-covalent methods (physical adsorption or entrapment), such a covalent

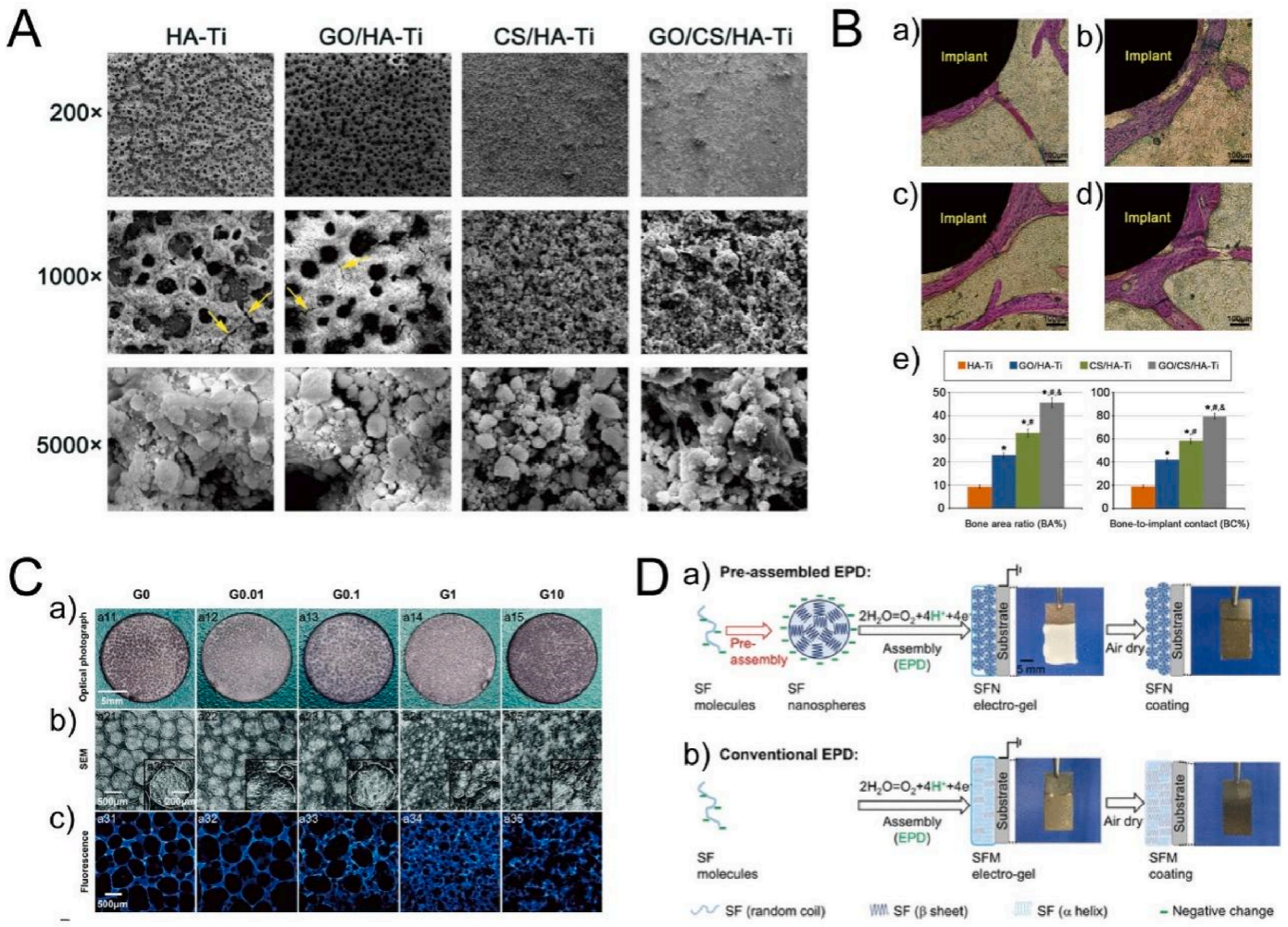

Fig. 9. (A) SEM images of HA-Ti, GO/HA-Ti, CS/HA-Ti, and GO/CS/HA-Ti prepared by electrophoretic deposition [209]. (B) Stained histological sections of the proximal tibiae (a: HA-Ti; b: GO/HA-Ti; c: CS/HA-Ti; d: GO/CS/HA-Ti) and the quantitative results (e) after implantation for 12 weeks [209]. Reprinted with permission from Ref. [209]. (C) Topography of chitosan/gelatin coating including (a) optical photographs, (b) SEM images and (c) fluorescence images [217]. Reprinted with permission from Ref. [217]. (D) Assembly mechanism of (a) pre-assembly and (b) conventional assembly of SF EPD coatings [222]. Reprinted with permission from Ref. [222].

immobilization method has some advantages, such as high specificity, low competitive replacement and the relatively low-loss rates [18]. It has been noted that the amount grafting on the surfaces should exceed the threshold levels to induce cellular activity. The Ti metal does not possess surface functional groups (e.g., -NH_2 and -COOH) required for the covalent immobilization of biomolecules by most of the binding strategies, but the passive oxide films on the metals can form surface hydroxyl groups upon immersion in aqueous environments, which provide potential binding sites for covalent attachment of a linker molecule for further bio-functionalization. In general, a pre-treatment step (e.g., acid or alkali immersion and O_2 plasma) is needed to enrich the surface hydroxyl groups for the dehydration/condensation reactions to covalently attach the linker molecules, which are either synthetic compounds, including silane and polyethylene glycol, or biologically-derived compounds, including heparin, dopamine and chitosan [18]. By reacting with the linker molecules, biomolecules, such as peptides and proteins, are immobilized on the Ti surface to promote the bioactivity.

Silanization is a most widely-used approach to link the surface with biomolecules. Typically, silane undergoes a condensation reaction between head groups of silane and -OH groups on the surface, leading to formation of Si-O bonding on the interface [223]. Because silane can be chemically tailored either on the head groups or on the alkyl tail, many types of functional groups on the tail (e.g., -NH_2 and -SH) can be introduced onto the Ti surface by using various kinds of coupling reagents for subsequent modification, such as aminosilanes, mercaptosilanes and glycidoxysilanes [18]. Biomolecules, such as peptides [224–226], collagen [227], BMP-2 [228] or ulvan polysaccharides [229], can be immobilized on the surface by one- or multiple-step post reactions with the tail group of silane to realize the improved osteoblast or stem cell activity and the reduced infection both in vitro and in vivo. As to the one-step post coupling, biomolecules are facilely attached to the silanized surface. For instance, the Ti surface was first modified with a silane reagent with alkynyl groups, and then conjugated with a fusion peptide (FP) containing antibacterial sequence and angiogenic sequence via Cu(I)-catalyzed azide–alkyne cycloaddition. Such a FP-engineered implant can kill up to 99.63% of *S. aureus*, and simultaneously enhance vascularization and osseointegration both in infection and non-infection bone-defect models (Fig. 10A and B) [230]. As to the multiple-step post coupling, one typical processing is the surface-initiated atom transfer radical polymerization (SI-ATRP) to introduce polymers on the surface for subsequent immobilization, where silanes containing halogen groups can act as initiators. For instance, Zhang et al. first added trichlorosilane on the hydroxylated Ti surface as an initiator to conduct the surface-initiated polymerization of methacrylic acid sodium salt (MAAS), and then conjugated sericin to the

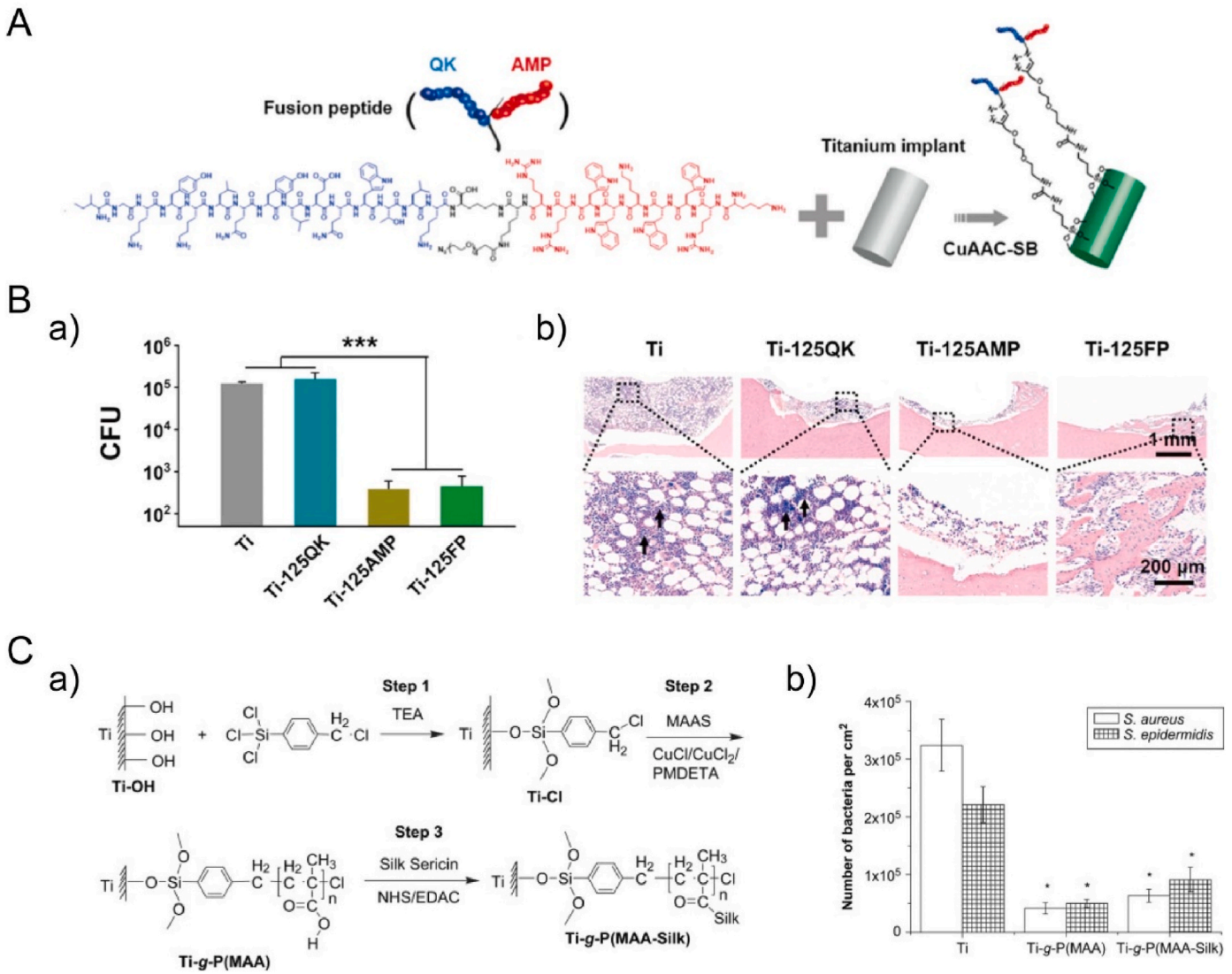

Fig. 10. (A) Schematic diagram of engineering titanium with fusion peptide (FP) by CuAAC-SB method [230]. (B) In vivo assay of implants with infection model: (a) antimicrobial activity against *S. aureus* by the agar plate method, and (b) H&E staining images of the decalcified bone sections after implantation for 7 days [230]. Reprinted with permission from Ref. [230]. (C) Schematic diagram (a) of the processes including silanization of the Ti-OH surface, surface-initiated ATRP of MAAS chains, and immobilization of silk sericin on the Ti surface. (b) The quantitative results of adherent of *S. aureus* and *S. epidermidis* cells on the different Ti substrates [231]. Reprinted with permission from Ref. [231].

pendant carboxyl groups of poly-(methacrylic acid) (P(MAA)) via carbodiimide chemistry, as shown in Fig. 10C [231]. The P(MAA) brushes obviously inhibited bacterial adhesion (*Staphylococcus aureus* and *Staphylococcus epidermidis*), but the silk sericin significantly enhanced attachment, proliferation, and ALP activity of MC3T3-E1 cells. Similar SI-ATRP was performed via using the silanes containing halogen groups including (6-(2-bromo-2-methyl)propionyloxy) hexyldimethylchlorosilane) [232] or 12-(2-bromoisobutyramido)dodecanoic acid [233] as an initiator, which was followed by the conjugation of ECM-derived peptide or osteoblast-binding motif peptide, respectively. It is noteworthy that the incorporation of peptide onto Ti surfaces with a polymer intermediate layer significantly improved cell adhesion proliferation and osteogenic mineralization.

Mussel-inspired dopamine and its analogues are another broadly adopted molecules to connect the surface with biomolecules. The mechanism of dopamine attached to Ti surface, which is still under exploration, is generally considered that the catechol groups react with hydroxyl groups on the TiO_2, resulting in bridged bidentate bonding [234]. Similar to silanes, biomolecules are immobilized on the surface by one- or multiple-step post reactions with the tail group of dopamine [235]. As to the one-step post coupling, peptides, proteins, polysaccharide and drugs are able to attach to the Ti surface via direct conjugation with the dopamine-based linker molecules. For instance, Wang et al. first pretreated Ti6Al4V surface with polydopamine (PDA) and then deposited fibrinogen (Fg), which was more stable than the physically adsorbed Fg (Ti-Fg) [236]. The Ti-PDA-Fg surface can greatly weaken soft tissue response and strengthen angiogenesis in subcutaneous parts of Sprague-Dawley (SD) rats, compared with Ti-Fg and Ti-PDA surfaces. The further implantation in percutaneous tibial parts indicated the Ti-PDA-Fg surface enhanced bone regeneration and inhibited epithelial downgrowth, maybe because Fg positively regulated hemostasis, inflammation and wound repair. As to the multiple-step post coupling, some other components with bioactivity can be used to link the biomolecules and dopamine-functionalized surfaces to achieve a multi-functional strategy. For example, oxidized dextran [237] and carboxymethyl chitosan [238], were used to bridge the BMP-2 and dopamine-functionalized surface to realize improved osteoblast response and reduced infection together. Because conventional chemical conjugation generally involves tedious chemical reactions and sophisticated technologies that require more than one reaction step for

surface-initiated immobilization, one-step modification of Ti surfaces with similar "grafting to" strategy has been developed to reduce reaction procedures and improve immobilization efficiency on surfaces. Recently, synthetic peptides that contain 3,4-Dihydroxy-L-phenylalanine (DOPA) have been widely investigated in this way [239–242]. The catecholic DOPA units can adhere the substrates to realize one-step modification if the bioactive peptides were conjugated with DOPA in advance. For instance, Pan et al. added mussel-derived bioactive peptides containing DOPA units, integrin-targeted sequence (RGD) or/and osteogenic growth sequence (OGP), to Ti surface by the catechol/TiO_2 coordinative interactions [239], as shown in Fig. 11A and B. The single- or co-existence of the two kinds of peptides can obviously enhance the adhesion, proliferation and differentiation of human bone marrow-derived mesenchymal stem cells. After implantation in the femoral condyles of rabbits for 4 weeks, the OGP/RGD (3:1) dual-treated Ti screws displayed 1.5-fold improvement in bone-implant contact (73.3 ± 8.9%), compared with the ones attached with single peptide (46.9 ± 6.7% and 47.2 ± 7.5% for the RGD-treated and OGP-treated screws, respectively), and even more than 2-fold improvement compared with the untreated screws (30.5 ± 5.7%). Furthermore, the dual-treated Ti screws presented the highest average value (155.3 ± 18.5 N) of maximum pull-out force, nearly 2-fold improvement compared with that of the untreated ones (79.7 ± 10.9 N), which suggested an enhanced synergism on osteogenicity and osseointegration.

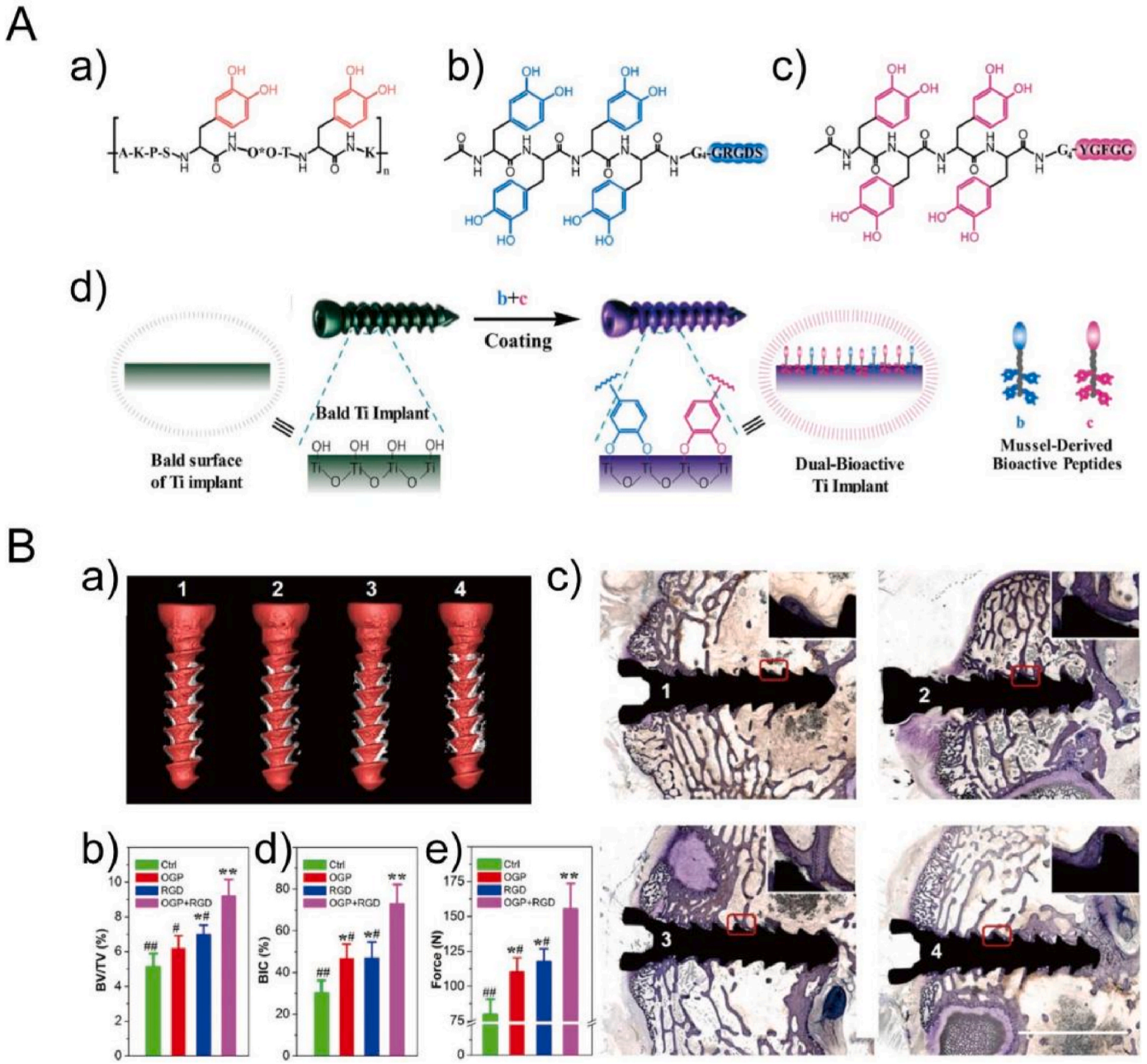

Fig. 11. (A) Structural formula (a) of mussel foot proteins (Mfp-1). (b and c) The biomimicry of mussel-derived peptides $(DOPA)_4$-G_4-GRGDS and $(DOPA)_4$-G_4-YGFGG. (d) Schematic diagram of the surface dual-biomodification of Ti implants by using the mussel-derived peptides b and c [239]. (B) The assay of osteogenesis and mechanical stability in vivo: (a) Micro-CT 3D reconstructed images, (b) quantitative evaluations of the percentage bone volume (BV) among tissue volume (TV) (BV/TV), (c) histological images of Ti screws with toluidine blue stain, (d) average histomorphometric values of bone-implant contact (BIC), and (e) results of biomechanical pull-out testing. Implant NO. 1–4 refer to untreated (control), OGP-treated, RGD-treated, and OGP/RGD (3:1) dual-treated Ti screws, respectively [239]. Reprinted with permission from Ref. [239].

Some other linking methods have also been well developed. PEGylation with terminally-modified PEG molecules has previously been explored to immobilize peptides or proteins, but the main application is to endow the surface with antifouling property by the hydrophilic nature of PEG [9,243,244]. In addition, phosphonic acids have been used as grafting groups as well, because it forms bidentate and tridentate phosphonate species by condensation and coordination of phosphonate coupling reagents with the hydroxyl groups on the oxide surface [245]. The multi-functional groups on the tail of phosphonate-based linkers can conjugate with biomolecules to obtain a versatile Ti platform with improved osteogenesis and decreased bacterial adhesion [246–249]. Because chemical covalent immobilization generally cannot greatly alter the substrate morphology, in some cases, this method is combined with other treatments to further improve the bioactivity of the original substrates, such as anodization [250], sandblasting/acid attacking (SLA) [251], and alkaline etching [252].

2.3.4.2. Layer-by-layer assembly. Layer-by-layer (LBL) assembly depends on a multitude of forces existing between two or more various materials that hold complementary interactions [253,254]. Typically, the LbL assembly is conducted by electrostatic interactions in which a charged material is first adsorbed onto a substrate, and after careful washing, an oppositely charged material is subsequently attracted on the first layer [255]. Such processing forms a single bi-layer, and it can be cycled to obtain a multilayer film of desired structure and thickness. Beyond electrostatic assembly, preparing multilayer films may result from short-range interactions, such as hydrogen bonding and van der Waals forces [253]. Many types of charged objectives can be coated onto the substrates, such as polymers, colloids, nanoparticles, biomolecules and even cells [254]. The widespread application of LbL assembly has produced several technologies to satisfy the various processing requirements related to the substrates (e.g., porous membranes, nanoparticles and solid plates), such as dipping, spinning, spraying, electrodeposition, centrifugation and immobilization [254,255]. The assembly technologies heavily affect the process parameters (e.g., time and scalability) and the physicochemical characteristics of the films (e.g., thickness and homogeneity) [255].

LbL assembly has been widely used to integrate Ti surfaces with versatile functions, such as osteogenesis, angiogenesis and antibacterial property. Polyelectrolytes, such as chitosan, hyaluronic acid and gelatin, are commonly applied as the components to construct the multilayered platforms. For instance, hyaluronic acid (HA) and chitosan (CH) were alternatively deposited on the Ti surface to form polyelectrolyte multilayers (PEMs), and arginine-glycine-aspartic acid (RGD) peptide was then immobilized on the outermost layer [256]. Such a surface not only significantly reduced *S. aureus* attachment, but also enhanced the proliferation and alkaline phosphatase activity of MC3T3-E1 cells by 100–200% over that of pristine Ti surface. Because of the unique processing, it is ready to incorporate bioactive components during the LBL deposition, such as peptides, proteins and drugs. For instance, Chen et al. first conjugated chitosan (Chi) with β-cyclodextrin (β-CD) as a reservoir of pitavastatin (PTT) to form Chi-β-CD@PTT, and then assembled the multilayered structure (LBL@PTT) comprised of Chi-β-CD@PTT and gelatin (Gel) [257]. The released pitavastatin improved osteogenic differentiation of mesenchymal stem cells (MSCs) and angiogenic capacity of endothelial cells (ECs). Additionally, the LBL@PTT might indirectly mediate the paracrine signaling that induced crosstalk effect between MSCs and ECs, which enhanced the angiogenic gene expression (VEGF, PDGF-bb, SDF-1α, and CXCR4) in MSCs and promoted the osteogenic gene expression (BMP-2, BMP-4, Wnt3a and Wnt5a) in ECs, respectively. The subcutaneous and femur implantation suggested that the maturity degree of bone for LBL@PTT surface was 34.1 ± 8.8%, much higher than the values of LBL (26.0 ± 7.7%) and pristine Ti (14.3 ± 3.8%) surfaces. In addition, nanomaterials with much larger sizes than biomolecules, including CaP-based or drug-loaded nanoparticles, are easily loaded via this technique during the preparation as well. For example, hydroxyapatite nanofibers [258], raloxifene-loaded MOFs [259] and β-estradiol loaded mesoporous silica nanoparticles [260], have been widely exploited to increase osteogenesis. Xing et al. first prepared a siRNA-decorated gold nanoparticles with polyelectrolyte multilayer coatings composed of chitosan (Chi) and gelatin (Gel), (AuNP@siRNA-*CTSK*)$_{cg}$, and then embedded it into the multilayers of Chi and Gel on Ti surface, [(AuNP@siRNA-CTSK)$_{cg}$]$_{CG}$ [261], as shown in Fig. 12. The release of the siRNA that targeted the regulation of cathepsin K (CTSK) expressed in osteoclasts obviously enhanced the behaviors of osteogenesis-related gene expressions and the key vascular regeneration factors in vitro, by regulating the CTSK-PDGF-BB-bone remodeling pathways, and it even significantly improved the osteogenesis and angiogenesis when implanted in ovariectomized rat and comprehensive beagle dogs.

LbL assembly usually integrates with other methods, such as acid etching [262], plasma spraying [263], and EPD [264], to improve the bioactivity of Ti surfaces. For instance, TiO_2 nanotube arrays produced by anodization have been widely used as nanoreservoirs for loading proteins or drugs, but in some cases, the release kinetics are unsatisfactory. Hence, LBL multilayers are prepared to cover the nanotube arrays to control the release and maintain the bioactivity of loaded molecules. The drugs with either large molecular weight (e.g., BMP-2 [265]) or small molecular weight (e.g., deferoxamine [266]) have been loaded into the TiO_2 nanotubes, where the outer surface was covered by multilayers composed of one or two biocompatible polymers (e.g., PLGA and Chi/Gel). Notably, such a construction can efficiently reduce the burst release and improve the antibacterial, anti-inflammatory and osteoblast activities. Briefly, LBL technique can realize high degrees of functionalization and diversity with superior performance and flexibility.

2.4. Micro/nanostructured surfaces

From the bionic viewpoint, it is better to construct a hierarchical hybrid micro/nanostructured surface on Ti implants to regulate osteoblast response in various scales. Recently, such a combination of micro- and nano-sized features has become a most promising strategy. It usually requires combined methods of the above techniques of the micro- and nano-scale morphology creation, such as acid etching and anodization [267], plasma spraying and anodization [268], acid etching and cathode sputtering [269], sandblasting and alkaline treatment [270], sandblasting/acid etching and calcination [271], etc. For instance, Zhao et al. prepared a hybrid micropitted/nanotubular surfaces by acid etching and anodization, and it is suggested that multiple functions of primary rat calvarial osteoblasts, including adhesion, proliferation, differentiation and mineralization, were somewhat similar or promoted compared with cells on micropitted and smooth surfaces [267]. Gittens et al. used a calcination treatment to add nanoscale protuberances to a micro-/submicro-scale surface via sandblasting/acid etching [271], as shown in Fig. 13B. Such nano-modified surfaces obviously improved differentiation and local factor production of MG63 cells, but depressed proliferation. Similar elevated regulations of cell functions were observed on micropitted/nanonetwork surface [272], and micropitted/nanospongelike surface [273]. In addition, some studies have tried to vary either the nanoscale or microscale features of the hierarchical surfaces and to investigate the corresponding osteogenic response because cells are sensitive to the surface scale dimensions. As to nanoscale feature regulation, TiO_2 nanonodules with different sizes (100, 300 and 500 nm) were sputter-deposited onto a micropitted Ti surface created via acid etching, producing a micropit-and-nanonodule hybrid morphology, as shown in Fig. 13A [269]. Such nanonodule-in-micropit surfaces all selectively improved both proliferation and differentiation of osteoblast (rat bone marrow-derived) but not fibroblast activities. The strength of bone-implant integration further showed more than two times greater for all the hybrid surface than for the micropitted surface.

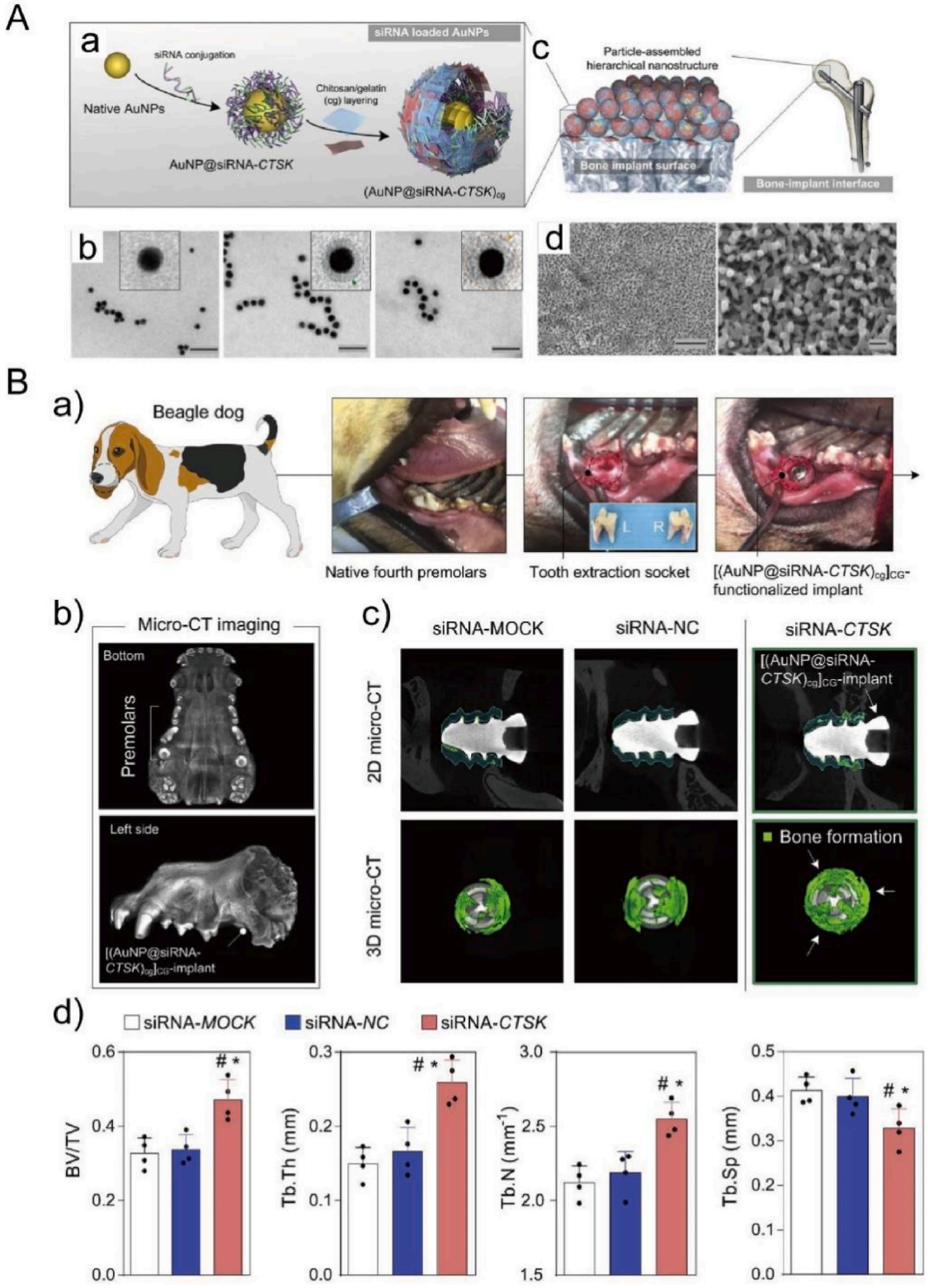

Fig. 12. (A) Particle-based nanostructured implant coatings: (a) Synthesis of siRNA-CTSK-loaded AuNPs by layer-by-layer assembly of chitosan and gelatin (cg) multilayers. (b) TEM images of monodispersed AuNPs, siRNA-loaded AuNPs, and $(AuNP@siRNACTSK)_{cg}$. (c) Preparation of $[(AuNP@siRNA\text{-}CTSK)_{cg}]_{CG}$ coatings by the assembly of $(AuNP@siRNA\text{-}CTSK)_{cg}$ on the implant surface. (d) SEM images of the Ti implant surface functionalized with $[(AuNP@siRNA\text{-}CTSK)_{cg}]_{CG}$ [261]. (B) The application of Ti surface functionalized with $[(AuNP@siRNA\text{-}CTSK)_{cg}]_{CG}$ as dental implants in a comprehensive beagle dog model. (a) The implantation of various Ti materials into the tooth extraction sockets. (b) Micro-CT images of dog maxillary bone after three months. (c) Micro-CT analysis of new bone formation around the implants after 12 weeks. (d) The quantitative data from the micro-CT analysis, including BV/TV, Tb.Th., Tb.N. (trabecular number), and Tb.Sp. (trabecular separation) [261]. Reprinted with permission from Ref. [261].

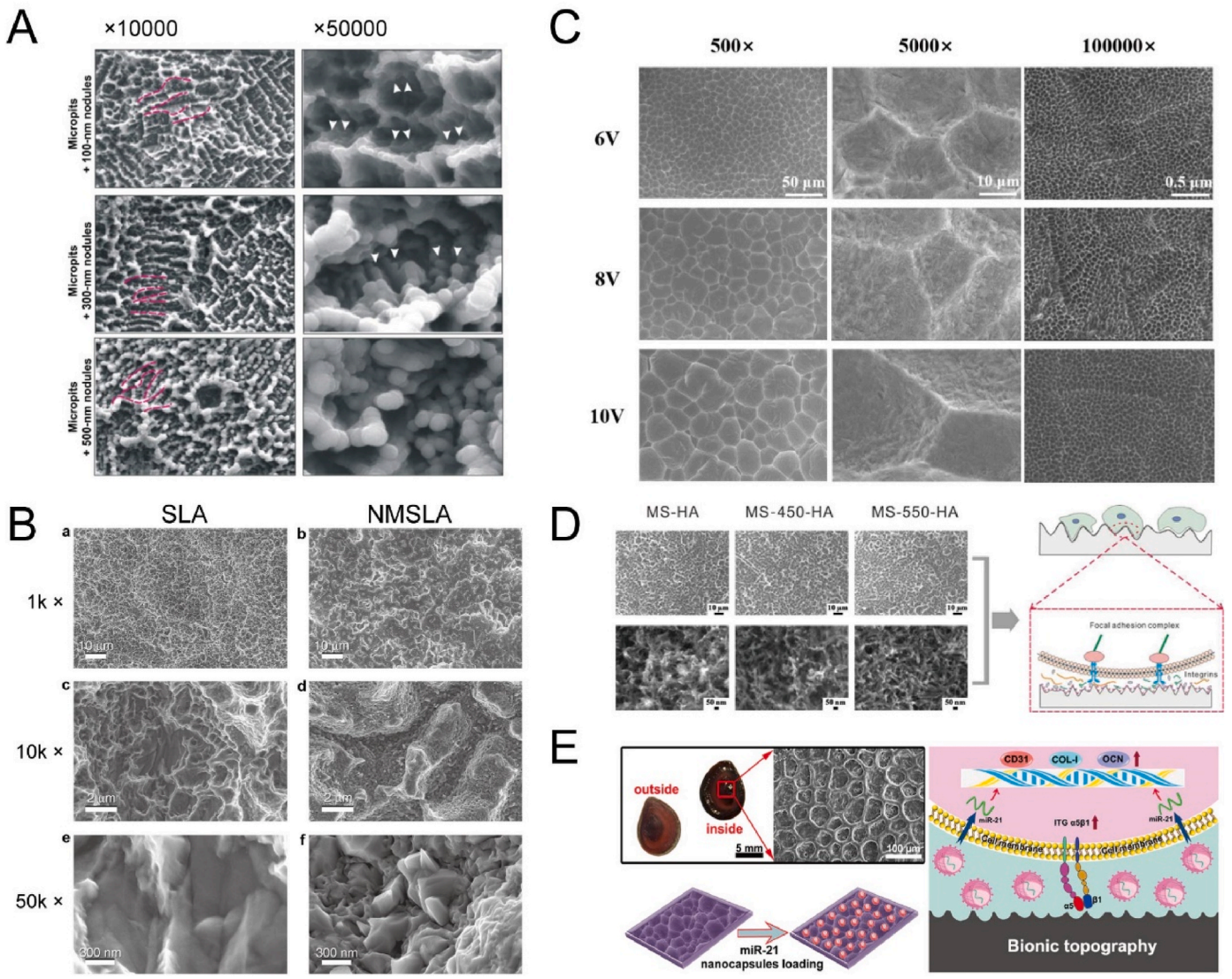

Fig. 13. (A) SEM images of micro-nano-hybrid topography created by deposition of TiO_2 nanonodules (100, 300 and 500 nm) onto the acid-etched (micropit) surface [269]. Reprinted with permission from Ref. [269]. (B) SEM images of SLA samples (a,c,e), and of NMSLA samples (b,d,f) generated via oxidation at 740 °C for 90 min [271]. Reprinted with permission from Ref. [271]. (C) SEM images of the prepared ordered micro-nano hierarchical Ti surfaces with varying micro-scaled pits [274]. Reprinted with permission from Ref. [274]. (D) SEM images of micropitted/nanospongelike TiO_2 surfaces with different crystalline phases after hydroxyapatite modification [283]. Reprinted with permission from Ref. [283]. (E) Schematic diagram of modification of Ti surfaces with micro/nanoscale bionic morphology and miR-21 nanocapsules coating [284]. Reprinted with permission from Ref. [284].

Amongst them, the surface of micropits with 300-nm nodules displayed the most pronounced biological effects, probably because the 300-nm nodules provided optimal inter-structure space, surface area and roughness for efficient osteoblast attachment and behaviors. As to microscale feature regulation, Zhang et al. first prepared various bowl-shaped microholes on Ti surface by electrochemical etching with average sizes ranging from 12.01 μm to 36.34 μm, and then similar sub-micro and nano structures were further introduced by chemical etching and electrochemical anodization without altering the original microholes (Fig. 13C) [274]. It is noteworthy that smaller microholes with lower roughness of the hierarchical micro/nanostructured surfaces benefitted faster cell propagation. However, larger cell-match-size microholes with higher roughness significantly enhanced osteogenic-related gene expressions despite of slight delay of cell growth, The reason may be related to the factor that the hierarchical morphology with larger microholes have a stronger effect on activating Wnt/β-catenin pathway for osteoblast differentiation. In short, a positive effect of the hierarchical hybrid surfaces is observed in all presented papers, even though some specific expressions of osteogenic activities are different.

Beyond positive effects on osteoblast behaviors, micro/nano-structured titania surfaces also obviously reduce inflammation and osteoclastogenesis [275,276], and even promote osteogenesis under oxidative stress conditions such as osteoporosis, and diabetes [276,277]. For instance, micro/nano-scale (MNS) titania with fiber-like network on Ti surface suppressed the expression of pro-inflammatory cytokines (IL1β, IL-6, and TNF-α) and activated autophagy-related genes, and thus downregulated inflammatory response [275]. Meanwhile, it enhanced the expression of osteogenic/angiogenic markers (VEGFA, RUNX2, TGF-β1, and BMP-2) of macrophages (MΦs). Additionally, bone marrow stromal cells (BMSCs) on the MNS surface induced an obvious immunomodulatory effect on MΦs by reducing IL-6 expression in inflammation-related signaling pathways. Thereafter, MNS showed a superior osteoimmune microenvironment to facilitate osteogenesis and angiogenesis via the crosstalk of multiple signaling pathways in vivo, which presented much better bone-implant contact and osteocyte

accumulation compared with single nanofiber structure (NS) and pristine Ti surfaces. In addition, the hierarchical micro/nanostructured surfaces can enhance osseointegration under osteoporotic conditions. Dai et al. prepared a micro/sub-micro-textured surface (EE-CE) by combined electrochemical etching and acid etching, and a sub-micro-roughened surface (CE) by only acid etching, respectively [276]. The EE-CE surface can inhibit pro-inflammatory reactions of M1 macrophage by suppressing TLR2/NF-κB signaling pathway, with downregulated expression of M1 markers (iNOS, CCR7 and TNF-α), and reduce osteoclast formation with low expression of the osteoclastogenesis regulator NFATc-1. Further, the EE-CE surface showed much higher values of bone-implant-contact (BIC) and bone volume around implants than the values from CE surface in osteoporotic rats. Thereafter, the hierarchical surface greatly mitigated inflammatory microenvironment, inhibited osteoclastogenesis, and thereby activated implant-bone integration in osteoporotic models.

It is still necessary to optimize surface components to tailor the micro/nanostructured surfaces because of the bioinert property of TiO_2, although such hierarchical hybrid structures provide promising strategies. As a result, some bioactive compounds are further added to enrich the biocompatibility of the micro/nanostructured surfaces. Normally, inorganic ions [278–280], metal nanoparticles [281], calcium phosphate compounds [282,283], and nucleic acids [284] were additionally deposited to improve bacterial resistance, angiogenesis and osteogenesis. As to the inorganic ions, the release of bio-functional ions, such as Mg^{2+} [278], Sr^{2+} [280], and Fe^{3+} [279], obviously influences cell activities and tissue response. For example, Sr-incorporated micro/-nanostructured surface (SLA-Sr) not only improved proliferation and differentiation of human mandible bone marrow stromal cells (hBMSCs), but also enhanced angiogenic capacity of human umbilical vein endothelial cells (HUVECs) by elevated expression of HIF-1α and Erk1/2 phosphorylation [280]. The in vivo data suggested that the SLA-Sr significantly enhanced early vascularized bone integration with increased type H vessel formation, with a much higher vessel area than that of without Sr-incorporated SLA surface, because of the synergistic effect of the micro/nanoscale topography and the release of Sr^{2+}. In the case of metal nanoparticles, Ag NPs were incorporated deeply into TiO_2 nanotubes prepared on the sandblasted and etched (SLA) Ti surface to realize both the “release bactericidal” and “contact bactericidal” effects, but without toxicity towards MC3T3-E1 cells [281]. Additionally, because of the bioactive and osteoconductive properties, CaP compounds, including OCP [282], and HA [283], are also applied. Jiang et al. first prepared micropitted/nanospongelike TiO_2 surfaces with different crystalline phases, and then added HA nanorods by a spin-assisted LBL assembly method [283], as shown in Fig. 13D. Interestingly, the added HA component greatly stimulated differentiation and mineralization of MCT3-E1 cells, but it cannot obviously influence the trend of cell proliferation caused by the different crystalline phases of the initial micro/nanostructured TiO_2 surfaces. Recently, biological-derived nucleic acids, such as MicroRNAs, were used to modify the surface as well [284]. Geng et al. immobilized miR-21 nanocapsules on the micro/nanoscale roughed surface, and observed that the combination of micro/nanoscale morphology and miR-21 coating synergistically improved MG63 cell adhesion and MSC angiogenic differentiation in vitro and promoted blood vessel growth and bone formation after implantation into the distal femur and tibia of New Zealand White rabbits [284], as shown in Fig. 13E.

The construction of a hierarchical hybrid structure on Ti surfaces is of great interest, because the interaction that occurs at the bone-implant interface with various scales mainly influences the long-term outcome. The combination of both micro- and nano-scale roughness provides feature sizes comparable to the structure of natural extracellular matrix, which positively regulates cell functions by acting on the protein and cell membrane receptors from multiple scales. More importantly, during bone remolding, resorption lacunae created by osteoclast possesses a hierarchical structural complexity. Generally, the resorption pits contain microscale pits (~100 μm in diameter and ~50 μm in depth [285,286]), submicro-scale features by the irregular acid-dissolution at the ruffled border of the osteoclast [287,288], and nanoscale roughness formed by undigested collagen fibrils on the surface [289,290]. Such a multiple-scale bone surface is sequentially for osteoblast to differentiate and secrete molecules that finally form new bone [291]. Hence, the micro/nanostructured modification, one of the most promising ways, is able to synergistically improve cell behaviors from various dimensions and to satisfy the requirements of bone-implant interaction. Additionally, the hierarchical hybrid structure may be more easily to combine or anchor other functional molecules, nanoparticles and coatings to fulfil multiple functions including bacterial resistance, angiogenesis and osteogenesis, because of the larger specific surface area and wider range of pore sizes, which indicates great possibility to reduce the healing period and improve the quality of implants in near future.

3. Dynamic responsive surfaces

Beyond control of materials with specific structure and size scales, biomaterials are evolving from a traditional static design to those having dynamic properties [292]. Historically, orthopedic implants tend to provide consistent functions, including mechanical support and bone integration. Such approaches have induced the successful application of Ti implants in clinic; however, advances in materials design, dynamic chemistry and nanomedicines allow us to introduce dynamic responsive properties into surface modification, because the implants need to respond to cues characteristic of specific cells and tissues spatiotemporally [293]. Spatial and temporal regulation of biomaterials provides unique avenues to recapitulate the dynamic features of the microenvironments in biological tissues, which plays a critical role in modulating cell behaviors and functions [294]. It is noted that dynamic biomaterials have been designed in response to a diverse set of stimuli. According to the stimuli sources, the signals can be divided into environmental triggers and physiological triggers [292,295]. The environmental triggers are introduced as external stimuli typically absent from living systems, which include the signal from light, electrical field, ultrasound or magnetic/electromagnetic field etc [292]. Under this mode, materials can be modulated with spatial and temporal control, even in four dimensions. Alternatively, as to physiological systems, it is generally triggered by pH, enzyme, redox conditions or hydrolysis [296]. Materials autonomously responding to cues show the ability to communicate and interact with cells at bodily locations, which can enrich bioresponsive behaviors for material design. In short, dynamic responsive materials greatly satisfy the requirement of the development of medical devices, with the aim to improve the biocompatibility on demand (e.g., osseointegration, antibacterial and anti-inflammation capability). Many efforts have been made to construct responsive surfaces on Ti substrates, which can modulate temporal signals to cells, reduce infection by controlled drug release or understand complex cellular processes, beyond control of Ti surfaces with specific morphology, wettability and composition. In this section, dynamic responsive surfaces on Ti implants are discussed, and such surfaces are grouped into eight types based on the triggers, namely light, X-ray, electrical field, piezoelectricity, ultrasound, magnetic/electromagnetic field, pH and enzyme.

3.1. Light

Light that functions as a type of non-invasive physical signal with precise control in microscale dimension [297], can spatiotemporally modulate Ti surfaces to induce cell or tissue behaviors because of the photocatalytic activity of TiO_2 and other added photo-responsive components. In general, the light is used to regulate the drug-release kinetics, improve the antibacterial ability, or to conduct cell and tissue repair on Ti surfaces. As stated above, TiO_2 TNTs can be served as drug carriers, however, the burst release usually occurs. As a strategy, hydrophobic molecules are used to achieve a “smart” platform. Among one

of the early studies, horseradish peroxidase was linked onto the lower part of TNTs via APTES/vitamin C monolayer linker, and octadecylphosphonic acid (ODPA) was for nanotube capping, forming an amphiphilic drug release platform [298]. Once exposure to UV-light irradiation, the ODPA and APTES linkers were decomposed by the produced peroxides and hydroxyl radicals due to the photocatalytic nature of TiO_2, leading to the controlled release of enzyme molecules. Because of the inherent limitations of UV wavelength, such as poor tissue penetration, some noble metals (e.g., Au and Ag) producing surface plasmon resonance (SPR) were deposited on TiO_2 TNTs to allow drug release upon using visible or infrared light [299,300]. The same group further improved the release kinetics of ampicillin from the amphiphilic TNT platform by using the (Au-SPR)-induced photocatalytic scission of the hydrophobic chain of ODPA cap and the drug-grafting linker in the hydrophilic bottom layer, under the visible light illumination (Fig. 14A and B) [299]. Beyond regulation of drug release, SPR-based hybrid surfaces can be directly used to achieve rapid biofilm elimination but without cytotoxicity towards tissues, namely photodynamic therapy with the production of reactive oxygen species (ROS). Ag NPs-based hybrid coatings, including graphene oxide/Ag/collagen [301] and tannic acid/Fe^{3+}/Ag [302] coatings, prepared on Ti surfaces showed an antibacterial efficiency of higher than 94% against both *Escherichia coli* and *Staphylococcus aureus*, under the synergistic action of visible-light-inspired photodynamic therapy and the innate antibacterial ability of Ag^{+}. In addition to SPR, heterostructures have also been explored, such as TiO_2-Bi_2WO_6 [303],

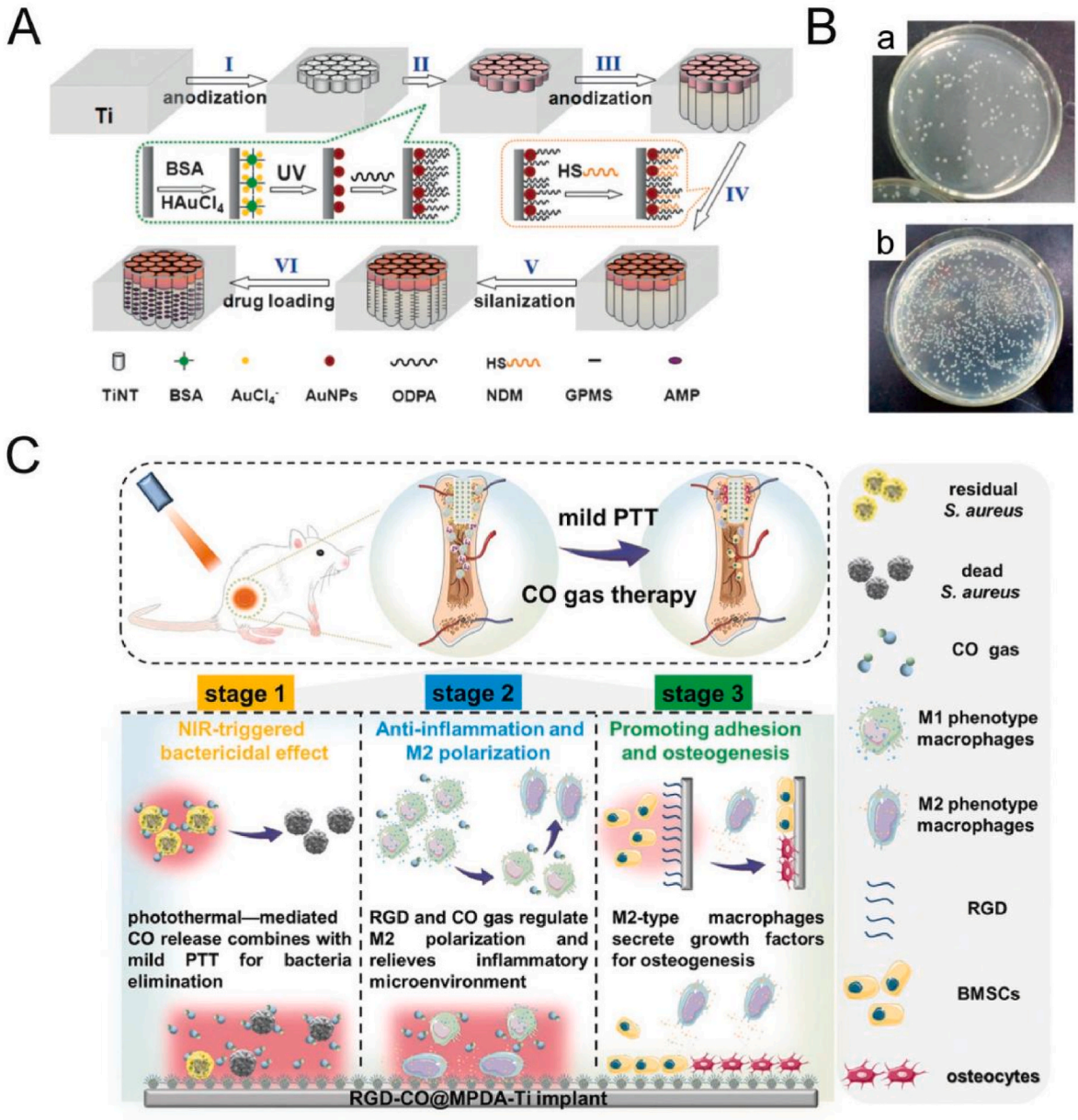

Fig. 14. (A) Preparation of TiNTs with visible-light-controlled drug-release property: (I) first anodization to prepare TiNTs, (II) deposition of Au NPs and hydrophobic monolayer to TiNTs, (III) second anodization for drug storage, (IV) link of hydrophobic monolayer to Au NPs by mercaptan, (V) silanization of lower nanotube layer with GPMS, and (VI) AMP loaded by GPMS linker [299].
(B) Optic images of bactericidal assay from drug-loaded amphiphilic TiNTs with (a) or without (b) treatment by visible light irradiation [299]. Reprinted with permission from Ref. [299].
(C) Schematic diagram of RGD-CO@MPDA-Ti surface for improving infected bone repair by CO-potentiated antibiosis, CO-induced anti-inflammation, and the cascade of immunomodulation-osteogenic differentiation [314]. Reprinted with permission from Ref. [314].

MnO_2/g-C_3N_4/Ti [304], and TiO_2/AgNPs/g-C_3N_4 [305]. For instance, the addition of MnO_2 to the g-C_3N_4 not only improved the photoconversion efficiency by 21.11% under visible-light irradiation, but also helped the oxidation of glutathione (GSH) to glutathione disulfide (GSSG) via thiol-disulfide that assisted oxidative stress in bacteria [304]. Hence, this coating displayed a high antibacterial efficiency but little influence on osteoblast viability, with an efficiency of 99.96% and 99.26% against *S. aureus* and *E. coli*, respectively.

Despite of great potential for clinical application, single mode of photodynamic action has some disadvantages that include short life span and limited diffusion distance [306]. Hence, other studies have focused on deposition of hybrid compounds with photodynamic and photothermal properties onto Ti surfaces to achieve synergistic systems, such as Bi_2S_3@Ag_3PO_4/Ti [307], red phosphorus/ZnO/Ti [308], chitosan/Ag/MoS_2-Ti [309], and Ti-polydopamine nanoparticles/indocyanine green/RGD [310]. In one case, a red-phosphorus–IR780–RGDC coating was prepared on the Ti surface, with red phosphorus (RP) as a photothermal agent and IR780 as a photosensitizer [311]. Under NIR (808 nm) light irradiation, the increment of temperature (up to 50 °C) and the production of singlet oxygen ($^1O_2$) caused the biofilm eradication of *Staphylococcus aureus*, with antibacterial efficiency of 89.3% in vitro and 96.2% in vivo,

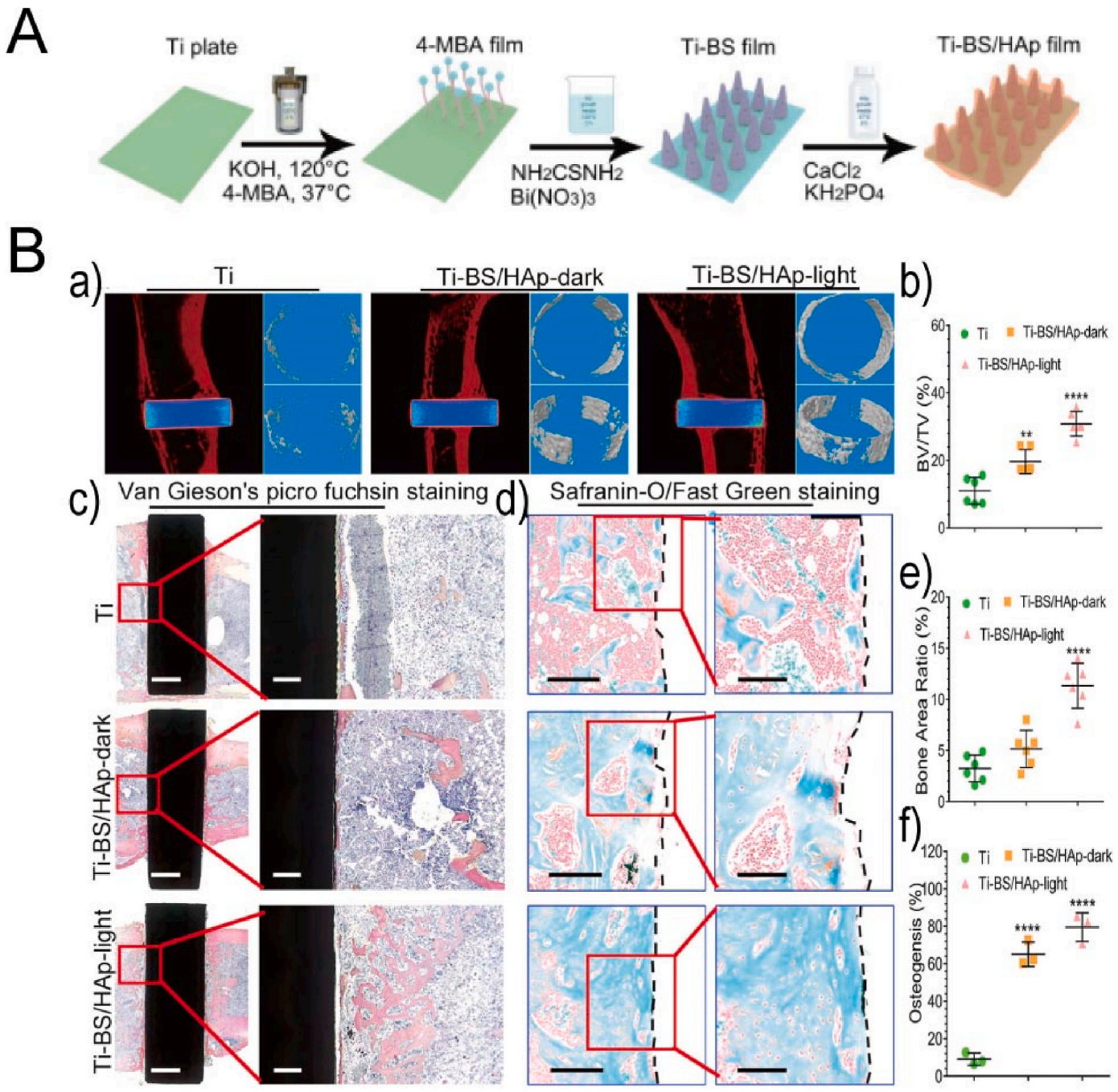

Fig. 15. (A) Schematic diagram of preparation process of Ti-BS and Ti-BS/HAp [315]. (B) Evaluation of in vivo bone formation of Ti, Ti-BS/HAp-dark, and Ti-BS/HAp-light implants after 4 weeks: (a) Micro-CT images of bone formation, (b) quantitative results by measurement of micro-CT 3D images, (c) Van Gieson's picrofuchsin staining, (d) Safranin-O/Fast Green staining, (e) histomorphometric results of bone area rate, and (f) histomorphometric results of osteogenesis [315]. Reprinted with permission from Ref. [315].

respectively. Similarly, a MoS_2-IR780-RGDC phototherapeutic system was developed as well [312]. Beyond the combination of photodynamic and photothermal therapy, other two synergetic modes were also developed, including photothermal and gas therapy [313,314]. The Ti surface was first integrated with a CO nanogenerator layer which contained mesoporous polydopamine (MPDA) nanoparticles loaded with a typical thermosensitive CO donor of $Fe_3(CO)_{12}$, and then covalently immobilized with RGD polypeptide as RGD-CO@MPDA-Ti (Fig. 14C) [314]. Under near-infrared (NIR) irradiation, RGD-CO@MPDA-Ti surface showed a strong antibacterial activity against planktonic MRSA by the CO gas-potentiated mild photothermal therapy at 42 °C. After bacteria elimination, CO inhibited M1 macrophages to secrete pro-inflammatory cytokines via activating heme oxygenase (HO-1) and inducing the down-regulation of p38 MAPK and NFκB (p50/p65). Thereafter, the co-existence of CO and RGD induced the polarization of M1-phenotype towards anti-inflammatory M2-phenotype by the JAK1/STAT6 pathways. In an implant-infected model in rat, the phototherapeutic platform not only introduced CO gas to synergistically eliminate residual bacteria, but also alleviated the inflammation and mediated immunomodulation which stimulated osteogenesis.

Alternatively, the light-responsive surface can also be used to modulate the osteogenic differentiation of mesenchymal stem cells [315], neuronal differentiation [316], and vessel repair as well as inflammation reduction [317]. As to osteogenic regulation, one example noted that bismuth sulfide and hydroxyapatite were deposited on Ti surface to form a photoelectric-responsive coating (BS/HAp) [315], as shown in Fig. 15. The HAp can reduce the recombination of photogenerated electrons and holes produced by BS under NIR light irradiation and help transfer the photoelectrons to the cell membrane, enhancing the photocatalytic capability of the hybrid film. The electrons not only influenced Na^+ channel and membrane potential which changed cell shape, but also made Ca^{2+} inflow from extracellular to intracellular compartments to activate the Wnt/Ca^{2+} signaling pathway, thus leading to the upregulation of the osteogenic differentiation of stem cells. After implantation in bilateral femurs of Sprague-Dawley (SD) rats, the osteogenic expression of such a Ti-BS/HAp-light substrate reached 82.41% compared with the values of 65.10% and 6.5% for Ti-BS/HAp-dark and blank Ti substrates, respectively. In another neuronal regulation, a heterointerface of rGO/g-C_3N_4/TiO_2 nanocoating was prepared on the Ti surface that can produce photoinduced separation of electron-hole pairs under blue LED irradiation [316]. The electrons moved towards cells can activate plasma membrane Ca^{2+} channels to enhance neural differentiation and neurite outgrowth of PC12 cells, which showed a higher aspect ratio, a larger cell area and a lower circularity level. The upregulated calcitonin gene-related peptide (CGRP) secreted by PC12 in turn benefitted osteogenic differentiation of MC3T3-E1 cells, because of its function as an anabolic agent to bone.

3.2. X-ray

X-ray as a typical electromagnetic radiation that is emitted by electrons around the atomic nucleus, has been widely applied in clinical diagnosis and treatment [318]. X-ray offers unique merits of a high tissue-penetrating capability and a minimal autofluorescence background compared with optical stimuli [319]. In general, X-ray is able to regulate osteoblast activities, trigger drug release, and assist implant infection imaging. It is noted that low-dose X-ray irradiation (<1 Gy) benefits differentiation and mineralization of osteoblast in vitro and favors mineralization of fracture callus in vivo [320,321]. For instance, She et al. investigated the influences of low-dose X-ray irradiation and added Ti particles on the osseointegration of hydroxyapatite-coated Ti6Al4V prosthesis after implantation in distal femurs of rabbits for 8 weeks [322]. As to the implant groups without addition of Ti particles, low-dose irradiation with 0.5 Gy X-ray obviously enhanced bone ingrowth into the prosthesis surface (Fig. 16A). Though the improved effects of bone formation modulated by low-dose irradiation were compromised by the introduction of wear particles, the thickness of interface membrane around the implant caused by Ti particles was significantly reduced when exposed to X-ray irradiation. Hence, the low-dose X-ray irradiation maybe helped promote the prosthesis stability in the presence of wear particles and inhibited the early development of aseptic loosening caused by wear particles. As to the triggered drug release, one typical example is based on the photocatalytic property of TiO_2 in response to X-ray irradiation. Schmidt-Stein et al. used the X-ray to induce the generation of electron-hole pairs of compact TiO_2 layer and TiO_2 nanotube arrays [323]. The improved production of separated electron-hole pairs observed in anatase phase can degrade organic compound Acid Orange 7 in both compact and nanotubular surfaces. Similarly, the TiO_2 nanotubular surface silanized with a monolayer of zinc porphyrin containing a triethoxysilane functional group (Zn-TESP) can even undergo monolayer chain scission to release attached Zn-porphyrin molecules under X-ray stimulation. It is clear that about 50% of the attached Zn-TESP units were removed after X-ray irradiation for 20 min, suggesting the feasibility of X-ray activation for regulating potential drug release patterns. Recently, X-ray excited luminescent chemical imaging (XELCI) is used to detect and monitor bacterial infection on implant surfaces in a non-invasive way [324]. XELCI is a combined technique consisting of X-ray excitation to produce high-resolution images and optical detection of infection degree, which is composed of an X-ray scintillator layer and pH-sensing layer [325]. The mechanism lies on that once exposure to an X-ray beam, the scintillator layer produces luminescence, and the emitted light is partially adsorbed by the pH-sensing layer that modulates the spectrum in response to the pH variation [325]. For instance, Uzair et al. first prepared an X-ray scintillator layer containing Gd_2O_2S:Eu in epoxy on orthopedic implant surfaces, and then added another PEG layer containing pH indicator dyes (bromocresol green (BCG) or bromothymol blue (BTB)) [326]. Under X-ray irradiation, the scintillator layer emitted 620 nm and 700 nm light, and the pH indicator layer presented different adsorption of 620 nm luminescence responding to different pH values but without adsorbing 700 nm light in all pH range, thus producing pH mapping. Both the pH dyes can obviously exhibit pH mapping effects when one half of the coated plate was immersed in pH 4 solution and another half in pH 7 solution with and without tissue covering, but only BTB dye layer can show appreciable pH mapping change with the formation of *S. aureus* biofilm under both the optical and XELCI imaging, because the BCG responded best during pH 3–5 while BTB responded best during pH 5–8 (Fig. 16B). Thereafter, such an epoxy-PEG pH film containing BTB on an implant rod can successfully image the acidic and basic pH regions after implantation in rabbit tibia parts. Hence, the XELCI technique shows a potential application for detecting local pH variations under acidosis conditions including tumors, inflammation and ischemia etc. In addition, X-ray excited luminescent chemical imaging can be combined with photodynamic therapy. Wang et al. prepared five layers of X-ray functional materials that can be coated on the surface of implantable medical devices [327]. The order of layers from the bottom to the top is (1) red fluorescence material of Eu^{3+}-doped $Y(PO_3)_3$, (2) green fluorescence material of Tb^{3+}-doped $Y(PO_3)_3$, (3) ultraviolet fluorescent material of Gd^{3+}-doped $Y(PO_3)_3$, (4) nanometer titanium oxide, and (5) dye layer of methyl orange. The efficient fluorescent materials of Tb^{3+}-, Eu^{3+}-doped $Y(PO_3)_3$ combined with fluorescent dye were able to label color change under pH 5–7 under X-ray irradiation even in the presence of meat tissue, while another two compounds of Gd^{3+}-doped $Y(PO_3)_3$ and TiO_2 were able to realize bactericidal effects because of the photocatalytic production of singlet oxygen and hydroxyl radicals. Therefore, such a precise treatment strategy may provide a new paradigm for implant infection. In short, X-ray provides promising applications for activating implant osteogenesis and monitoring surface infection, with minimum attenuation by the soft tissue and elevated spatial resolution.

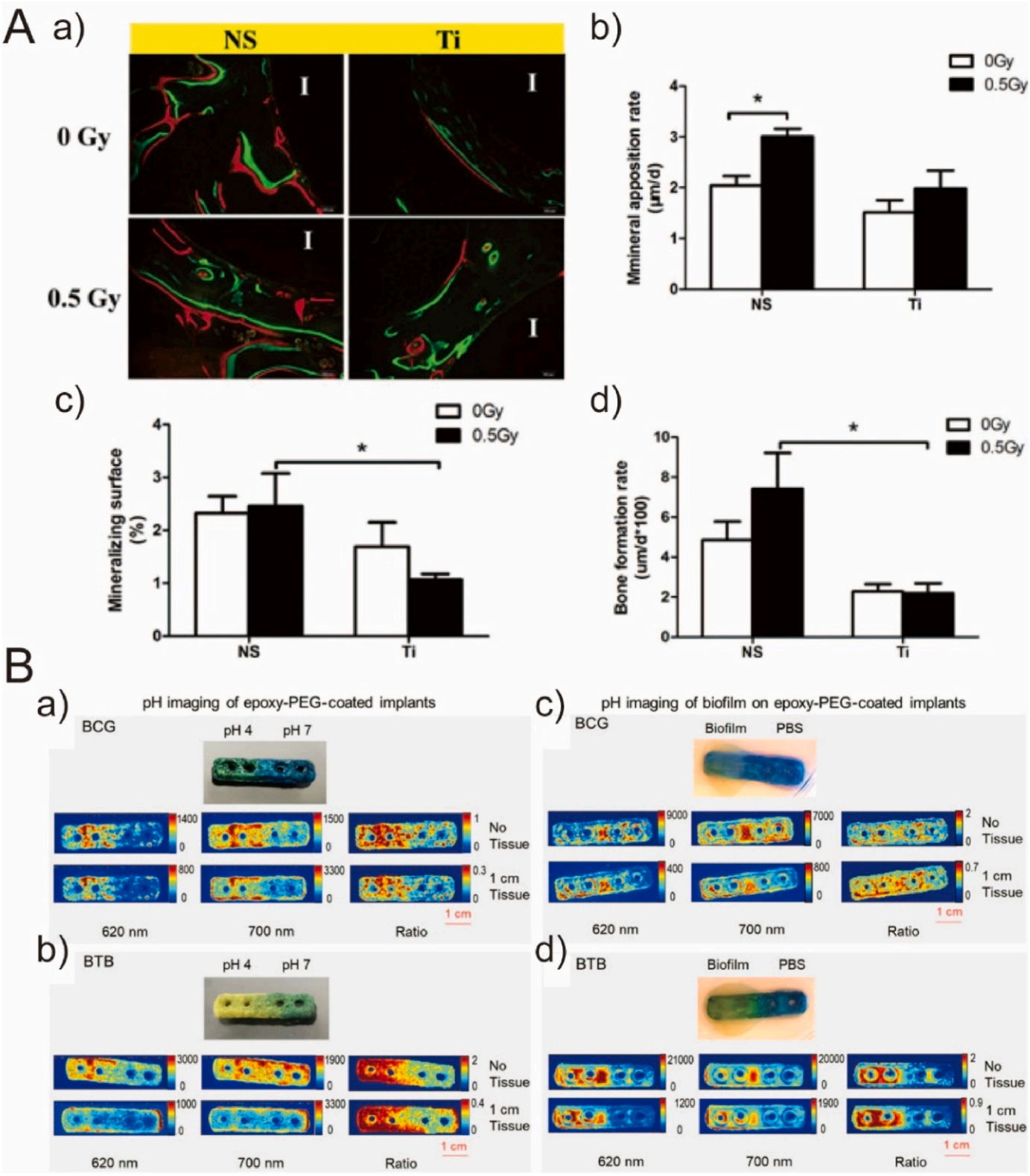

Fig. 16. (A) In vivo bone regeneration results. (a) Fluorescent images of implants in distal femur sections with the xylenol (red) and calcein (green) labels. Scale bars, 100 μm. (b) The mineral apposition rate (MAR) of different groups. (c) The mineralized surface (MS) of different groups. (d) The bone formation rate (BFA) of different groups. Note: NS = injection of sterile saline group, Ti = addition of Ti particles [322]. Reprinted with permission from Ref. [322]. (B) pH imaging of orthopedic plates with an epoxy-PEG pH film. (a and b) Photograph of a respective plate with the epoxy-PEG film containing (a) BCG dye and (b) BTB dye with one half of the plate in pH 4 solution and the other half in pH 7 solution. XELCI images of the respective plate at 620 nm, 700 nm, and ratio of 620/720 nm without tissue and with porcine tissue (1 cm). (c and d) Photographs of a respective (c) epoxy-PEG-BCG-coated plate and (d) epoxy-PEG-BTB-coated plate after growing a biofilm on the left half and keeping the right half in agar (pH 7.4) after 24 h. XELCI images of the respective plate of biofilm growth (at 620 nm, 700 nm, and ratio of 620/720 nm) without tissue and with porcine tissue (1 cm) after 24 h [326]. Reprinted with permission from Ref. [326].

3.3. Electrical field

Electrical stimulation refers to an external electric signaling to regulate cell or tissue response, because a variety of behaviors and mechanisms involve electric signaling, such as angiogenesis, mitosis, migration and would healing [328]. As to the Ti implants, the applied electrical signaling can stimulate cell and tissue activities or trigger the release of drugs. One of the early studies indicated that the proliferation, and differentiation (ALP synthesis and calcium deposition) of osteoblasts were enhanced upon both the creation of a nanotubular surface and biphasic electrical stimulation (15V, pulses) [329]. Although such application of electric signaling to stimulate cell behaviors has been widely observed, the molecular mechanism to osteogenic differentiation remains elusive. Park et al. noted that osteogenic differentiation of clonal rat MSCs (mesenchymal stem cells) was obviously improved on TiO_2 nanotubular surface by triggering of constant electric fields (EFs), even in the absence of osteogenic chemical supplements [330]. This was explained by the fact that EFs induced membrane protrusions with Connexin 43 (Cx43) transported to plasma membrane, and Cx43 appeared to mediate extracellular Ca^{2+} influx and rapid propagation of intracellular Ca^{2+} increase by gap junctions. The increased Ca^{2+} ions further modulated downstream signaling, calcineurin/CAMKII phosphorylation and NFAT dephosphorylation, resulting in osteogenic gene expressions. Because the above TiO_2 on the outer surface is a type of semiconductors, the conductivity and electron transport are unsatisfactory in some cases, which may require a long-term EF application in terms of days. Hence, in order to promote sensitivity and reduce stimulation time, Mazare et al. prepared Ar/H_2-reduced black TiO_2 nanotube arrays, with a strongly decreased resistivity (15.5 kΩ) compared with the as-formed TNTs (1.17 MΩ) [331]. The faster proliferation and intracellular Ca^{2+} level elevation of clonal rat MSCs were observed on black TiO_2 TNTs under a lower EF intensity in contrast to the as-formed TNTs, suggesting the enhanced substrate sensitivity, as shown in Fig. 17A and B. The hypothetical mechanism was that the enhanced conductivity of the reduced TiO_2 nanotube surface can provoke elevated Ca^{2+} influx via calcium channels under minimal EF stimulation. As the increase in intracellular Ca^{2+} level, downstream signaling cascades containing calmodulin (CaM)/calcineurin may improve cell proliferation via the transcriptional activation including NFAT/NFκB.

Electric stimulation can also be used to regulate surface wettability, osteogenic and antibacterial activity based on the added coating functions beyond TiO_2 properties. The polymers with switchable orientation transformation by the electrochemical oxidation/reduction process are commonly used to generate a reversible surface to dynamically regulate on-demand properties, such as polypyrrole (PPy) [332,333] and polydopamine [334]. For instance, Liao et al. doped an amphiphilic

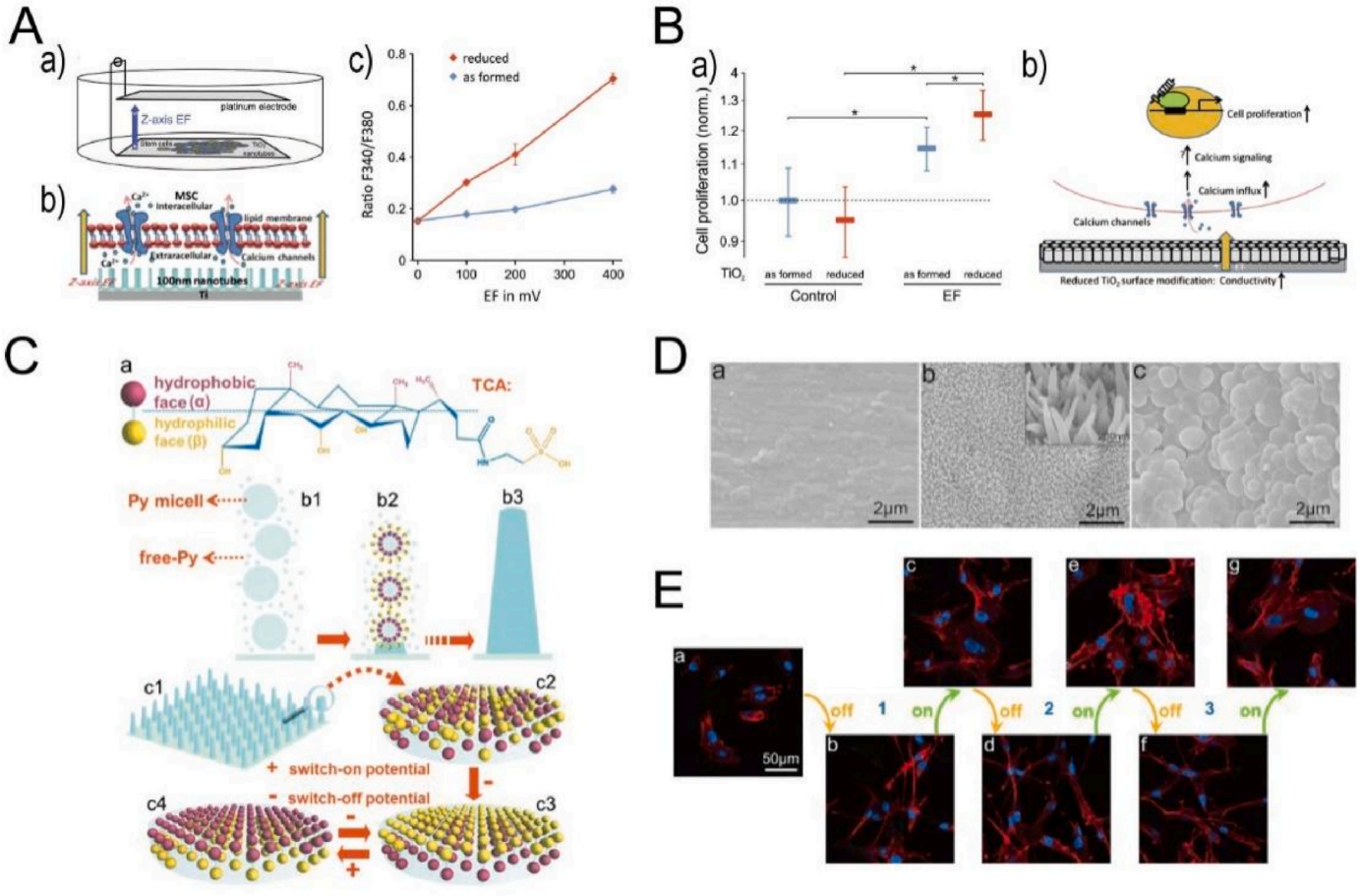

Fig. 17. (A) Illustration (a) of electric field stimulation of MSC. (b) Schematic diagram of EF-triggered calcium influx. (c) The voltage-dependent elevation of intracellular calcium in as formed and reduced TiO_2 after 10 min-EF stimulation [331]. (B) Cell proliferation in reduced and as formed TiO_2 nanotubes under EF stimulation: (a) Cell proliferation analysis by WST1 test, and (b) a hypothetical diagram of EF-triggered MSC cell proliferation [331]. Reprinted with permission from Ref. [331]. (C) The chair conformation (a) of TCA. (b) The possible mechanism of preparing 1D NAPPy/TCA (b3). (c) Schematic diagram of the electrical-potential-induced wettability of 1D NAPPy/TCA: c1-c2) the random orientation of TCA without an applied potential, c3) the switch-off state, and c4) the switch-on state [332]. (D) SEM images of NAPPy/TCA prepared in PBS containing 0.01 M (a), 0.07 M (b), and 0.20 M (c) of TCA [332]. (E) Immunofluorescence staining images of MC3T3-E1 cells on 1D NAPPy/TCA in the original state (a), and cycles between switch-off (b, d, and f) and switch-on states (c, e, and g) [332]. Reprinted with permission from Ref. [332].

biomolecule, taurocholic acid (TCA) into 1D nano-architectured polypyrrole (NAPPy) array on Ti surface [332], as shown in Fig. 17C–E. The doping TCA enabled the surface with reversible wettability between superhydrophobic (152°, switch-on state) and hydrophilic (55°, switch-off state) in response to two weak electrical potentials (+0.50 and −0.80 V applied as a swtich-on and swtich-off potential, respectively), which was caused by potential-tunable orientation between α-face (hydrophobic) and β-face (hydrophilic) of TCA. Such a potential-switchable surface induced preferential protein adsorption and subsequently modulated the adhesion and spreading of MC3T3-E1 cells in situ. Similarly, another hybrid PPy coating was prepared on Ti-5Al-2.5Fe surfaces containing negatively charged chondroitin sulphate (CS) and positively charged antibacterial peptide (OP-145) [333]. The PPy underwent reversible switching between the oxidation state (+0.5 V) and the reduction state (−0.5 V) in response to the electrical stimuli, which resulted in the preferential presence of CS (−0.5 V) or OP-145 (+0.5 V) on the outmost surface. Interestingly, the coating in switch (−0.5 V) facilitated osteogenic activity of MC3T3-E1 cells because of the exposure of osteocyte-philic CS, while it in switch (+0.5 V) exhibited strong antibacterial property due to the exposure of OP-145, suggesting a dynamic switching between enhanced osteogenic and antibacterial activity on demand. In addition, some drugs can be incorporated into the conductive polymer coatings and released once exposure to the electric stimulation [335]. For instance, Wu et al. prepared a polypyrrole/dexamethasone (Ppy/Dex) composite coating on Ti surface by electrochemical deposition, and further added the composites of extracellular matrix (ECM) to gain a Ppy/Dex/ECM coating [336]. The release of Dex can be realized by changing redox status of Ppy, whose positively charged surface was reduced to neutrality to reduce electrostatic attraction under the negative pulse electrical stimulation. Therefore, the on-demand released Dex and the Ppy/Dex/ECM coating with three-dimensional nano-network structure synergistically improved osteogenic differentiation and reduced inflammatory factors secreted by RAW264.7 cells. In short, electrical stimulation provides an approach of dynamically manipulating the Ti interfaces.

3.4. Piezoelectricity

Piezoelectricity as a biomimetic mode to regulate bone tissue regeneration is based on the fact that natural bones show piezoelectric properties. The piezoelectric properties of bone mainly originate from its specific dense fibrillar assembly of non-centrosymmetric collagenous matrix with embedded apatite nanocrystals [337]. The piezoelectric response of bone presents anisotropic because of its structural anisotropy, and also relies on the direction, frequency and intensity of the stimuli [338]. It is reported that the highest piezoelectric coefficient (d_{14}) of femoral bone is 0.7 pC/N^{-1} measured in shear mode [337]. According to previous studies, natural bone accumulates negative charges under physiologic conditions due to piezoelectric potential in bone, with a zeta potential of −5 mV [339]. Because compression of collagen produces negative charges on the surface that augment the zeta potential under bone compression and enhance dynamic bone stiffness [339]. On the contrary, the tensile force likely generates positive charges that attenuate the zeta potential and may reduce dynamic bone stiffness [339]. Once it undergoes damage, the fractured region of bone displays more electronegative than other regions. It is reported that the accumulated charges benefit the functionality of osteoblast cells, enhance matrix mineralization at the fractured parts and thus promote bone regeneration [340]. In addition, molecular physiological analysis shows that a cascade of cellular events (namely galvanotaxis) also produce endogenous electrical signal, which include cell membrane depolarization and hyperpolarization, Ca^{2+}/Mg^{2+} ions influx through hyperpolarized ends and actin depolymerization, etc [337]. Hence, from both cellular and tissular levels, piezoelectric stimulation can effectively regulate osteoblast and bone activities.

The piezoelectric responses of Ti surfaces are realized by introduction of piezoelectric coatings. Piezoelectric materials can be divided into three groups, such as piezoceramics, piezopolymers and piezocomposites [337,341]. Piezoceramics contains $BaTiO_3$, $KNbO_3$, $MgSiO_3$ and ZnO etc., piezopolymers include polyvinylidene fluorid (PVDF), poly(vinylidene fluoride-trifluoroethylene) (P(VDF-TrFE)), poly(l-lactic acid) (PLLA) and collagen etc., and piezocomposites usually comprise of the above piezoceramic and piezopolymers [337,341]. Piezoelectric materials are able to modulate cellular behaviors through surface charges produced in response to deformation induced by cellular communication, vibration stimulus or both [342]. Piezoelectric coatings generally need polarization to achieve unidirectional orientation of randomly aligned dipoles via corona poling (1–10 kV) or thermal poling (25–1000 °C) before the biological studies [337]. The piezoelectric coatings on Ti surfaces are used to stimulate osteoblast and bone behaviors, and improve antibacterial activities. As to osteogenesis regulation, a $BaTiO_3$ coating was deposited on a porous Ti6Al4V (pTi/$BaTiO_3$) to investigate its effect on osteogenesis and angiogenesis [343]. The pTi/$BaTiO_3$ (poled) by corona polarization with a surface potential of −30 mV promoted the migration, proliferation and osteogenic differentiation of mesenchymal stem cells of rat femurs via the Ca^{2+}/p38MAPK/osterix axis, compared with the functions observed from pTi/$BaTiO_3$ (unpoled) and pTi. Meanwhile, the migration, proliferation and secretion of VEGF and PDGF-BB of human umbilical vein endothelial cells were promoted via the PDGF-BB/PDGFR-β axis. In vivo results suggested that pTi/$BaTiO_3$ (poled) implant was covered by new bone with an area ratio of 58.68% after 8 months using interbody fusion cage implantation model in sheep, which was much higher than that of pTi/$BaTiO_3$ (unpoled) (46.88%) and pTi (33.16%). Because the above animal model lacked a physiological loading environment where the material acted as interbody cages and bone fillers, the same group implanted such a poled $BaTiO_3$/Ti6Al4V (BT/Ti) scaffold in a sheep cervical corpectomy model (Fig. 18A) [344]. As such, piezoelectric effects can be effectively produced by dynamic pressure from cervical movement. The in vitro and in vivo data both indicated that the BT/Ti (poled) scaffold can suppress MAPK/JNK signaling cascade but activate oxidative phosphorylation (OXPHOS) and ATP synthesis of macrophages, and thus facilitate macrophage M2 polarization. The new bone volume ratio (BV/TV) of BT/Ti (poled) group was 33.97% compared with the value of 23.97% of the Ti group after one year, suggesting an active immunoregulatory bone repair. Beyond only using the piezoelectric property, it can be combined with other stimuli to achieve synergetic or switching efforts on osteogenesis, such as ultrasound and magnetic field. For instance, Cai et al. prepared a $BaTiO_3$ coating on TC4 titanium substrate (BT/TC4) with a piezoelectric coefficient (d_{33}) of 0.42 pC/N [345]. The mechanical wave introduced by LIPUS not only stimulated the BT/TC4 to produce a microcurrent of 10 $\mu A/cm^2$, but also positively affected cell activities. As a result, the piezoelectric BT/TC4 surface with LIPUS stimulation synergistically enhanced osteogenic expressions of MC3T3-E1 cells which were mediated by the elevated influx of calcium ions. Similar LIPUS-induced synergetic effects of $BaTiO_3$-coated Ti surfaces on osteogenesis and osseointegration were also observed by Chen et al. [346] and Fan et al. [347]. Recently, an electrical stimulation platform of $BaTiO_3$ nanoarrays on Ti surface for selectively regulating antiosteosarcoma and osteogenesis was relegalized by switching on and off ultrasound assistance (Fig. 18B), respectively [348]. In the switch-on state, the polarized $BaTiO_3$ nanorod arrays under US stimulation can produce a high-intensity output potential (−237–139 mV) to dynamically disturb the tubulin orientation, disrupt the spindle structure and arrest the G2/M phase of mitosis of osteosarcoma cells (143B). Therefore, a mouse survival rate of ~60% was obtained in the PNBTO + US group after 60 days, but none survived after 25 days observed in the control groups. In the switch-off state, the positively charged PNBTO surface with a surface potential of ~530.8 mV can form a static electrical stimulation towards the negatively charged bone defect. As a result, the combination of mechano-conduction from 1-D nanorod structure and the static electrical

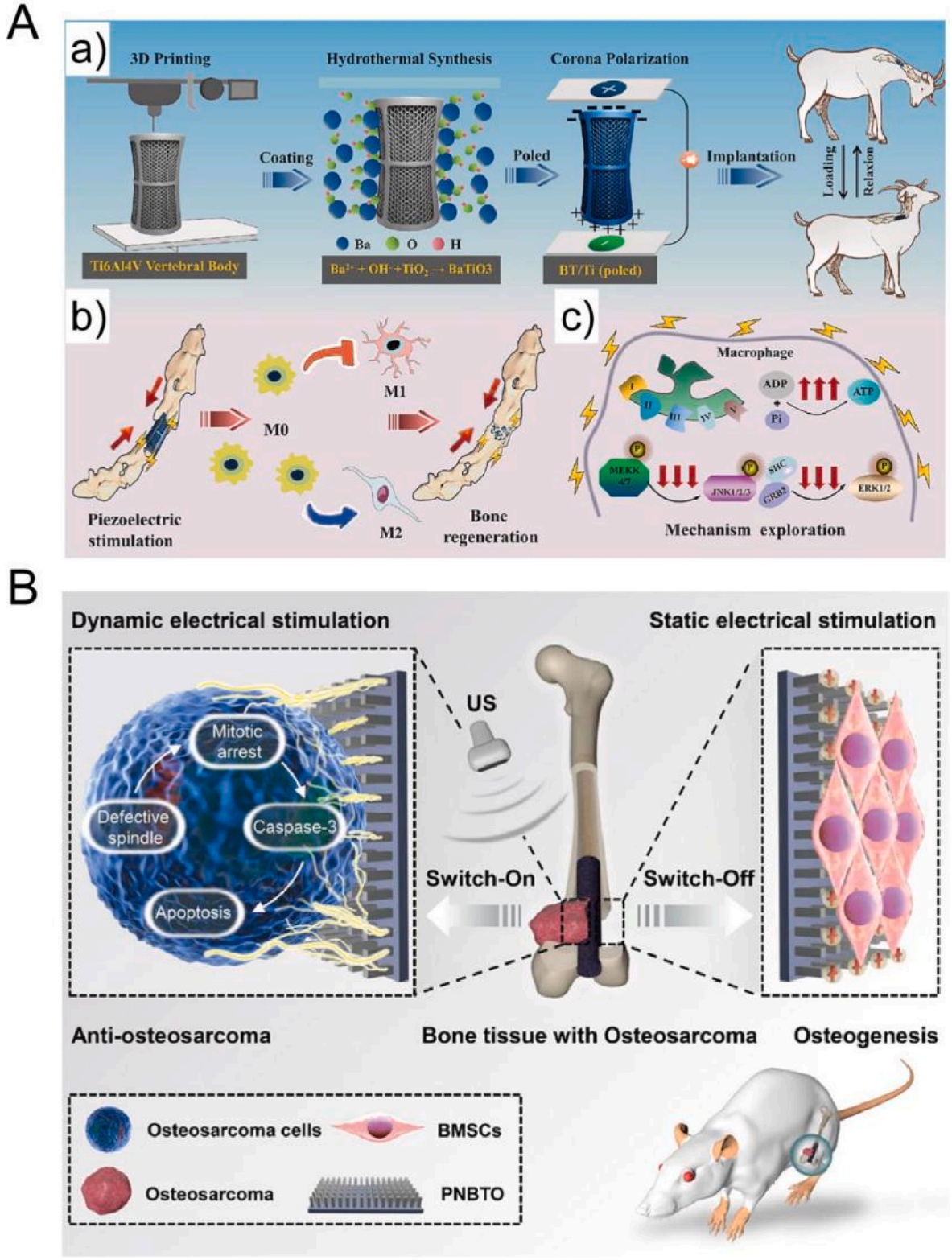

Fig. 18. (A) Schematic diagram of porous Ti6Al4V scaffolds coated with $BaTiO_3$. (a) Preparation of porous Ti6Al4V scaffolds coated with $BaTiO_3$ and the implantation in a cervical en-bloc spondylectomy model of sheep. (b) BT/Ti (poled) artificial vertebrae bodies enhanced M2 polarization during bone repair process. (c) Piezoelectric stimulation suppressed MAPK/JNK signaling but activated OXPHOS of macrophages [344]. Reprinted with permission from Ref. [344]. (B) One-dimensional ferroelectric nanoarrays with switchable effects for selectively regulating osteogenesis (US switch-off) and antiosteosarcoma (US switch-on) under static and dynamic electrical stimulation, respectively [348]. Reprinted with permission from Ref. [348].

stimulation synergistically promoted osseointegration in the femoral condyle parts of rats. For instance, the value of bone volume to tissue volume (BV/TV) in PNBTO group (29.3 ± 0.25%) was 1.7- and 2.3-fold higher than that in the BaTiO3 flat coating (PBTO) group (17.5 ± 0.61%) and pure Ti group (13.0 ± 1.37%), respectively, after 4 weeks. Beyond US mode, magnetic field can also be introduced to strengthen the piezoelectric effects. P(VDF-TrFE)-based magnetoelectric coatings consisting of piezoelectric polymer and magne-tostrictive phase, were prepared to unite ferromagnetism and ferroelectricity, including $CoFe_2O_4$/P(VDF-TrFE) [349], and $Tb_xDy_{1-x}Fe_2$ alloy/P(VDF-TrFE) [350]. Once exposure to magnetic field, the charged magne-tostrictive phase would be elongated or contracted along the magnetic field direction, and it thus causes the stress/strain transferring between the magne-tostrictive and piezoelectric phases, finally increasing surface potential [351]. Hence, the expended range of surface potential can provide an accurate platform to investigate the relationship between surface potential and osteogenic differentiation of mesenchymal stem cells. In short, piezoelectric response provides a biomimetic method to activate osteogenesis efforts.

3.5. Ultrasound

Ultrasound, as a mechanical wave, can directly modulate the cell-material interaction or control the release of drugs from the surface in a non-intrusive manner. Amongst them, low-intensity pulse ultrasound (LIPUS) has been approved by the US Food and Drug Administration (FDA) to improve fresh fracture healing and bone nonunion reconstitution [352]. As to the regulation of cell-material interaction, one

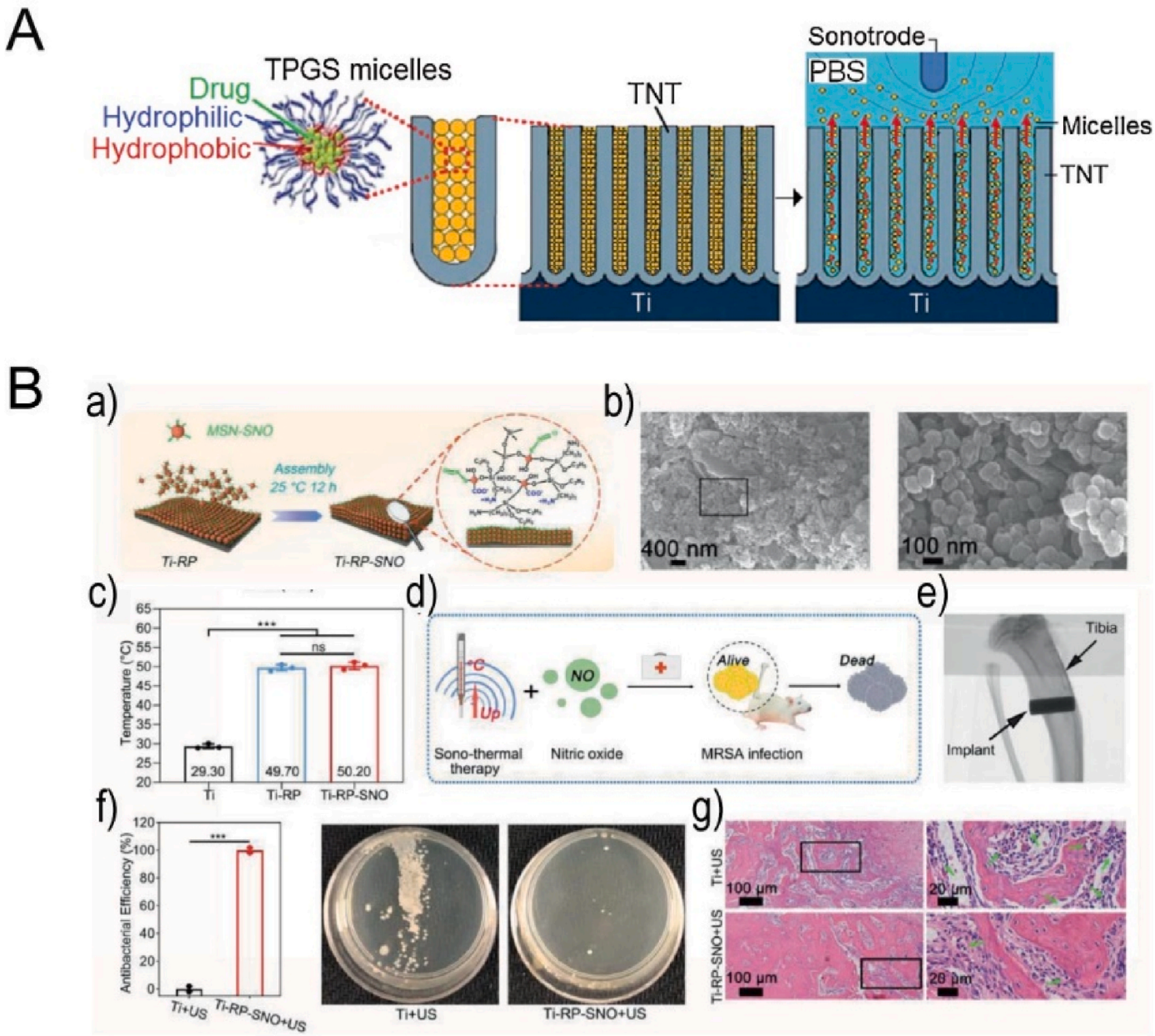

Fig. 19. (A) Schematic diagram of ultrasound-stimulated drug release from TiO_2 nanotubes (TNTs) arrays [354]. Reprinted with permission from Ref. [354]. (B) Preparation of the MSN coating on Ti–RP and the synergetic antibacterial results of sonothermal and NO therapy: (a) the preparation method of Ti–RP-SNO, (b) SEM images of Ti–RP-SNO, (c) the corresponding temperatures of different samples under US stimulation, (d) schematic diagram of the antibacterial test in vivo, (e) Micro-CT image of the position of implant in the tibia, (f) the antibacterial efficiency and corresponding spread plate photographs under continuous US in vivo, and (g) H&E staining images of the bone tissues around implants in rats [357]. Reprinted with permission from Ref. [357].

example observed the combined effect of MAO method and LIPUS on MG63 cell behaviors [353]. Cells under LIPUS stimulation bound more tightly to the surface with more pseudofeet, and showed a faster proliferation and higher expressions of osteogenic differentiation compared with the only MAO-treated surface, which may be related with the fact that LIPUS vibration could influence the permeability and the diffusion process of the cell membrane as well as intracellular material movement. Another application is that the ultrasonic wave can modulate the release of drugs on demand. Aw et al. loaded micelles carried with water-insoluble drug (indomethacin) into the TNTs [354], as shown in Fig. 19A. Under ultrasonic stimulation, the drug-micelles were released in a responsive way, with even 100% release in a desirable time of 5–50 min. The mechanism might involve a combination of cavitations and thermal processes produced by mechanical vibration of ultrasound waves in interaction with the aqueous buffer and rigid TNTs structures. In another study, Zhou et al. first prepared superhydrophobic TNT arrays by modifying hydrophilic TNTs with 1H,1H,2H,2H-perfluorooctyl-triethoxysilane (POTS), and then loaded different amounts of tetracycline hydrochloride [355]. The loaded drug can be triggered in response to the multiple and controlled ultrasonic waves, because of the selective removal of the trapped air layer. Alternatively, ultrasonic stimulation can also be combined with sonothermal therapy and triggered gas therapy for infected bone regeneration models. Compared with phototherapy, ultrasonic waves can penetrate deeply into tissues and be focused to a single discrete point spatially [356]. Recently, red-phosphorus-coated Ti surface (Ti-RP) exhibited an obvious sonothermal activity of more than 20 °C increase under continuous ultrasound excitation (1.0 W cm^{-2}, 1 MHz), which was related with the fact that ultrasound-activated electron motion in the RP was able to turn the mechanical energy of ultrasound into phonons in the forms of lattice thermal vibration [357], as shown in Fig. 19B. To achieve a more effective antibacterial treatment, the Ti-RP was functionalized with another nanomesoporous silica nanoparticle (MSN) coating that contained thermal-responsive NO precursor. Such a hybrid surface under ultrasound excitation showed an antibacterial efficiency of more than 93.40% against multidrug-resistant *Staphylococcus aureus* (MRSA) in vitro and validly combatted bone infection by MRSA in vivo without side effect, because of the synergism of the hyperthermia and the released

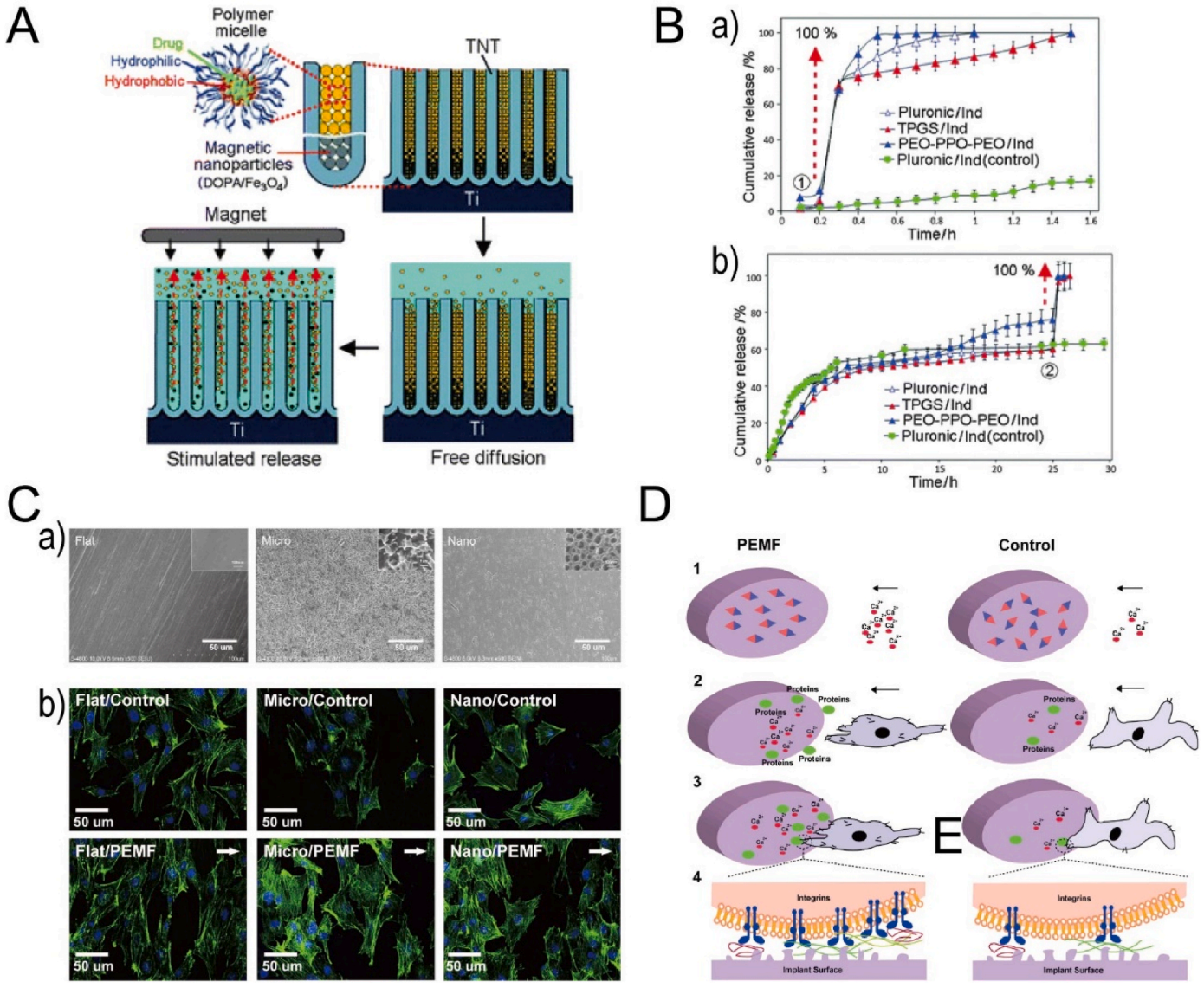

Fig. 20. (A) Schematic diagram of the responsive drug release from TNTs by magnetic stimuli [359]. (B) Release profile of indomethacin encapsulated micelles at different stages of release process by addition of magnetic stimuli: a) at the beginning, and b) during 50–60% of release [359]. Reprinted with permission from Ref. [359]. (C) SEM images (a) of the overall topography and (b) CLSM images of cells stained with DAPI (blue) and FITC (green) [362]. (D) Schematic diagram of the effects of the PEMF on cell adhesion [362]. Reprinted with permission from Ref. [362].

NO. Briefly, ultrasonic stimulation provides an attractive approach because ultrasonic waves can target the region in a precise, narrow and deep way.

3.6. Magnetic and electromagnetic field

The magnetic field is derived from either static magnets or the flow of electric charges through the wires or electrical devices (electromagnetic field) based on the sources, which shows high tissue penetration and minimum adverse effects under low strength magnetic field [358]. Magnetic and electromagnetic field can be used to trigger drug release with the assistance of magnetic NPs, and to stimulate cell and tissue behaviors. In one case, a magnetic-responsive delivery platform was prepared on TNT arrays by loading dopamine-modified iron oxide nanoparticles (MNPs) at the bottom and indomethacin-encapsulated polymer micelles at the top, respectively [359], as shown in Fig. 20A. Upon addition of a magnet on top of the TNTs, immediate 100% release of drug-encapsulated micelles was observed within 1–1.5 h, and similar triggered-release result was achieved at desirable times during the release process (Fig. 20B). This strategy shows some limitations including uncontrolled release triggered by external magnetic field, but it may satisfy the requirement where on-demand release is needed without delay. In another application, the magnetic field produced by movement of electric charges can stimulate cell functions or tissue regeneration. For instance, Fassina et al. observed the higher proliferation and the increased of matrix deposition via upregulated osteogenic-related expressions (type-I collagen, decorin, and osteopontin) of SAOS-2 cells on Ti fiber-mesh scaffolds [360] or titanium plasma-spray surface [361], under the pulse electromagnetic field (PEMF). Although some positive results have been reported on the osteogenic effects, few works have concerned about the combination of the electromagnetic stimulation and different surface topographies. As a result, Wang et al. cultured primary rat calvarial osteoblast on three types of Ti surface, namely micro-structured surface (Micro) by sand-blasting/acid etching, nanotubular-structured surface (Nano) by anodization, and a polished surface (Flat) [362], as shown in Fig. 20C. Interestingly, osteoblasts were oriented perpendicular to the electromagnetic field lines, with more microfilaments and stress fibers as well. The proliferation, expressions of osteogenesis-related genes and extracellular mature were promoted to different extents in respect to different topographies by the PEMF, where greater promotion was observed on Micro and Nano surfaces. The mechanism may be explained as follows (Fig. 20D): (1) the PEMF stimulation endowed the Ti/TiO_2 surface with oriented dipoles and amplified surface potential gradient; (2) the polarized surface adsorbed more cations and proteins; (3) polarized cells were drift to the charged surface; and (4) specific binding occurred at the focal adhesion. The further study revealed that the PEMF may enhance osteoblast activities and the skeletal anabolism via a Wnt/β-catenin signaling-induced mechanism [363]. In addition to healthy cell and animal models, it is noteworthy that PEMF is able to efficiently reduce osteopenia and osteoporosis, and to promote bone defect/fracture healing. Cai et al. adopted two animal modes of osteoporosis, including rabbits with Type 1 diabetes mellitus (T1DM) [364] or rabbits with glucocorticoids (GC) treatment [365]. The PEMF can reverse the adverse effects of T1DM or GC on bone formation via activating canonical Wnt/β-catenin signaling, which obviously promoted bone anabolism (mass, architecture and mechanical properties) between bone and porous implant interaction to a similar levels observed from healthy controls.

Beyond regulation mode based on TiO_2 and Ti properties, magnetic-responsive cell regulation can also be realized by the introduction of surface coatings containing magnetic NPs. Lin et al. prepared a magnetized collagen coatings (MCCs) containing Fe_3O_4 NPs, and investigated the effects of magnetic drive (MA) direction on osteogenic differences [366]. The MA parallel to the randomly-oriented MCC surface can significantly improve osteogenic differentiation of bone marrow mesenchymal stem cells (BMSCs) in contrast to the down-regulated behavior under the perpendicular direction. The reason may be related to the fact that the tensile status of collagen fibers responded differently to MA direction under parallel or perpendicular modes, resulting in strengthening or weakening the α5β1 integrin expression. The elevated expression of α5β1 as a receptor as mechanical conduction can activate order arrangement of cytoskeletons and osteogenic differentiation. In short, the external magnetic or electromagnetic stimulation provides a valuable approach to improve the interaction between Ti surfaces and biological tissues.

3.7. pH

The pH-responsive strategy is generally realized on Ti surfaces by single or combined modes of pH-triggered protonation and deprotonation of chemical groups in polymer caps, pH-sensitive chemical bonds, pH-induced dissolution of nanoparticles [367]. As to pH-triggered protonation and deprotonation, chitosan with abundant amino groups is one of the commonly-used molecules for modifying Ti surfaces [368–370]. For example, Zhou et al. first prepared a micelles composed of tobramycin (Tob) and heparin (HET), and then alternatively deposited positively charged chitosan (CHT) and negatively charged HET on the polydopamine-modified Ti surface [368]. The release of Tob from Tob-loaded CHT/HET multilayer coatings showed a pH-dependent pattern, with the total amount of 72.52 μg/cm^2 (~66.7%, pH 4.3) and 108.77 μg/cm^2 (~100%, pH 7.3) over the 320 h, respectively. The reason is related with the fact that more amino groups that were protonated in acid condition made CHT higher positively charged and strengthened the electrostatic interaction with micelle-loaded HET layer, thus hindering Tob release. Such a coating not only inhibited initial bacterial adhesion (*E. coli* and *S. aureus*) and disrupted biofilm formation, but also showed a "long-term antibacterial" pattern (up to 10 days) in acid condition, whereas slight decreases in adhesion and proliferation of MC3T3-E1 cells were observed. Other chitosan-based surfaces can realize the responsive release of Cu^{2+} [369], and Ag^{+}/gentamicin [370], to reduce the bacterial adhesion and proliferation. Beyond chitosan, poly(methacrylic acid) (PMAA) is also used as a gate molecule. PMAA undergoes swelling at pH 7.4 because the deprotonation of the carboxyl groups (-COOH) into carboxylate ions ($-COO^{-}$) produces strong electrostatic repulsion and high degree of hydration, but it collapses in acidic aqueous solution because the protonation reduces the electrostatic repulsion [371]. Chen et al. loaded the AMPs (HHC36 peptides) inside the TiO_2 nanotubes and encapsulated the surface with PMAA as a gate, which turned the TNT surface into a Pandora' box (Fig. 21 A-C) [372]. The box extended the release time from dozens of hours to 10 days under physiological conditions where PMAA swelled. However, when the pH value decreased to the simulated infection conditions, it was opened to release an adequate amount of AMPs to kill bacteria immediately. The in vitro results showed the "on-demand" bactericidal activity against a panel of four clinical bacteria of the Pandora' box, and the vivo data confirmed that the system can inhibit bacterial activity during the acute infection period using a bacterial infection/bone defect model.

Furthermore, some pH-sensitive chemical bonds, such as metal-coordination bonds [373] and schiff base [374], are exploited in the prepared coatings. For instance, a hybrid TNT array system with loaded vancomycin or nanosilver particles was sealed with 1,4-bis (imidazol-1-ylmethyl) benzene (BIX) via the Zn^{2+}- or Ag^{+}-induced coordination bond between TNTs and BIX [373], as shown in Fig. 21D. Once exposure to an acidic environment, the caps on TNTs underwent erosion by cleaving the ion-induced bonds to open and release drugs from TNTs, which efficiently killed the *S. aureus* and *E. coli* but without significantly inhibiting proliferation and differentiation of MC3T3-E1 cells. As to pH-induced dissolution, one typical approach is to use ZnO nanoparticles on Ti surface for triggered release. For instance, Xiang et al. coated vancomycin-loaded TNTs with folic acid/ZnO quantum dots

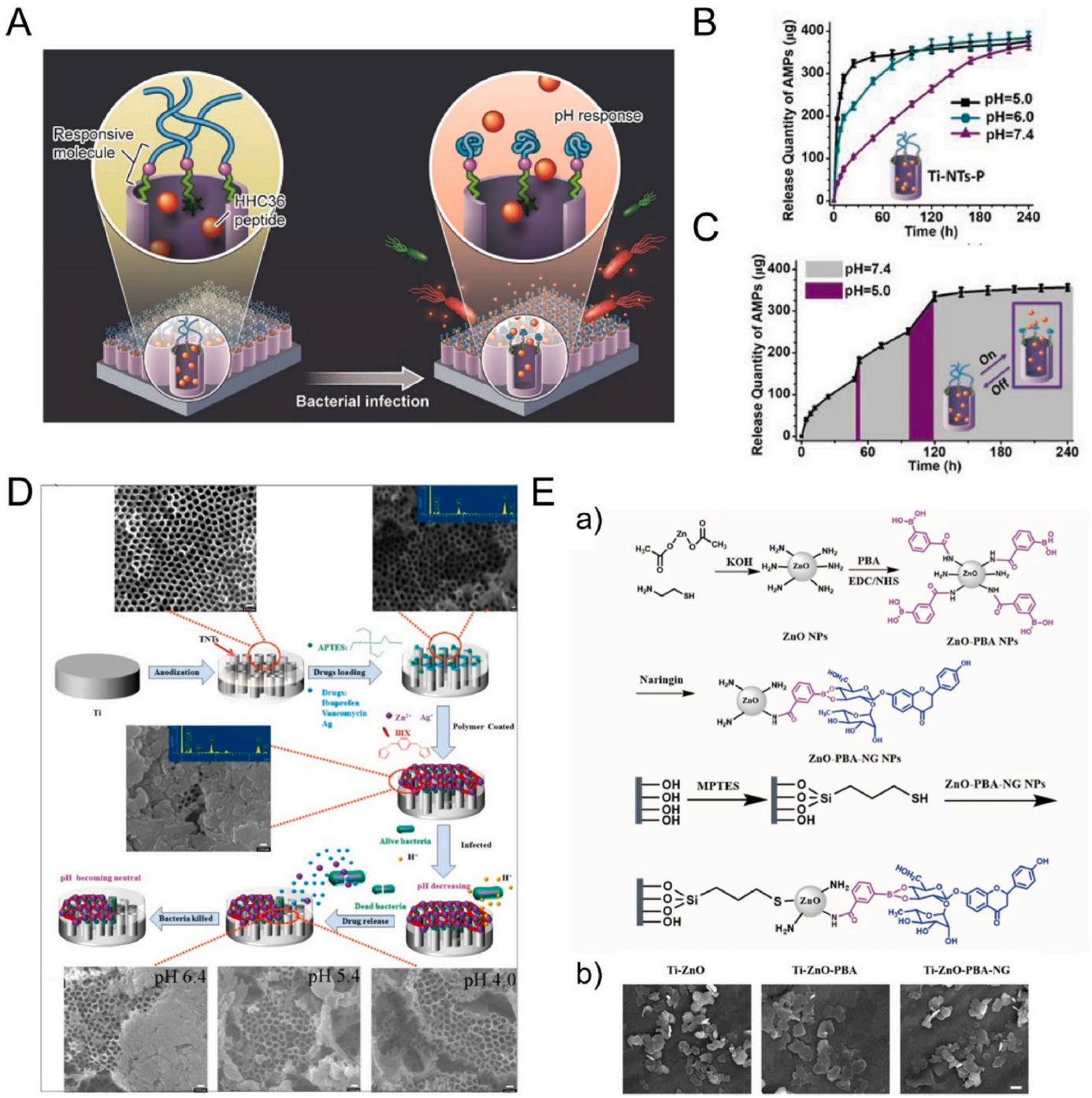

Fig. 21. (A) Schematic diagram of the release of AMPs from the Pandora's box under bacterial infection [372]. (B) Release profile of HHC36 peptides from Ti-NTs-P-A (Ti-NTs treated with dopamine, PMAA and HHC36) at different pH [372].
(C) Release profile of HHC36 peptides from Ti-NTs-P-A with a pH trigger at 48 h and 96 h [372]. Reprinted with permission from Ref. [372].
(D) Schematic diagram of preparation of the metal ion coordination polymer/titania nanotube system and SEM images of the samples before and after release for 400 h at different pH values of 6.4, 5.4, and 4.0, respectively [373]. Reprinted with permission from Ref. [373]. (E) Schematic diagram of (a) the preparation process of Ti-ZnO-PBA-NG system and (b) SEM images of the prepared samples [376]. Reprinted with permission from Ref. [376].

(TNTs-Van@ZnO-FA surface) [375]. A greater extent of improved antibacterial ratio against *Staphylococcus aureus* was obtained on such a surface when the pH switched from 7.4 to 5.5 compared with the one without capping, because of the both accelerated release of Van and Zn^{2+} via the dissolution of ZnO-FA caps under acidic environments. In addition, beyond single mode, two above modes are facilely combined to achieve a responsive way. One case with the combination of pH-sensitive boronic ester bonding and pH-induced dissolution of ZnO nanoparticles is that ZnO NPs were conjugated with naringin (NG) via using 3-carboxyphenylboronic acid (PBA) as a bridging molecule (ZnO-PBA-NG NPs), where dynamic boronic ester structure was induced [376], as shown in Fig. 21E. The Ti surface immobilized with these NPs showed "off-on" release patterns of Zn^{2+} and NG responding to bacterial infections and tumor extracellular acidity, where both dissolution of ZnO and hydrolysis of boronate ester bonding took place. The released Zn^{2+} and NG can obviously increase oxidative stress in both bacteria

(*Escherichia coli* and *Staphylococcus aureus*) and osteosarcoma (Saos-2 cells) with the production of ROS, which caused damage of bacteria and apoptosis of osteosarcoma cells. However, the proliferation and differentiation of neonatal rat calvaria osteoblast were promoted. The result suggested that ZnO-PBA-NG-modified surface provided a prospective strategy to prevent implants from infection and tumor recurrence when applied in reconstruction and osteosarcoma resection.

Beyond the above patterns, pH-sensitive strategy can also combine catalytic therapy and gas therapy for infected arthroplasty model. For instance, the CaO_2 nanoparticles were first functionalized with tannic acid (TA), and then deposited on Ti surface to prepare a nano-painting with the assistance of mussel-bioinspired adhesion and Cu^{2+}-facilitated metal-phenolic network (interparticle locking) [377]. The nano-painting was rapidly disassembled upon exposure to bacteria-induced acidic niche. Thereafter, ROS from Cu^{2+}-mediated Fenton-like reactions and O_2 from CaO_2-induced hydrolysis were promptly triggered during the degradation of the nano-painting. The produced ROS can effectively eradicate methicillin-resistant *staphylococcus aureus* (MRSA), and the released O_2 can relieve the hypoxic infected microenvironment and even induce pro-inflammatory polarization of macrophages together with Cu^{2+} ions. The arthroplasty rat model suggested that the nano-painting surface obviously inhibited periprosthetic joint infection and enhanced the peri-implant osteogenesis by aborting the immunosuppressive milieu [377]. In short, the pH-responsive strategy provides a smart platform mainly for the infected model therapy.

3.8. Enzyme

Enzyme-responsive way usually takes the advantage of the secreted enzymes by prokaryotic or eukaryotic cells to hydrolyze the coating to trigger drug release or activate specific cell behaviors. One of the biological enzymes, hyaluronidase secreted by a variety of bacteria, is commonly used to cleave the hyaluronan-contained caps to regulate drug release kinetics. For instance, Yuan et al. first loaded vancomycin (Van) into the TNTs, and then sealed the array by alternatively depositing 3,4-dihydroxyhydrocinnamic acid-modified chitosan (Chi-c) and dopamine-modified hyaluronic acid (HA-c) [378]. In the presence of HAase or *S. aureus*, the degradation of the multilayer films caused more than 50% Van released from the TNTs during 24 h, with an antibacterial rate of higher than 80%. Meanwhile, the hybrid surface obviously improved the initial adhesion of rat calvaria osteoblast, and significantly cleared infection from the surrounding medulla because of the self-responsiveness after implantation in distal femur of Sprague-Dawley (SD) rats. In some cases, hyaluronate can be further conjugated with antibacterial agents as the capping component, while another drug facilitating osteogenic differentiation is loaded into the TNTs to a achieve a bi-functional property. For instance, the sodium hyaluronate-lauric acid (SL) conjugates [379] or hyaluronic acid (HA)-gentamicin (Gen) conjugates along with chitosan [380], were used

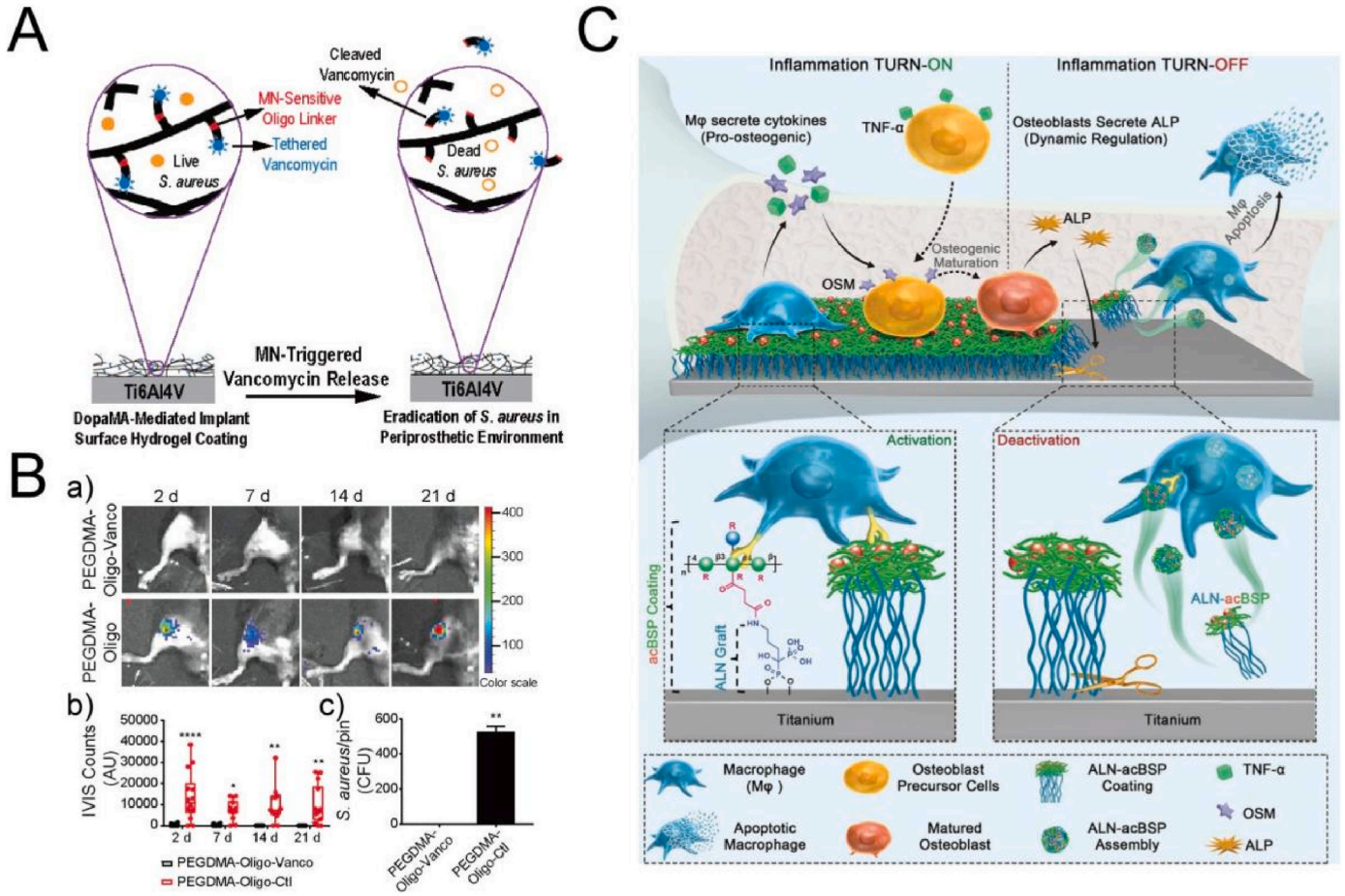

Fig. 22. (A) Schematic diagram of micrococcal-nuclease-triggered vancomycin from implant coating [381].
(B) Eradication assay of *S. aureus* inoculated in the part of mouse femoral canal: (a) IVIS images of femurs injected with *S. aureus* and implanted with IM pins modified with PEGDMA-Oligo-Vanco or PEGDMA-Oligo coatings, (b) quantitative results of longitudinal bioluminescence signals of femurs injected with *S. aureus* and implanted with different hydrogel-coated pins, and (c) *S. aureus* recovery of explanted pins after 21 days [381]. Reprinted with permission from Ref. [381].
(C) Schematic diagram of a "bridge-burning" coating consisting of acetyl glucomannan (acBSP) and alendronate (ALN) on Ti surface to switch on and off macrophages during bone healing [384]. Reprinted with permission from Ref. [384].

to cap the BMP-2- or deferoxamine (DFO)-loaded TNTs, respectively. Such constructed surfaces not only showed antifouling and antibacterial properties, but also exhibited improved osteogenic differentiation. In addition, other enzymes including micrococcal nucleases [381,382] and serine protease-like protease (SplB) [383] both secreted by *S. aureus*, have been exploited to trigger the surface response as well. For instance, Ghimire et al. conjugated vancomycin to a poly(ethylene glycol) dimethacrylate hydrogel coating on Ti6Al4V surface with an oligonucleotide linker sensitive to *S. aureus* micrococcal nuclease (MN) [381], as shown in Fig. 22A and B. The coating effectively prevented *S. aureus* infection in mouse femoral canals, because the released vancomycin triggered by MN caused the timely eradication of *S. aureus* around the implant surface and inhibited the subsequent development of osteomyelitis. The effective tethering vancomycin dose (0.6 μg/mg PEGDMA) was >200 times lower than the prophylactic antibiotic amounts used in bone cements, suggesting a potential application in timely bacterial elimination. Beyond the bacteria-related enzymes, another osteoblast-related enzymes, including ALP [384], are also used to modify the surface response. A "bridge-burning" coating consisting of acetyl glucomannan (acBSP) and alendronate (ALN) was constructed on Ti surface to switch on and off macrophages during bone healing, where ALN served as a linker molecule to bridge the acBSP and Ti surface, as shown in Fig. 22C [384]. In vitro evaluations showed that acBSP activated macrophages (primary murine bone marrow-derived) to express pro-osteogenic cytokines that contained oncostatin M (OSM). OSM as a member of pro-inflammatory interleukin-6 (IL-6) family cytokines can directly induce osteogenesis, which greatly stimulated the expression of ALP and osteocalcin (OCN) of MC3T3-E1 cells during 14 days ("switch-on"). The gradually elevated ALP contents in turn hydrolyzed the ALN linker to release ALN-acBSP complexes ("switch-off"), which killed the pro-inflammatory macrophage. In vivo results in an osteoporotic rat model showed that such a bioresponsive coating significantly improved bone-implant contact ratio (94.35% at day 28) via regulating local inflammatory niches, which provided a strategy for immunomodulatory surface modification.

4. Conclusions and perspectives

Ti and its alloys have been widely used as orthopedic implants for several decades. Though diverse applications have been realized such as artificial joints, dental implants and bone fixtures, there are still many avenues available for further development of the current approaches to meet the clinical requirements. Recent explorations in connecting fields open such interdisciplinary reach up to new strategies and methods. The development of new alloying and additive methods, the emergence of various types of biological molecules (biomolecular chemistry) and the deep understanding towards regulatory mechanism of bone-implant interaction, make Ti-based implants more potent multifunctional and high-performance, which provide emerging and prospective approaches for surface engineering.

Some new types of Ti-based alloys have been developed by adding specific elements, to improve the mechanical properties, corrosion resistance and biocompatibility. As stated above, the modulus of pure Ti is ~120 GPa, which is much higher than that for cortical bone of 10–30 GPa. The mismatched modulus between implants and adjacent bone tissue can induce stress shielding effect with bone resorption surrounding the materials [37]. Therefore, it is necessary to develop low modulus Ti-alloys to reduce modulus mismatch. Historically, Ti6Al4V is the first developed alloy for artificial implants, however, the toxicity of Al and V have aroused great concern because both of them may cause long-term side effects, including Alzheimer and neuropathy diseases [385]. Instead of such toxic components, less toxic elements as β-stabilizers are involved, including Nb, Mo, Ta, Zr, Mn as well as Sn [386]. Some types of multi-element alloys, such as Ti-Mo-Ta, Ti-Mn-Mo, Ti-Nb-Zr and Ti-Mo-Zr-Fe series, were designed to lower elastic modulus, enhance corrosion resistance, and advance biocompatibility [387]. Amongst them, Ti-Nb-Ta-Zr alloys show the moduli within the range of 40–80 GPa, suggesting a great improvement in modulus matching [386]. In addition, many studies have focused on the preparation of surface coatings with good antibacterial properties; however, the added coatings have some disadvantages that include susceptibility to exfoliation and attenuation of antibacterial effect. Alternatively, antibacterial-type Ti alloys become an increasing interest as a promising strategy [388], by the addition of bio-functional elements including Cu, Ag and Zn during the alloying [389]. For instance, Cu [390], Ag [391] and Au [392] powders have been mixed with Ti powders to form Ti-Cu, Ti-Ag and Ti-Au sintered binary alloys, respectively, all of which have significantly inhibited bacterial adhesion and growth. Beyond binary alloys, the additions of Cu and Ag to Ti-13Nb-13Zr to form Ti-13Nb-13Zr-10Cu and Ti-13Nb-13Zr-12.5Ag, not only show enhanced antibacterial activity, but also exhibit a low elastic modulus of 66 GPa and 79 GPa, respectively [388]. Hence, it is facile to prepare titanium oxide layers with specific structures containing bio-functional elements on the substrate, which avoids further doping processing and also provides a rich content of the components. As such, the appearance of new types of functional Ti alloys with lower modulus and better biocompatibility, and its combination with advanced surface modification methods would greatly enrich the applications as orthopedic implants.

The advancement in biological molecules provides great potential for further innovation in implant modification, although the field of biomimetic functionalization has achieved great progress. Developments in protein and peptide chemistry allow synthesis of more specific and targeted molecules by chemical approach or recombinant expression methods [393,394]. Some recombinant proteins and synthetic peptides have the advantages over their full protein counterparts, such as the increased yielding and the decreased base sequences without compromising bioactive domain. The reduction in the length of amino acid sequences favors its biochemical stability by attenuating peptide-bond hydrolysis and conformation destruction. The peptides with various functions, including pro-angiogenic, anti-inflammatory and pro-adherence properties, can endow Ti surfaces with desirable regulations after placement in vivo [394]. Another kind of biomolecules such as oligonucleotides beyond double-stranded nucleic acids may enrich the surface modification as well. Aptamers obtained by SELEX (systematic evolution of ligands by exponential enrichment) are short oligonucleotide sequences that can bind with various targets with high affinity and high specificity, ranging from small metal ions, amino acids, proteins to even whole cells and live animals [395]. Amongst them, aptamers targeting some physiologically related molecules, such as VEGF, PDGF, coagulation factor IXa and thrombin, have been exploited and developed [396]. One typical aptamer (Macugen/pegaptanib) binding VEGF has even been approved by FDA for ophthalmic use [397]. Hence, some aptamers that target against physiologically related molecules can be applied to Ti implants to regulate the angiogenesis and osteogenesis. In one case, an aptamer (Apt19s) binding mesenchymal stem cells (MSCs) was used to modify porous hydroxyapatite-coating Ti surface via oxidize hyaluronic acid (OHA) as a linker [398]. The introduced Apt19s obviously promoted the migration towards Ti surface of bone marrow mesenchymal stem cells (MSCs) for subsequent osteogenesis differentiation. In vivo results confirmed that aptamer/hydroxyapatite-functionalized Ti surface was able to enhance MSC recruitment around the peri-implant interface to promote new bone mineralization. As such, the future development of aptamers aiming to osteogenesis-related cells or tissues may provide routines to improve the bioactivity of Ti surfaces. In addition, other classes of biomolecules including polysaccharides beyond chitosan are biological active when coating Ti surface [399]. In brief, for successful osseointegration, cells must undergo a series of cascade reactions, implying that more than one type of biological molecules and cells involve. The deeper understanding of biomolecular chemistry shows the opportunity to innovate by the selection of biomolecules to form potent interface.

The further understanding towards regulatory mechanism of bone-

implant interaction brings about new advances from different aspects. It is well known that one critical step for deciding successful implantation is no adverse host immune response occurred during the early wound healing [400]. The interaction between implants and host immune system is currently an intense field for exploration. The production of osteoimmunology is due to the fact that the immune and skeletal systems are closely related, both sharing a variety of cytokines, receptors, signaling molecules as well as transcription factors [401,402]. As a foreign body, orthopedic implants are discerned by immune cells and thus induce an obvious immune reaction which influences biological activities of osteogenesis-related cells. Such a correlative event may affect the final fate of orthopedic implants. However, the immune response used to be ignored when examining the osteogenic behavior of orthopedic implants. Therefore, the design approaches for advanced orthopedic implants should switch from being "immune friendly" to having "immunomodulatory reprogramming" capacity, which is able to regulate local immune environment and thus stimulate osteogenesis and osseointegration [403]. The immune cells exert the effects on osteogenic regulation by releasing various cytokines, thus enhancing or depressing bone formation. Amongst different immune cells, macrophages act as a significant role in the immune response, whose polarization patterns greatly influence the wound healing process [401]. The majority of macrophages typically display pro-inflammatory M1 phenotype at the early stage after injury, and thereafter, the phenotype shifts to anti-inflammatory M2 polarization [404]. The timely switching from M1 to M2 phenotype leads to the release of osteogenic cytokines that favor osteogenesis, whereas the prolonged M1 state causes the expression of fibro-enhancing cytokines that benefit the formation of fibrous capsules [405]. From the viewpoint of material design, surface properties of biomaterials, such as surface wettability, charge and morphology, significantly regulate biological behaviors of immune cells [401]. Generally, hydrophilic surfaces tend to tune macrophage activation in addition to the improved osteoblast behaviors in vitro. Hydrophilic Ti surfaces tend to downregulate the expression of pro-inflammatory cytokines including TNF-α and IL-1α, and upregulate the secretion of anti-inflammatory cytokines such as interleukins IL-4 and IL-10 [406,407]. Surface charge also influences immune response, because immune cells similar to other mammalian cells are negatively charged. The changes in surface charge of the cell membranes by the adhesion to positively charged implant surface may affect protein location and conformation, thus altering signal transduction and immune response [408]. In some cases, the movements of holes and electrons between Ti surface and cell membranes induce M2 polarization of macrophages, leading to favorable bone formation [409]. Surface morphology is of great concern for immune regulation, because surface modification about constructing specific structures plays a dominant role in improving the biocompatibility and bioactivity of orthopedic implants [407]. Ti surfaces with various dimensions ranging from nanoscale to microscale features greatly influence the attachment, spreading, cytokine/chemokine secretion of macrophages [410–412]. For instance, TiO_2 honeycomb-like structure were prepared on Ti surfaces, with various diameters of 90, 500, 1000 and 5000 nm [410]. Amongst them, 90-nm surface performed the highest expression levels of CD206, IL-4, IL-10 and BMP-2 with the polarization of macrophage towards M2 phenotype, because smaller scale provided more anchor points and minor spatial confinement for cells that benefitted filopodia formation and mechanotransduction, and activated the RhoA/Rho-associated signaling pathway. In addition, proper surface modification by improving both surface roughness and hydrophility can even compensate for the compromised function of M2 macrophage in Type 2 diabetic rat by reducing the pro-inflammatory activity and enhancing anti-inflammatory response, which restored macrophage homeostasis and provided a favorable cellular environment for osseous healing [413]. As such, the optimized relationship between osteoimmunology and surface physicochemical properties via modification not only favors the design of bioactive implants, but also polarizes the adaptive immune response towards a pro-would healing phenotype. The Ti surface with dynamic properties may spatiotemporally regulate immune system with timely macrophage phenotype transition, resulting in faster resolution of inflammation and better stem cell recruitment around implants [414].

In short, surface modification is still the dominant strategy for improving the bioactivity and biocompatibility of Ti implants. Herein, an overview of surface modification methods has been performed. Firstly, according to the formation mechanism of surface layers, conventional methods are grouped into mechanical, physical, and chemical approaches. These methods endow Ti surface with some specific properties, but it is still far from the ideal. With the development of surface engineering, surface modification methods are needed to move forward to meet the requirements of spatiotemporal modulation. Secondly, the construction of dynamic responsive surfaces is introduced as well, to satisfy the dynamic growth requirements of living cells and tissues. Such responsive surfaces are classified into light, X-ray, electrical field, piezoelectricity, ultrasound, magnetic/electromagnetic field, pH and enzyme based on the stimuli sources derived from environmental triggers or physiological triggers, which render Ti surface "smart" and responsive to surrounding environments on demand. Finally, the progress of new alloying processing, the advancement in biological molecules and the deep understanding of osteoimmunology are prospected, and all thus provide new avenues to program Ti surface with osteointegretion, which would help produce more potent bioactive implants to satisfy various clinical requirements.

CRediT authorship contribution statement

Pinliang Jiang: Writing - Original Draft, Writing - Review & Editing.
Yanmei Zhang: Writing - Original Draft.
Ren Hu: Writing - Review & Editing.
Bin Shi: Writing - Review & Editing.
Lihai Zhang: Writing - Review & Editing.
Qiaoling Huang: Writing - Review & Editing.
Yun Yang: Writing - Review & Editing.
Peifu Tang: Writing - Review & Editing.
Changjian Lin: Supervision, Writing - Review & Editing.

Ethics approval and consent to participate

The authors declare no studies related to ethics problems.

Declaration of competing interest

The authors declare no conflict of interest.

All authors have read and approved the submission of this manuscript. And we also confirm that this manuscript, or its contents in some other form, has not been published previously by any of the authors and/or is not under consideration for publication in another journal at the time of submission.

Acknowledgements

This work was financially supported by National Key Research and Development Program of China (grant Nos. 2020YFC2004900, 2016YFC1100300) and the National Natural Science Foundation of China (grant Nos. 21773199, 51571169, 52001265).

References

[1] D.F. Williams, On the nature of biomaterials, Biomaterials 30 (30) (2009) 5897–5909.
[2] I. Kulinets, 1 - biomaterials and their applications in medicine, in: S.F. Amato, R. M. Ezzell (Eds.), Regulatory Affairs for Biomaterials and Medical Devices, Woodhead Publishing, 2015, pp. 1–10.

[3] T. Hanawa, 2.1 - transition of surface modification of titanium for medical and dental use, in: F.H. Froes, M. Qian (Eds.), Titanium in Medical and Dental Applications, Woodhead Publishing, 2018, pp. 95–113.
[4] S. Bandopadhyay, N. Bandyopadhyay, S. Ahmed, V. Yadav, R.K. Tekade, Chapter 10 - current research perspectives of orthopedic implant materials, in: R. K. Tekade (Ed.), Biomaterials and Bionanotechnology, Academic Press, 2019, pp. 337–374.
[5] M. Sloan, A. Premkumar, N.P. Sheth, Projected volume of primary total joint arthroplasty in the U.S., 2014 to 2030, JBJS 100 (17) (2018).
[6] M. Abdel-Hady Gepreel, M. Niinomi, Biocompatibility of Ti-alloys for long-term implantation, J. Mech. Behav. Biomed. Mater. 20 (2013) 407–415.
[7] F.H. Froes, 1.1 - titanium for medical and dental applications—an introduction, in: F.H. Froes, M. Qian (Eds.), Titanium in Medical and Dental Applications, Woodhead Publishing, 2018, pp. 3–21.
[8] F. Variola, J.-H. Yi, L. Richert, J.D. Wuest, F. Rosei, A. Nanci, Tailoring the surface properties of Ti6Al4V by controlled chemical oxidation, Biomaterials 29 (10) (2008) 1285–1298.
[9] T. Hanawa, A comprehensive review of techniques for biofunctionalization of titanium, J Periodontal Implant Sci 41 (6) (2011) 263–272.
[10] M. Geetha, A.K. Singh, R. Asokamani, A.K. Gogia, Ti based biomaterials, the ultimate choice for orthopaedic implants – a review, Prog. Mater. Sci. 54 (3) (2009) 397–425.
[11] N.S. Manam, W.S.W. Harun, D.N.A. Shri, S.A.C. Ghani, T. Kurniawan, M. H. Ismail, M.H.I. Ibrahim, Study of corrosion in biocompatible metals for implants: a review, J. Alloys Compd. 701 (2017) 698–715.
[12] M. Prestat, D. Thierry, Corrosion of titanium under simulated inflammation conditions: clinical context and in vitro investigations, Acta Biomater. 136 (2021) 72–87.
[13] S. Grosse, H.K. Haugland, P. Lilleng, P. Ellison, G. Hallan, P.J. Høl, Wear particles and ions from cemented and uncemented titanium-based hip prostheses—a histological and chemical analysis of retrieval material, J. Biomed. Mater. Res. B Appl. Biomater. 103 (3) (2015) 709–717.
[14] D.J. Hall, R. Pourzal, J.J. Jacobs, R.M. Urban, Metal wear particles in hematopoietic marrow of the axial skeleton in patients with prior revision for mechanical failure of a hip or knee arthroplasty, J. Biomed. Mater. Res. B Appl. Biomater. 107 (6) (2019) 1930–1936.
[15] D.F. Williams, On the mechanisms of biocompatibility, Biomaterials 29 (20) (2008) 2941–2953.
[16] B.D. Ratner, Chapter 3 - the biocompatibility of implant materials, in: S. F. Badylak (Ed.), Host Response to Biomaterials, Academic Press, Oxford, 2015, pp. 37–51.
[17] X. Liu, P.K. Chu, C. Ding, Surface modification of titanium, titanium alloys, and related materials for biomedical applications, Mater. Sci. Eng. R Rep. 47 (3–4) (2004) 49–121.
[18] C. Stewart, B. Akhavan, S.G. Wise, M.M.M. Bilek, A review of biomimetic surface functionalization for bone-integrating orthopedic implants: mechanisms, current approaches, and future directions, Prog. Mater. Sci. 106 (2019), 100588.
[19] J.J. Li, H. Zreiqat, Tissue response to biomaterials, in: R. Narayan (Ed.), Encyclopedia of Biomedical Engineering, Elsevier, Oxford, 2019, pp. 270–277.
[20] S. Qiu, J. Ji, W. Sun, J. Pei, J. He, Y. Li, J.J. Li, G. Wang, Recent advances in surface manipulation using micro-contact printing for biomedical applications, Smart Materials in Medicine 2 (2021) 65–73.
[21] F.A. Shah, P. Thomsen, A. Palmquist, Osseointegration and current interpretations of the bone-implant interface, Acta Biomater. 84 (2019) 1–15.
[22] C. Hu, D. Ashok, D.R. Nisbet, V. Gautam, Bioinspired surface modification of orthopedic implants for bone tissue engineering, Biomaterials 219 (2019), 119366.
[23] J. Hasan, R. Bright, A. Hayles, D. Palms, P. Zilm, D. Barker, K. Vasilev, Preventing peri-implantitis: the quest for a next generation of titanium dental implants, ACS Biomater. Sci. Eng. 8 (11) (2022) 4697–4737.
[24] J. Raphel, M. Holodniy, S.B. Goodman, S.C. Heilshorn, Multifunctional coatings to simultaneously promote osseointegration and prevent infection of orthopaedic implants, Biomaterials 84 (2016) 301–314.
[25] M. Sundfeldt, L. V Carlsson, C. B Johansson, P. Thomsen, C. Gretzer, Aseptic loosening, not only a question of wear: a review of different theories, Acta Orthop. 77 (2) (2006) 177–197.
[26] W. Yin, M. Chen, J. Bai, Y. Xu, M. Wang, D. Geng, G. Pan, Recent advances in orthopedic polyetheretherketone biomaterials: material fabrication and biofunction establishment, Smart Materials in Medicine 3 (2022) 20–36.
[27] G.L. Koons, M. Diba, A.G. Mikos, Materials design for bone-tissue engineering, Nat. Rev. Mater. 5 (8) (2020) 584–603.
[28] H. Cao, S. Qiao, H. Qin, K.D. Jandt, Antibacterial designs for implantable medical devices: evolutions and challenges, J. Funct. Biomater. 13 (3) (2022) 86.
[29] Z. Yuan, Y. He, C. Lin, P. Liu, K. Cai, Antibacterial surface design of biomedical titanium materials for orthopedic applications, J. Mater. Sci. Technol. 78 (2021) 51–67.
[30] E. Nikoomanzari, M. Karbasi, W. C.M.A. Melo, H. Moris, K. Babaei, S. Giannakis, A. Fattah-alhosseini, Impressive strides in antibacterial performance amelioration of Ti-based implants via plasma electrolytic oxidation (PEO): a review of the recent advancements, Chem. Eng. J. 441 (2022), 136003.
[31] R.C. Costa, B.E. Nagay, C. Dini, M.H.R. Borges, L.F.B. Miranda, J.M. Cordeiro, J. G.S. Souza, C. Sukotjo, N.C. Cruz, V.A.R. Barão, The race for the optimal antimicrobial surface: perspectives and challenges related to plasma electrolytic oxidation coating for titanium-based implants, Adv. Colloid Interface Sci. 311 (2023), 102805.
[32] A.G. Gristina, Biomaterial-centered infection: microbial adhesion versus tissue integration, Science (New York, N.Y.) 237 (4822) (1987) 1588–1595.
[33] C.R. Arciola, D. Campoccia, L. Montanaro, Implant infections: adhesion, biofilm formation and immune evasion, Nat. Rev. Microbiol. 16 (7) (2018) 397–409.
[34] S.B. Goodman, Z. Yao, M. Keeney, F. Yang, The future of biologic coatings for orthopaedic implants, Biomaterials 34 (13) (2013) 3174–3183.
[35] J.C.M. Souza, M.B. Sordi, M. Kanazawa, S. Ravindran, B. Henriques, F.S. Silva, C. Aparicio, L.F. Cooper, Nano-scale modification of titanium implant surfaces to enhance osseointegration, Acta Biomater. 94 (2019) 112–131.
[36] S. Bauer, P. Schmuki, K. von der Mark, J. Park, Engineering biocompatible implant surfaces: Part I: materials and surfaces, Prog. Mater. Sci. 58 (3) (2013) 261–326.
[37] L.-C. Zhang, L.-Y. Chen, L. Wang, Surface modification of titanium and titanium alloys: technologies, developments, and future interests, Adv. Eng. Mater. 22 (5) (2020), 1901258.
[38] O. Yetik, H. Koçoğlu, Y. Yıldıran Avcu, E. Avcu, T. Sınmazçelik, The effects of grit size and blasting pressure on the surface properties of grit blasted Ti6Al4V alloy, Mater. Today Proc. 32 (2020) 27–36.
[39] L. Le Guéhennec, A. Soueidan, P. Layrolle, Y. Amouriq, Surface treatments of titanium dental implants for rapid osseointegration, Dent. Mater. 23 (7) (2007) 844–854.
[40] A. Wennerberg, T. Albrektsson, B. Andersson, An animal study of c.p. titanium screws with different surface topographies, J. Mater. Sci. Mater. Med. 6 (5) (1995) 302–309.
[41] A. Wennerberg, T. Albrektsson, J. Lausmaa, Torque and histomorphometric evaluation of c.p. titanium screws blasted with 25- and 75-μm-sized particles of Al2O3, J. Biomed. Mater. Res. 30 (2) (1996) 251–260.
[42] A. Wennerberg, T. Albrektsson, Effects of titanium surface topography on bone integration: a systematic review, Clin. Oral Implants Res. 20 (s4) (2009) 172–184.
[43] H.J. Rønold, J.E. Ellingsen, Effect of micro-roughness produced by TiO2 blasting—tensile testing of bone attachment by using coin-shaped implants, Biomaterials 23 (21) (2002) 4211–4219.
[44] G. Thompson, D. Puleo, Ti-6Al-4V ion solution inhibition of osteogenic cell phenotype as a function of differentiation timecourse in vitro, Biomaterials 17 (20) (1996) 1949–1954.
[45] Z.L. Sun, J.C. Wataha, C.T. Hanks, Effects of metal ions on osteoblast-like cell metabolism and differentiation, J. Biomed. Mater. Res. 34 (1) (1997) 29–37.
[46] A. Canabarro, M.G. Diniz, S. Paciornik, L. Carvalho, E.M. Sampaio, M.M. Beloti, A.L. Rosa, R.G. Fischer, High concentration of residual aluminum oxide on titanium surface inhibits extracellular matrix mineralization, J. Biomed. Mater. Res. 87A (3) (2008) 588–597.
[47] S. Stea, L. Savarino, A. Toni, A. Sudanese, A. Giunti, A. Pizzoferrato, Microradiographic and histochemical evaluation of mineralization inhibition at the bone-alumina interface, Biomaterials 13 (10) (1992) 664–667.
[48] M. B, F. K, B. S, I. S, A. W, H.Jr P, K. K, Adverse tissue reactions to wear particles from Co-alloy articulations, increased by alumina-blasting particle contamination from cementless Ti-based total hip implants, The Journal of Bone and Joint Surgery. British 84-B (1) (2002) 128–136.
[49] M. Rüger, T.J. Gensior, C. Herren, M.v. Walter, C. Ocklenburg, R. Marx, H.-J. Erli, The removal of Al2O3 particles from grit-blasted titanium implant surfaces: effects on biocompatibility, osseointegration and interface strength in vivo, Acta Biomater. 6 (7) (2010) 2852–2861.
[50] A. Citeau, J. Guicheux, C. Vinatier, P. Layrolle, T.P. Nguyen, P. Pilet, G. Daculsi, In vitro biological effects of titanium rough surface obtained by calcium phosphate grid blasting, Biomaterials 26 (2) (2005) 157–165.
[51] I. Bajpai, I. Hidayat, I. Song, J. Lee, S. Kim, Comparison of hydroxyapatite and alumina grits blasted Ti surface for in-vitro cell adhesion and proliferation, Journal of Biomaterials and Tissue Engineering 5 (5) (2015) 403–410.
[52] R.K. Guduru, U. Dixit, A. Kumar, A critical review on thermal spray based manufacturing technologies, Mater. Today Proc. 62 (2022) 7265–7269.
[53] T.-Y. Liao, A. Biesiekierski, C.C. Berndt, P.C. King, E.P. Ivanova, H. Thissen, P. Kingshott, Multifunctional cold spray coatings for biological and biomedical applications: a review, Prog. Surf. Sci. 97 (2) (2022), 100654.
[54] N. Jagadeeshanayaka, S. Awasthi, S.C. Jambagi, C. Srivastava, Bioactive surface modifications through thermally sprayed hydroxyapatite composite coatings: a review of selective reinforcements, Biomater. Sci. 10 (10) (2022) 2484–2523.
[55] S. Kuroda, J. Kawakita, M. Watanabe, H. Katanoda, Warm spraying—a novel coating process based on high-velocity impact of solid particles, Sci. Technol. Adv. Mater. 9 (3) (2008), 033002.
[56] A.S.M. Ang, C.C. Berndt, A review of testing methods for thermal spray coatings, Int. Mater. Rev. 59 (4) (2014) 179–223.
[57] D. Tejero-Martin, M. Rezvani Rad, A. McDonald, T. Hussain, Beyond traditional coatings: a review on thermal-sprayed functional and smart coatings, J. Therm. Spray Technol. 28 (4) (2019) 598–644.
[58] S.R. Paital, N.B. Dahotre, Calcium phosphate coatings for bio-implant applications: materials, performance factors, and methodologies, Mater. Sci. Eng. R Rep. 66 (1–3) (2009) 1–70.
[59] A.H. Choi, S. Akyol, A. Bendavid, B. Ben-Nissan, 2.3 - nanobioceramic thin films: surface modifications and cellular responses on titanium implants, in: F.H. Froes, M. Qian (Eds.), Titanium in Medical and Dental Applications, Woodhead Publishing, 2018, pp. 147–173.
[60] A. Schroeder, E. van der Zypen, H. Stich, F. Sutter, The reactions of bone, connective tissue, and epithelium to endosteal implants with titanium-sprayed surfaces, J. Maxillofac. Surg. 9 (1981) 15–25.
[61] J.Y. Martin, Z. Schwartz, T.W. Hummert, D.M. Schraub, J. Simpson, J. Lankford Jr., D.D. Dean, D.L. Cochran, B.D. Boyan, Effect of titanium surface

roughness on proliferation, differentiation, and protein synthesis of human osteoblast-like cells (MG63), J. Biomed. Mater. Res. 29 (3) (1995) 389–401.
[62] A. Bagno, C. Di Bello, Surface treatments and roughness properties of Ti-based biomaterials, J. Mater. Sci. Mater. Med. 15 (9) (2004) 935–949.
[63] M.V. Capilla, M.N.R. Olid, M.V.O. Gaya, C.R. Botella, C.Z. Romera, Cylindrical dental implants with hydroxyapatite- and titanium plasma spray–coated surfaces: 5-year results, J. Oral Implantol. 33 (2) (2007) 59–68.
[64] M. Browne, P.J. Gregson, Effect of mechanical surface pretreatment on metal ion release, Biomaterials 21 (4) (2000) 385–392.
[65] M. Franchi, E. Orsini, D. Martini, V. Ottani, M. Fini, G. Giavaresi, R. Giardino, A. Ruggeri, Destination of titanium particles detached from titanium plasma sprayed implants, Micron 38 (6) (2007) 618–625.
[66] D. Martini, M. Fini, M. Franchi, V.D. Pasquale, B. Bacchelli, M. Gamberini, A. Tinti, P. Taddei, G. Giavaresi, V. Ottani, M. Raspanti, S. Guizzardi, A. Ruggeri, Detachment of titanium and fluorohydroxyapatite particles in unloaded endosseous implants, Biomaterials 24 (7) (2003) 1309–1316.
[67] R.B. Heimann, Structure, properties, and biomedical performance of osteoconductive bioceramic coatings, Surf. Coating. Technol. 233 (2013) 27–38.
[68] F. Ma, P. P.-B, Early migration and late aseptic failure of proximal femoral prostheses, The Journal of Bone and Joint Surgery. British 76-B (3) (1994) 432–438.
[69] D.D. D'Lima, R.H. Walker, C.W. Colwell Jr., Omnifit-HA stem in total hip arthroplasty. A 2- to 5-year followup, Clin. Orthop. Relat. Res. (363) (1999) 163–169.
[70] W.N. Capello, J.A. D'Antonio, W.L. Jaffe, R.G. Geesink, M.T. Manley, J. R. Feinberg, Hydroxyapatite-coated femoral components - 15-year minimum followup, Clin. Orthop. Relat. Res. (453) (2006) 75–80.
[71] J.-A. Epinette, M.T. Manley, Uncemented stems in hip replacement - hydroxyapatite or plain porous: does it matter? Based on a prospective study of HA Omnifit stems at 15-years minimum follow-up, HIP Int. 18 (2) (2008) 69–74.
[72] R.B. Heimann, Plasma-sprayed hydroxylapatite-based coatings: chemical, mechanical, microstructural, and biomedical properties, J. Therm. Spray Technol. 25 (5) (2016) 827–850.
[73] C.C. Berndt, F. Hasan, U. Tietz, K.P. Schmitz, A review of hydroxyapatite coatings manufactured by thermal spray, in: B. Ben-Nissan (Ed.), Advances in Calcium Phosphate Biomaterials, Springer Berlin Heidelberg, Berlin, Heidelberg, 2014, pp. 267–329.
[74] W.S.W. Harun, R.I.M. Asri, J. Alias, F.H. Zulkifli, K. Kadirgama, S.A.C. Ghani, J.H. M. Shariffuddin, A comprehensive review of hydroxyapatite-based coatings adhesion on metallic biomaterials, Ceram. Int. 44 (2) (2018) 1250–1268.
[75] X. Liu, D. He, Z. Zhou, G. Wang, Z. Wang, X. Guo, Effect of post-heat treatment on the microstructure of micro-plasma sprayed hydroxyapatite coatings, Surf. Coating. Technol. 367 (2019) 225–230.
[76] C.-W. Yang, T.-S. Lui, T.-M. Lee, E. Chang, Effect of hydrothermal treatment on microstructural feature and bonding strength of plasma-sprayed hydroxyapatite on Ti-6Al-4V, Mater. Trans. 45 (9) (2004) 2922–2929.
[77] R. Kumar, P. Cheang, K.A. Khor, Radio frequency (RF) suspension plasma sprayed ultra-fine hydroxyapatite (HA)/zirconia composite powders, Biomaterials 24 (15) (2003) 2611–2621.
[78] S. Singh, C. Prakash, H. Singh, Deposition of HA-TiO2 by plasma spray on β-phase Ti-35Nb-7Ta-5Zr alloy for hip stem: characterization, mechanical properties, corrosion, and in-vitro bioactivity, Surf. Coating. Technol. 398 (2020), 126072.
[79] J. Singh, S.S. Chatha, H. Singh, Characterization and corrosion behavior of plasma sprayed calcium silicate reinforced hydroxyapatite composite coatings for medical implant applications, Ceram. Int. 47 (1) (2021) 782–792.
[80] R.S. Lima, K.A. Khor, H. Li, P. Cheang, B.R. Marple, HVOF spraying of nanostructured hydroxyapatite for biomedical applications, Mater. Sci. Eng., A 396 (1) (2005) 181–187.
[81] F. Ghadami, S. Saber-Samandari, G. Rouhi, M. Amani Hamedani, M.M. Dehghan, S. Farzad Mohajeri, F. Mashhadi-Abbas, H. Gholami, The effects of bone implants' coating mechanical properties on osseointegration: in vivo, in vitro, and histological investigations, J. Biomed. Mater. Res. 106 (10) (2018) 2679–2691.
[82] R.S. Lima, S. Dimitrievska, M.N. Bureau, B.R. Marple, A. Petit, F. Mwale, J. Antoniou, HVOF-sprayed nano TiO2-HA coatings exhibiting enhanced biocompatibility, J. Therm. Spray Technol. 19 (1) (2010) 336–343.
[83] A.M. Vilardell, N. Cinca, A. Concustell, S. Dosta, I.G. Cano, J.M. Guilemany, Cold spray as an emerging technology for biocompatible and antibacterial coatings: state of art, J. Mater. Sci. 50 (13) (2015) 4441–4462.
[84] A.M. Vilardell, N. Cinca, N. Garcia-Giralt, S. Dosta, I.G. Cano, X. Nogués, J. M. Guilemany, Osteoblastic cell response on high-rough titanium coatings by cold spray, J. Mater. Sci. Mater. Med. 29 (2) (2018) 19.
[85] J. Tang, Z. Zhao, X. Cui, J. Wang, T. Xiong, Microstructure and bioactivity of a cold sprayed rough/porous Ta coating on Ti6Al4V substrate, Sci. China Technol. Sci. 63 (5) (2020) 731–739.
[86] A.M. Vilardell, N. Cinca, N. Garcia-Giralt, S. Dosta, I.G. Cano, X. Nogués, J. M. Guilemany, In-vitro comparison of hydroxyapatite coatings obtained by cold spray and conventional thermal spray technologies, Mater. Sci. Eng. C 107 (2020), 110306.
[87] D. Li, X. Chen, Y. Gong, B. Zhang, Y. Liu, P. Jin, H. Li, Synthesis and vacuum cold spray deposition of biofunctionalized nanodiamond/hydroxyapatite nanocomposite for biomedical applications, Adv. Eng. Mater. 19 (12) (2017), 1700363.
[88] D. Li, Y. Gong, X. Chen, B. Zhang, H. Zhang, P. Jin, H. Li, Room-temperature deposition of hydroxyapatite/antibiotic composite coatings by vacuum cold spraying for antibacterial applications, Surf. Coating. Technol. 330 (2017) 87–91.
[89] T. Lu, Y. Qiao, X. Liu, Surface modification of biomaterials using plasma immersion ion implantation and deposition, Interface Focus 2 (3) (2012) 325–336.
[90] W. Jin, P.K. Chu, Surface functionalization of biomaterials by plasma and ion beam, Surf. Coating. Technol. 336 (2018) 2–8.
[91] S. Mändl, D. Manova, Modification of metals by plasma immersion ion implantation, Surf. Coating. Technol. 365 (2019) 83–93.
[92] P. Liu, G. Wang, Q. Ruan, K. Tang, P.K. Chu, Plasma-activated interfaces for biomedical engineering, Bioact. Mater. 6 (7) (2021) 2134–2143.
[93] H.-H. Huang, D.-K. Shiau, C.-S. Chen, J.-H. Chang, S. Wang, H. Pan, M.-F. Wu, Nitrogen plasma immersion ion implantation treatment to enhance corrosion resistance, bone cell growth, and antibacterial adhesion of Ti-6Al-4V alloy in dental applications, Surf. Coating. Technol. 365 (2019) 179–188.
[94] C.-S. Chen, J.-H. Chang, V. Srimaneepong, J.-Y. Wen, O.-H. Tung, C.-H. Yang, H.-C. Lin, T.-H. Lee, Y. Han, H.-H. Huang, Improving the in vitro cell differentiation and in vivo osseointegration of titanium dental implant through oxygen plasma immersion ion implantation treatment, Surf. Coating. Technol. 399 (2020), 126125.
[95] D.-K. Shiau, C.-H. Yang, Y.-S. Sun, M.-F. Wu, H. Pan, H.-H. Huang, Enhancing the blood response and antibacterial adhesion of titanium surface through oxygen plasma immersion ion implantation treatment, Surf. Coating. Technol. 365 (2019) 173–178.
[96] Y. Xie, X. Liu, A. Huang, C. Ding, P.K. Chu, Improvement of surface bioactivity on titanium by water and hydrogen plasma immersion ion implantation, Biomaterials 26 (31) (2005) 6129–6135.
[97] J. Tan, C. Wang, D. Wang, H. Jiang, Y. Qiao, D. Zhang, X. Zhang, R. Xu, C. Liu, J. Su, W. Weng, X. Liu, Tailoring time-varying alkaline microenvironment on titanium for sequential anti-infection and osseointegration, Chem. Eng. J. 431 (2022), 133940.
[98] H. Cao, X. Liu, F. Meng, P.K. Chu, Biological actions of silver nanoparticles embedded in titanium controlled by micro-galvanic effects, Biomaterials 32 (3) (2011) 693–705.
[99] G. Wang, W. Jin, A.M. Qasim, A. Gao, X. Peng, W. Li, H. Feng, P.K. Chu, Antibacterial effects of titanium embedded with silver nanoparticles based on electron-transfer-induced reactive oxygen species, Biomaterials 124 (2017) 25–34.
[100] Y. Qiao, W. Zhang, P. Tian, F. Meng, H. Zhu, X. Jiang, X. Liu, P.K. Chu, Stimulation of bone growth following zinc incorporation into biomaterials, Biomaterials 35 (25) (2014) 6882–6897.
[101] G. Jin, H. Qin, H. Cao, S. Qian, Y. Zhao, X. Peng, X. Zhang, X. Liu, P.K. Chu, Synergistic effects of dual Zn/Ag ion implantation in osteogenic activity and antibacterial ability of titanium, Biomaterials 35 (27) (2014) 7699–7713.
[102] H. Cao, K. Tang, X. Liu, Bifunctional galvanics mediated selective toxicity on titanium, Mater. Horiz. 5 (2) (2018) 264–267.
[103] L. Wang, Q. Luo, X. Zhang, J. Qiu, S. Qian, X. Liu, Co-implantation of magnesium and zinc ions into titanium regulates the behaviors of human gingival fibroblasts, Bioact. Mater. 6 (1) (2021) 64–74.
[104] S. Mei, H. Wang, W. Wang, L. Tong, H. Pan, C. Ruan, Q. Ma, M. Liu, H. Yang, L. Zhang, Y. Cheng, Y. Zhang, L. Zhao, P.K. Chu, Antibacterial effects and biocompatibility of titanium surfaces with graded silver incorporation in titania nanotubes, Biomaterials 35 (14) (2014) 4255–4265.
[105] X. Zhao, J. Yang, J. You, Surface modification of TiO2 coatings by Zn ion implantation for improving antibacterial activities, Bull. Mater. Sci. 39 (1) (2016) 285–291.
[106] M. Cheng, Y. Qiao, Q. Wang, G. Jin, H. Qin, Y. Zhao, X. Peng, X. Zhang, X. Liu, Calcium plasma implanted titanium surface with hierarchical microstructure for improving the bone formation, ACS Appl. Mater. Interfaces 7 (23) (2015) 13053–13061.
[107] X. Lin, L. Zhou, S. Li, H. Lu, X. Ding, Behavior of acid etching on titanium: topography, hydrophility and hydrogen concentration, Biomed. Mater. 9 (1) (2013), 015002.
[108] N. Ren, G. Wang, H. Liu, T. Ohachi, In situ synthesis of TiH2 layer on metallic titanium foil through gaseous hydrogen free acid-hydrothermal method, Mater. Res. Bull. 50 (2014) 379–384.
[109] S. Ban, Y. Iwaya, H. Kono, H. Sato, Surface modification of titanium by etching in concentrated sulfuric acid, Dent. Mater. 22 (12) (2006) 1115–1120.
[110] J.E. Davies, Understanding peri-implant endosseous healing, J. Dent. Educ. 67 (8) (2003) 932–949.
[111] S.F. Lamolle, M. Monjo, M. Rubert, H.J. Haugen, S.P. Lyngstadaas, J.E. Ellingsen, The effect of hydrofluoric acid treatment of titanium surface on nanostructural and chemical changes and the growth of MC3T3-E1 cells, Biomaterials 30 (5) (2009) 736–742.
[112] L.F. Cooper, Y. Zhou, J. Takebe, J. Guo, A. Abron, A. Holmén, J.E. Ellingsen, Fluoride modification effects on osteoblast behavior and bone formation at TiO2 grit-blasted c.p. titanium endosseous implants, Biomaterials 27 (6) (2006) 926–936.
[113] D. Li, S.J. Ferguson, T. Beutler, D.L. Cochran, C. Sittig, H.P. Hirt, D. Buser, Biomechanical comparison of the sandblasted and acid-etched and the machined and acid-etched titanium surface for dental implants, J. Biomed. Mater. Res. 60 (2) (2002) 325–332.
[114] S.K. Roehling, B. Meng, D.L. Cochran, Sandblasted and acid-etched implant surfaces with or without high surface free energy: experimental and clinical background, in: A. Wennerberg, T. Albrektsson, R. Jimbo (Eds.), Implant Surfaces and Their Biological and Clinical Impact, Springer Berlin Heidelberg, Berlin, Heidelberg, 2015, pp. 93–136.

[115] J.-Y. Choi, S. Kim, S.B. Jo, H.K. Kang, S.Y. Jung, S.W. Kim, B.-M. Min, I.-S.L. Yeo, A laminin-211-derived bioactive peptide promotes the osseointegration of a sandblasted, large-grit, acid-etched titanium implant, J. Biomed. Mater. Res. 108 (5) (2020) 1214–1222.
[116] D. Buser, S.F.M. Janner, J.-G. Wittneben, U. Brägger, C.A. Ramseier, G.E. Salvi, 10-Year survival and success rates of 511 titanium implants with a sandblasted and acid-etched surface: a retrospective study in 303 partially edentulous patients, Clin. Implant Dent. Relat. Res. 14 (6) (2012) 839–851.
[117] H.-M. Kim, F. Miyaji, T. Kokubo, T. Nakamura, Preparation of bioactive Ti and its alloys via simple chemical surface treatment, J. Biomed. Mater. Res. 32 (3) (1996) 409–417.
[118] T. Kokubo, S. Yamaguchi, Novel bioactive materials developed by simulated body fluid evaluation: surface-modified Ti metal and its alloys, Acta Biomater. 44 (2016) 16–30.
[119] T. Kokubo, S. Yamaguchi, Simulated body fluid and the novel bioactive materials derived from it, J. Biomed. Mater. Res. 107 (5) (2019) 968–977.
[120] S. Yamaguchi, H. Takadama, T. Matsushita, T. Nakamura, T. Kokubo, Cross-sectional analysis of the surface ceramic layer developed on Ti metal by NaOH-heat treatment and soaking in SBF, J. Ceram. Soc. Jpn. 117 (1370) (2009) 1126–1130.
[121] H.M. Kim, F. Miyaji, T. Kokubo, T. Nakamura, Bonding strength of bonelike apatite layer to Ti metal substrate, J. Biomed. Mater. Res. 38 (2) (1997) 121–127.
[122] S. Nishiguchi, T. Nakamura, M. Kobayashi, H.-M. Kim, F. Miyaji, T. Kokubo, The effect of heat treatment on bone-bonding ability of alkali-treated titanium, Biomaterials 20 (5) (1999) 491–500.
[123] Y. Su, S. Komasa, T. Sekino, H. Nishizaki, J. Okazaki, Nanostructured Ti6Al4V alloy fabricated using modified alkali-heat treatment: characterization and cell adhesion, Mater. Sci. Eng. C 59 (2016) 617–623.
[124] T. Kizuki, H. Takadama, T. Matsushita, T. Nakamura, T. Kokubo, Preparation of bioactive Ti metal surface enriched with calcium ions by chemical treatment, Acta Biomater. 6 (7) (2010) 2836–2842.
[125] A. Fukuda, M. Takemoto, T. Saito, S. Fujibayashi, M. Neo, S. Yamaguchi, T. Kizuki, T. Matsushita, M. Niinomi, T. Kokubo, T. Nakamura, Bone bonding bioactivity of Ti metal and Ti–Zr–Nb–Ta alloys with Ca ions incorporated on their surfaces by simple chemical and heat treatments, Acta Biomater. 7 (3) (2011) 1379–1386.
[126] M. Tanaka, M. Takemoto, S. Fujibayashi, T. Kawai, S. Yamaguchi, T. Kizuki, T. Matsushita, T. Kokubo, T. Nakamura, S. Matsuda, Bone bonding ability of a chemically and thermally treated low elastic modulus Ti alloy: gum metal, J. Mater. Sci. Mater. Med. 25 (3) (2014) 635–643.
[127] Y. Tian, S. Fujibayashi, S. Yamaguchi, T. Matsushita, T. Kokubo, S. Matsuda, In vivo study of the early bone-bonding ability of Ti meshes formed with calcium titanate via chemical treatments, J. Mater. Sci. Mater. Med. 26 (12) (2015) 271.
[128] A. Rodríguez-Contreras, D. Torres, B. Rafik, M. Ortiz-Hernandez, M.P. Ginebra, J. A. Calero, J.M. Manero, E. Ruperez, Bioactivity and antibacterial properties of calcium- and silver-doped coatings on 3D printed titanium scaffolds, Surf. Coating. Technol. 421 (2021), 127476.
[129] S. Yamaguchi, S. Nath, T. Matsushita, T. Kokubo, Controlled release of strontium ions from a bioactive Ti metal with a Ca-enriched surface layer, Acta Biomater. 10 (5) (2014) 2282–2289.
[130] T. Kokubo, H.-M. Kim, M. Kawashita, T. Nakamura, REVIEW Bioactive metals: preparation and properties, J. Mater. Sci. Mater. Med. 15 (2) (2004) 99–107.
[131] K. Kawanabe, K. Ise, K. Goto, H. Akiyama, T. Nakamura, A. Kaneuji, T. Sugimori, T. Matsumoto, A new cementless total hip arthroplasty with bioactive titanium porous-coating by alkaline and heat treatment: average 4.8-year results, J. Biomed. Mater. Res. B Appl. Biomater. 90B (1) (2009) 476–481.
[132] K. So, A. Kaneuji, T. Matsumoto, S. Matsuda, H. Akiyama, Is the bone-bonding ability of a cementless total hip prosthesis enhanced by alkaline and heat treatments? Clin. Orthop. Relat. Res. 471 (12) (2013) 3847–3855.
[133] D. Gong, C.A. Grimes, O.K. Varghese, W. Hu, R.S. Singh, Z. Chen, E.C. Dickey, Titanium oxide nanotube arrays prepared by anodic oxidation, J. Mater. Res. 16 (12) (2001) 3331–3334.
[134] P. Roy, S. Berger, P. Schmuki, TiO2 nanotubes: synthesis and applications, Angew. Chem. Int. Ed. 50 (13) (2011) 2904–2939.
[135] A. Gao, R. Hang, L. Bai, B. Tang, P.K. Chu, Electrochemical surface engineering of titanium-based alloys for biomedical application, Electrochim. Acta 271 (2018) 699–718.
[136] D. Kowalski, D. Kim, P. Schmuki, TiO2 nanotubes, nanochannels and mesosponge: self-organized formation and applications, Nano Today 8 (3) (2013) 235–264.
[137] J. Park, S. Bauer, K. von der Mark, P. Schmuki, Nanosize and vitality: TiO2 nanotube diameter directs cell fate, Nano Lett. 7 (6) (2007) 1686–1691.
[138] S. Oh, K.S. Brammer, Y.S.J. Li, D. Teng, A.J. Engler, S. Chien, S. Jin, Stem cell fate dictated solely by altered nanotube dimension, Proc. Natl. Acad. Sci. USA 106 (7) (2009) 2130–2135.
[139] Y. Zhang, R. Luo, J. Tan, J. Wang, X. Lu, S. Qu, J. Weng, B. Feng, Osteoblast behaviors on titania nanotube and mesopore layers, Regenerative Biomaterials 4 (2) (2016) 81–87.
[140] B. Voltrova, V. Hybasek, V. Blahnova, J. Sepitka, V. Lukasova, K. Vocetkova, V. Sovkova, R. Matejka, J. Fojt, L. Joska, M. Daniel, E. Filova, Different diameters of titanium dioxide nanotubes modulate Saos-2 osteoblast-like cell adhesion and osteogenic differentiation and nanomechanical properties of the surface, RSC Adv. 9 (20) (2019) 11341–11355.
[141] E. Filova, J. Fojt, M. Kryslova, H. Moravec, L. Joska, L. Bacakova, The diameter of nanotubes formed on Ti-6Al-4V alloy controls the adhesion and differentiation of Saos-2 cells, Int. J. Nanomed. 10 (2015) 7145–7163.
[142] Y. Yu, X. Shen, Z. Luo, Y. Hu, M. Li, P. Ma, Q. Ran, L. Dai, Y. He, K. Cai, Osteogenesis potential of different titania nanotubes in oxidative stress microenvironment, Biomaterials 167 (2018) 44–57.
[143] S. Oh, K.S. Brammer, Y.S.J. Li, D. Teng, A.J. Engler, S. Chien, S. Jin, Reply to von der Mark et al.: looking further into the effects of nanotube dimension on stem cell fate, Proc. Natl. Acad. Sci. USA 106 (24) (2009) E61.
[144] Y.T. Sul, Electrochemical growth behavior, surface properties, and enhanced in vivo bone response of TiO2 nanotubes on microstructured surfaces of blasted, screw-shaped titanium implants, Int. J. Nanomed. 5 (2010) 87–100.
[145] P. S. E, F. J. D, R. P. C, K. S. V, S. N. V, S. O, S. J, Effects of titanium nanotubes on the osseointegration, cell differentiation, mineralisation and antibacterial properties of orthopaedic implant surfaces, The Bone & Joint Journal 100-B (1_Supple_A) (2018) 9–16.
[146] L.M. Bjursten, L. Rasmusson, S. Oh, G.C. Smith, K.S. Brammer, S. Jin, Titanium dioxide nanotubes enhance bone bonding in vivo, J. Biomed. Mater. Res. 92A (3) (2010) 1218–1224.
[147] C. Wang, Y. Liu, X. Hu, X. Shang, S. Ma, H. Guo, X. Ma, D. Cai, Z. Hu, Y. Zhao, Y. Zhu, Z. Cao, H. Yu, W. Cheng, Titanium dioxide nanotubes increase purinergic receptor P2Y6 expression and activate its downstream PKCα-ERK1/2 pathway in bone marrow mesenchymal stem cells under osteogenic induction, Acta Biomater. 157 (2023) 670–682.
[148] W.Q. Yu, Y.L. Zhang, X.Q. Jiang, F.Q. Zhang, In vitro behavior of MC3T3-E1 preosteoblast with different annealing temperature titania nanotubes, Oral Dis. 16 (7) (2010) 624–630.
[149] J. Park, S. Bauer, P. Schmuki, K. von der Mark, Narrow window in nanoscale dependent activation of endothelial cell growth and differentiation on TiO2 nanotube surfaces, Nano Lett. 9 (9) (2009) 3157–3164.
[150] I.-H. Bae, K.-D. Yun, H.-S. Kim, B.-C. Jeong, H.-P. Lim, S.-W. Park, K.-M. Lee, Y.-C. Lim, K.-K. Lee, Y. Yang, J.-T. Koh, Anodic oxidized nanotubular titanium implants enhance bone morphogenetic protein-2 delivery, J. Biomed. Mater. Res. B Appl. Biomater. 93B (2) (2010) 484–491.
[151] W. Zhang, Y. Jin, S. Qian, J. Li, Q. Chang, D. Ye, H. Pan, M. Zhang, H. Cao, X. Liu, X. Jiang, Vacuum extraction enhances rhPDGF-BB immobilization on nanotubes to improve implant osseointegration in ovariectomized rats, Nanomed. Nanotechnol. Biol. Med. 10 (8) (2014) 1809–1818.
[152] Q. Ma, W. Wang, P.K. Chu, S. Mei, K. Ji, L. Jin, Y. Zhang, Concentration- and time-dependent response of human gingival fibroblasts to fibroblast growth factor 2 immobilized on titanium dental implants, Int. J. Nanomed. 7 (2012) 1965–1976.
[153] L. Draghi, V. Preda, M. Moscatelli, M. Santin, R. Chiesa, Gentamicin-loaded TiO2 nanotubes as improved antimicrobial surfaces for orthopedic implants, Frontiers in Materials 7 (2020).
[154] L. Peng, A.D. Mendelsohn, T.J. LaTempa, S. Yoriya, C.A. Grimes, T.A. Desai, Long-term small molecule and protein elution from TiO2 nanotubes, Nano Lett. 9 (5) (2009) 1932–1936.
[155] S. Sun, Y. Zhang, D. Zeng, S. Zhang, F. Zhang, W. Yu, PLGA film/Titanium nanotubues as a sustained growth factor releasing system for dental implants, J. Mater. Sci. Mater. Med. 29 (9) (2018) 141.
[156] A.K. Baranwal, G. Keerthiga, L. Mohan, S.D. Dutta, P. Gupta, K.-T. Lim, T. S. Santra, Controlled and localized drug delivery using Titania nanotubes, Mater. Today Commun. 32 (2022), 103843.
[157] W.-E. Yang, H.-H. Huang, Improving the biocompatibility of titanium surface through formation of a TiO2 nano-mesh layer, Thin Solid Films 518 (24) (2010) 7545–7550.
[158] W.-E. Yang, H.-H. Huang, Multiform TiO2 nano-network enhances biological response to titanium surface for dental implant applications, Appl. Surf. Sci. 471 (2019) 1041–1052.
[159] A.L. Yerokhin, X. Nie, A. Leyland, A. Matthews, S.J. Dowey, Plasma electrolysis for surface engineering, Surf. Coating. Technol. 122 (2–3) (1999) 73–93.
[160] Y. Wang, H. Yu, C. Chen, Z. Zhao, Review of the biocompatibility of micro-arc oxidation coated titanium alloys, Mater. Des. 85 (2015) 640–652.
[161] A.L. Yerokhin, X. Nie, A. Leyland, A. Matthews, Characterisation of oxide films produced by plasma electrolytic oxidation of a Ti–6Al–4V alloy, Surf. Coating. Technol. 130 (2) (2000) 195–206.
[162] K. Li, T. Yan, Y. Xue, L. Guo, L. Zhang, Y. Han, Intrinsically ferromagnetic Fe-doped TiO2 coatings on titanium for accelerating osteoblast response in vitro, J. Mater. Chem. B 6 (36) (2018) 5756–5767.
[163] Y.-T. Sul, The significance of the surface properties of oxidized titanium to the bone response: special emphasis on potential biochemical bonding of oxidized titanium implant, Biomaterials 24 (22) (2003) 3893–3907.
[164] L.-H. Li, Y.-M. Kong, H.-W. Kim, Y.-W. Kim, H.-E. Kim, S.-J. Heo, J.-Y. Koak, Improved biological performance of Ti implants due to surface modification by micro-arc oxidation, Biomaterials 25 (14) (2004) 2867–2875.
[165] B.S. Necula, J.P.T.M. van Leeuwen, L.E. Fratila-Apachitei, S.A.J. Zaat, I. Apachitei, J. Duszczyk, In vitro cytotoxicity evaluation of porous TiO2–Ag antibacterial coatings for human fetal osteoblasts, Acta Biomater. 8 (11) (2012) 4191–4197.
[166] J. Ye, B. Li, M. Li, Y. Zheng, S. Wu, Y. Han, ROS induced bactericidal activity of amorphous Zn-doped titanium oxide coatings and enhanced osseointegration in bacteria-infected rat tibias, Acta Biomater. 107 (2020) 313–324.
[167] B. He, C. Xin, Y. Chen, Y. Xu, Q. Zhao, Z. Hou, Y. Tang, H. Liu, X. Su, Y. Zhao, Biological performance and tribocorrosion behavior of in-situ synthesized CuxO/TiO2 coatings, Appl. Surf. Sci. 600 (2022), 154096.
[168] X. Zhang, Y. Lv, F. Shan, Y. Wu, X. Lu, Z. Peng, B. Liu, L. Yang, Z. Dong, Microstructure, corrosion resistance, osteogenic activity and antibacterial capability of Mn-incorporated TiO2 coating, Appl. Surf. Sci. 531 (2020), 147399.

[169] M. Degidi, D. Nardi, A. Piattelli, 10-Year follow-up of immediately loaded implants with TiUnite porous anodized surface, Clin. Implant Dent. Relat. Res. 14 (6) (2012) 828–838.
[170] J. Zhang, C. Lin, Z. Feng, Z. Tian, Mechanistic studies of electrodeposition for bioceramic coatings of calcium phosphates by an in situ pH-microsensor technique, J. Electroanal. Chem. 452 (2) (1998) 235–240.
[171] N. Eliaz, M. Eliyahu, Electrochemical processes of nucleation and growth of hydroxyapatite on titanium supported by real-time electrochemical atomic force microscopy, J. Biomed. Mater. Res. 80A (3) (2007) 621–634.
[172] S.K. Yen, C.M. Lin, Cathodic reactions of electrolytic hydroxyapatite coating on pure titanium, Mater. Chem. Phys. 77 (1) (2003) 70–76.
[173] Y.-L. Lai, P.-Y. Cheng, C.-C. Yang, S.-K. Yen, Electrolytic deposition of hydroxyapatite/calcium phosphate-heparin/gelatin-heparin tri-layer composites on NiTi alloy to enhance drug loading and prolong releasing for biomedical applications, Thin Solid Films 649 (2018) 192–201.
[174] S. Pang, Y. He, P. He, X. Luo, Z. Guo, H. Li, Fabrication of two distinct hydroxyapatite coatings and their effects on MC3T3-E1 cell behavior, Colloids Surf. B Biointerfaces 171 (2018) 40–48.
[175] D. Richard, N. Dumelié, H. Benhayoune, S. Bouthors, C. Guillaume, N. Lalun, G. Balossier, D. Laurent-Maquin, Behavior of human osteoblast-like cells in contact with electrodeposited calcium phosphate coatings, J. Biomed. Mater. Res. B Appl. Biomater. 79B (1) (2006) 108–115.
[176] S. Pang, M. Sun, Z. Huang, Y. He, X. Luo, Z. Guo, H. Li, Bioadaptive nanorod array topography of hydroxyapatite and TiO2 on Ti substrate to preosteoblast cell behaviors, J. Biomed. Mater. Res. 107 (10) (2019) 2272–2281.
[177] H. Wang, N. Eliaz, Z. Xiang, H.-P. Hsu, M. Spector, L.W. Hobbs, Early bone apposition in vivo on plasma-sprayed and electrochemically deposited hydroxyapatite coatings on titanium alloy, Biomaterials 27 (23) (2006) 4192–4203.
[178] Y.C. Chai, G. Kerckhofs, S.J. Roberts, S. Van Bael, E. Schepers, J. Vleugels, F. P. Luyten, J. Schrooten, Ectopic bone formation by 3D porous calcium phosphate-Ti6Al4V hybrids produced by perfusion electrodeposition, Biomaterials 33 (16) (2012) 4044–4058.
[179] Z. Jia, X. Xu, D. Zhu, Y. Zheng, Design, printing, and engineering of regenerative biomaterials for personalized bone healthcare, Prog. Mater. Sci. 134 (2023), 101072.
[180] A.M. Pietak, J.W. Reid, M.J. Stott, M. Sayer, Silicon substitution in the calcium phosphate bioceramics, Biomaterials 28 (28) (2007) 4023–4032.
[181] R. Schmidt, A. Gebert, M. Schumacher, V. Hoffmann, A. Voss, S. Pilz, M. Uhlemann, A. Lode, M. Gelinsky, Electrodeposition of Sr-substituted hydroxyapatite on low modulus beta-type Ti-45Nb and effect on in vitro Sr release and cell response, Mater. Sci. Eng. C 108 (2020), 110425.
[182] Y. Yan, X. Zhang, Y. Huang, Q. Ding, X. Pang, Antibacterial and bioactivity of silver substituted hydroxyapatite/TiO2 nanotube composite coatings on titanium, Appl. Surf. Sci. 314 (2014) 348–357.
[183] Y. Huang, X. Zhang, R. Zhao, H. Mao, Y. Yan, X. Pang, Antibacterial efficacy, corrosion resistance, and cytotoxicity studies of copper-substituted carbonated hydroxyapatite coating on titanium substrate, J. Mater. Sci. 50 (4) (2015) 1688–1700.
[184] Y. Huang, X. Zhang, H. Mao, T. Li, R. Zhao, Y. Yan, X. Pang, Osteoblastic cell responses and antibacterial efficacy of Cu/Zn co-substituted hydroxyapatite coatings on pure titanium using electrodeposition method, RSC Adv. 5 (22) (2015) 17076–17086.
[185] D. Gopi, A. Karthika, S. Nithiya, L. Kavitha, In vitro biological performance of minerals substituted hydroxyapatite coating by pulsed electrodeposition method, Mater. Chem. Phys. 144 (1) (2014) 75–85.
[186] R. Hu, C. Lin, H. Wang, T. Tao, Modulation effects of collagen I on the structure of electrochemically deposited hydroxyapatite coating, Mater. Lett. 64 (8) (2010) 915–917.
[187] L. Yan, Y. Xiang, J. Yu, Y. Wang, W. Cui, Fabrication of antibacterial and antiwear hydroxyapatite coatings via in situ chitosan-mediated pulse electrochemical deposition, ACS Appl. Mater. Interfaces 9 (5) (2017) 5023–5030.
[188] B. Bozzini, A. Barca, F. Bogani, M. Boniardi, P. Carlino, C. Mele, T. Verri, A. Romano, Electrodeposition of nanostructured bioactive hydroxyapatite-heparin composite coatings on titanium for dental implant applications, J. Mater. Sci. Mater. Med. 25 (6) (2014) 1425–1434.
[189] R. Drevet, A. Lemelle, V. Untereiner, M. Manfait, G.D. Sockalingum, H. Benhayoune, Morphological modifications of electrodeposited calcium phosphate coatings under amino acids effect, Appl. Surf. Sci. 268 (2013) 343–348.
[190] H. Wang, C.J. Lin, R. Hu, F. Zhang, L.W. Lin, A novel nano-micro structured octacalcium phosphate/protein composite coating on titanium by using an electrochemically induced deposition, J. Biomed. Mater. Res. 87A (3) (2008) 698–705.
[191] H. Wang, C.J. Lin, R. Hu, Effects of structure and composition of the CaP composite coatings on apatite formation and bioactivity in simulated body fluid, Appl. Surf. Sci. 255 (7) (2009) 4074–4081.
[192] Y. Yang, H. Wang, F.-Y. Yan, Y. Qi, Y.-K. Lai, D.-M. Zeng, G. Chen, K.-Q. Zhang, Bioinspired porous octacalcium phosphate/silk fibroin composite coating materials prepared by electrochemical deposition, ACS Appl. Mater. Interfaces 7 (10) (2015) 5634–5642.
[193] Y. Yang, H. Wang, J.-C. Zhu, Y.-F. Shao, F.-J. Bai, X.-M. Chen, X. Li, M. Guo, Z. Shao, K.-Q. Zhang, Silk-fibroin-assisted cathodic electrolytic deposition of calcium phosphate for biomedical applications, ACS Biomater. Sci. Eng. 5 (9) (2019) 4302–4310.
[194] Z. Hadzhieva, A.R. Boccaccini, Recent developments in electrophoretic deposition (EPD) of antibacterial coatings for biomedical applications - a review, Current Opinion in Biomedical Engineering 21 (2022), 100367.
[195] R. Sikkema, K. Baker, I. Zhitomirsky, Electrophoretic deposition of polymers and proteins for biomedical applications, Adv. Colloid Interface Sci. 284 (2020), 102272.
[196] I. Zhitomirsky, Cathodic electrodeposition of ceramic and organoceramic materials. Fundamental aspects, Adv. Colloid Interface Sci. 97 (1) (2002) 279–317.
[197] M. Ammam, Electrophoretic deposition under modulated electric fields: a review, RSC Adv. 2 (20) (2012) 7633–7646.
[198] L. Besra, M. Liu, A review on fundamentals and applications of electrophoretic deposition (EPD), Prog. Mater. Sci. 52 (1) (2007) 1–61.
[199] P. Ducheyne, W. Van Raemdonck, J.C. Heughebaert, M. Heughebaert, Structural analysis of hydroxyapatite coatings on titanium, Biomaterials 7 (2) (1986) 97–103.
[200] A.R. Boccaccini, S. Keim, R. Ma, Y. Li, I. Zhitomirsky, Electrophoretic deposition of biomaterials, J. R. Soc. Interface 7 (2010) S581–S613.
[201] F. Chen, W.M. Lam, C.J. Lin, G.X. Qiu, Z.H. Wu, K.D.K. Luk, W.W. Lu, Biocompatibility of electrophoretical deposition of nanostructured hydroxyapatite coating on roughen titanium surface: in vitro evaluation using mesenchymal stem cells, J. Biomed. Mater. Res. B Appl. Biomater. 82B (1) (2007) 183–191.
[202] A. Tahmasbi Rad, M. Solati-Hashjin, N.A.A. Osman, S. Faghihi, Improved bio-physical performance of hydroxyapatite coatings obtained by electrophoretic deposition at dynamic voltage, Ceram. Int. 40 (8) (2014) 12681–12691. Part B).
[203] F.E. Baştan, M. Atiq Ur Rehman, Y.Y. Avcu, E. Avcu, F. Üstel, A.R. Boccaccini, Electrophoretic co-deposition of PEEK-hydroxyapatite composite coatings for biomedical applications, Colloids Surf. B Biointerfaces 169 (2018) 176–182.
[204] M. Li, Q. Liu, Z. Jia, X. Xu, Y. Cheng, Y. Zheng, T. Xi, S. Wei, Graphene oxide/hydroxyapatite composite coatings fabricated by electrophoretic nanotechnology for biological applications, Carbon 67 (2014) 185–197.
[205] S. Tang, B. Tian, Y.-J. Guo, Z.-A. Zhu, Y.-P. Guo, Chitosan/carbonated hydroxyapatite composite coatings: fabrication, structure and biocompatibility, Surf. Coating. Technol. 251 (2014) 210–216.
[206] R.V. Chernozem, M.A. Surmeneva, B. Krause, T. Baumbach, V.P. Ignatov, O. Prymak, K. Loza, M. Epple, F. Ennen-Roth, A. Wittmar, M. Ulbricht, E. A. Chudinova, T. Rijavec, A. Lapanje, R.A. Surmenev, Functionalization of titania nanotubes with electrophoretically deposited silver and calcium phosphate nanoparticles: structure, composition and antibacterial assay, Mater. Sci. Eng. C 97 (2019) 420–430.
[207] S. Singh, G. Singh, N. Bala, Electrophoretic deposition of hydroxyapatite-iron oxide-chitosan composite coatings on Ti–13Nb–13Zr alloy for biomedical applications, Thin Solid Films 697 (2020), 137801.
[208] A. Clifford, B.E.J. Lee, K. Grandfield, I. Zhitomirsky, Biomimetic modification of poly-l-lysine and electrodeposition of nanocomposite coatings for orthopaedic applications, Colloids Surf. B Biointerfaces 176 (2019) 115–121.
[209] L. Suo, N. Jiang, Y. Wang, P. Wang, J. Chen, X. Pei, J. Wang, Q. Wan, The enhancement of osseointegration using a graphene oxide/chitosan/hydroxyapatite composite coating on titanium fabricated by electrophoretic deposition, J. Biomed. Mater. Res. B Appl. Biomater. 107 (3) (2019) 635–645.
[210] M. Stevanović, M. Đošić, A. Janković, V. Kojić, M. Vukašinović-Sekulić, J. Stojanović, J. Odović, M. Crevar Sakač, K.Y. Rhee, V. Mišković-Stanković, Gentamicin-loaded bioactive hydroxyapatite/chitosan composite coating electrodeposited on titanium, ACS Biomater. Sci. Eng. 4 (12) (2018) 3994–4007.
[211] M. Sumathra, M. Rajan, R. Amarnath Praphakar, N. Marraiki, A.M. Elgorban, Vivo assessment of a hydroxyapatite/κ-carrageenan–maleic anhydride–casein/doxorubicin composite-coated titanium bone implant, ACS Biomater. Sci. Eng. 6 (3) (2020) 1650–1662.
[212] S. Seuss, A.R. Boccaccini, Electrophoretic deposition of biological macromolecules, drugs, and cells, Biomacromolecules 14 (10) (2013) 3355–3369.
[213] A. Tozar, I.H. Karahan, Y. Yucel, Optimization of the electrophoretic deposition parameters for biocomposite hydroxyapatite/chitosan/collagen/h-BN coatings on Ti6Al4V biomedical implants, Metall. Mater. Trans. A 50A (2) (2019) 1009–1020.
[214] M. Li, P. Xiong, M. Mo, Y. Cheng, Y. Zheng, Electrophoretic-deposited novel ternary silk fibroin/graphene oxide/hydroxyapatite nanocomposite coatings on titanium substrate for orthopedic applications, Front. Mater. Sci. 10 (3) (2016) 270–280.
[215] T. Jiang, Z. Zhang, Y. Zhou, Y. Liu, Z. Wang, H. Tong, X. Shen, Y. Wang, Surface functionalization of titanium with chitosan/gelatin via electrophoretic deposition: characterization and cell behavior, Biomacromolecules 11 (5) (2010) 1254–1260.
[216] Z. Zhang, T. Jiang, K. Ma, X. Cai, Y. Zhou, Y. Wang, Low temperature electrophoretic deposition of porous chitosan/silk fibroin composite coating for titanium biofunctionalization, J. Mater. Chem. 21 (21) (2011) 7705–7713.
[217] Z. Zhang, X. Cheng, Y. Yao, J. Luo, Q. Tang, H. Wu, S. Lin, C. Han, Q. Wei, L. Chen, Electrophoretic deposition of chitosan/gelatin coatings with controlled porous surface topography to enhance initial osteoblast adhesive responses, J. Mater. Chem. B 4 (47) (2016) 7584–7595.
[218] X. Cai, J. Cai, K. Ma, P. Huang, L. Gong, D. Huang, T. Jiang, Y. Wang, Fabrication and characterization of Mg-doped chitosan–gelatin nanocompound coatings for titanium surface functionalization, J. Biomater. Sci. Polym. Ed. 27 (10) (2016) 954–971.
[219] K. Ma, D. Huang, J. Cai, X. Cai, L. Gong, P. Huang, Y. Wang, T. Jiang, Surface functionalization with strontium-containing nanocomposite coatings via EPD, Colloids Surf. B Biointerfaces 146 (2016) 97–106.

[220] P. Huang, K. Ma, X. Cai, D. Huang, X. Yang, J. Ran, F. Wang, T. Jiang, Enhanced antibacterial activity and biocompatibility of zinc-incorporated organic-inorganic nanocomposite coatings via electrophoretic deposition, Colloids Surf. B Biointerfaces 160 (2017) 628–638.
[221] P. Zhao, Y. Zhao, L. Xiao, H. Deng, Y. Du, Y. Chen, X. Shi, Electrodeposition to construct free-standing chitosan/layered double hydroxides hydro-membrane for electrically triggered protein release, Colloids Surf. B Biointerfaces 158 (2017) 474–479.
[222] X. Cheng, D. Deng, L. Chen, J.A. Jansen, S.G.C. Leeuwenburgh, F. Yang, Electrodeposited assembly of additive-free silk fibroin coating from pre-assembled nanospheres for drug delivery, ACS Appl. Mater. Interfaces 12 (10) (2020) 12018–12029.
[223] J.P. Matinlinna, S. Areva, L.V.J. Lassila, P.K. Vallittu, Characterization of siloxane films on titanium substrate derived from three aminosilanes, Surf. Interface Anal. 36 (9) (2004) 1314–1322.
[224] K.V. Holmberg, M. Abdolhosseini, Y. Li, X. Chen, S.-U. Gorr, C. Aparicio, Bio-inspired stable antimicrobial peptide coatings for dental applications, Acta Biomater. 9 (9) (2013) 8224–8231.
[225] J. Chen, Y. Zhu, M. Xiong, G. Hu, J. Zhan, T. Li, L. Wang, Y. Wang, Antimicrobial titanium surface via click-immobilization of peptide and its in vitro/vivo activity, ACS Biomater. Sci. Eng. 5 (2) (2019) 1034–1044.
[226] S. Acosta, A. Ibañez-Fonseca, C. Aparicio, J.C. Rodríguez-Cabello, Antibiofilm coatings based on protein-engineered polymers and antimicrobial peptides for preventing implant-associated infections, Biomater. Sci. 8 (10) (2020) 2866–2877.
[227] P. Rezvanian, R. Daza, P.A. López, M. Ramos, D. González-Nieto, M. Elices, G. V. Guinea, J. Pérez-Rigueiro, Enhanced biological response of AVS-functionalized Ti-6Al-4V alloy through covalent immobilization of collagen, Sci. Rep. 8 (1) (2018) 3337.
[228] G. Voggenreiter, K. Hartl, S. Assenmacher, M. Chatzinikolaidou, H.P. Jennissen, H.M. Rumpf, Assesment of the biological activity of chemically immobilized rhBMP-2 on titanium surfaces in vivo, Mater. Werkst. 32 (12) (2001) 942–948.
[229] V. Gadenne, L. Lebrun, T. Jouenne, P. Thebault, Antiadhesive activity of ulvan polysaccharides covalently immobilized onto titanium surface, Colloids Surf. B Biointerfaces 112 (2013) 229–236, 0.
[230] J. Chen, G. Hu, T. Li, Y. Chen, M. Gao, Q. Li, L. Hao, Y. Jia, L. Wang, Y. Wang, Fusion peptide engineered "statically-versatile" titanium implant simultaneously enhancing anti-infection, vascularization and osseointegration, Biomaterials 264 (2021), 120446.
[231] F. Zhang, Z. Zhang, X. Zhu, E.-T. Kang, K.-G. Neoh, Silk-functionalized titanium surfaces for enhancing osteoblast functions and reducing bacterial adhesion, Biomaterials 29 (36) (2008) 4751–4759.
[232] S. Desseaux, H.-A. Klok, Fibroblast adhesion on ECM-derived peptide modified poly(2-hydroxyethyl methacrylate) brushes: ligand co-presentation and 3D-localization, Biomaterials 44 (2015) 24–35.
[233] L. Fu, M. Omi, M. Sun, B. Cheng, G. Mao, T. Liu, G. Mendonça, S.E. Averick, Y. Mishina, K. Matyjaszewski, Covalent attachment of P15 peptide to Ti alloy surface modified with polymer to enhance osseointegration of implants, ACS Appl. Mater. Interfaces 11 (42) (2019) 38531–38536.
[234] Y. Liu, K. Ai, L. Lu, Polydopamine and its derivative materials: synthesis and promising applications in energy, environmental, and biomedical fields, Chem. Rev. 114 (9) (2014) 5057–5115.
[235] H.-y. Li, D.-n. Huang, K.-f. Ren, J. Ji, Inorganic-polymer composite coatings for biomedical devices, Smart Materials in Medicine 2 (2021) 1–14.
[236] X. Wang, X. Lei, Y. Yu, S. Miao, J. Tang, Y. Fu, K. Ye, Y. Shen, J. Shi, H. Wu, Y. Zhu, L. Yu, G. Pei, L. Bi, J. Ding, Biological sealing and integration of a fibrinogen-modified titanium alloy with soft and hard tissues in a rat model, Biomater. Sci. 9 (15) (2021) 5192–5208.
[237] Z.L. Shi, K.G. Neoh, E.T. Kang, C. Poh, W. Wang, Titanium with surface-grafted dextran and immobilized bone morphogenetic protein-2 for inhibition of bacterial adhesion and enhancement of osteoblast functions, Tissue Eng. 15 (2) (2009) 417–426.
[238] D. Zheng, K.G. Neoh, Z. Shi, E.-T. Kang, Assessment of stability of surface anchors for antibacterial coatings and immobilized growth factors on titanium, J. Colloid Interface Sci. 406 (2013) 238–246.
[239] G. Pan, S. Sun, W. Zhang, R. Zhao, W. Cui, F. He, L. Huang, S.-H. Lee, K.J. Shea, Q. Shi, H. Yang, Biomimetic design of mussel-derived bioactive peptides for dual-functionalization of titanium-based biomaterials, J. Am. Chem. Soc. 138 (45) (2016) 15078–15086.
[240] J. Bai, H. Wang, H. Chen, G. Ge, M. Wang, A. Gao, L. Tong, Y. Xu, H. Yang, G. Pan, P.K. Chu, D. Geng, Biomimetic osteogenic peptide with mussel adhesion and osteoimmunomodulatory functions to ameliorate interfacial osseointegration under chronic inflammation, Biomaterials 255 (2020), 120197.
[241] X. Guo, J. Bai, G. Ge, Z. Wang, Q. Wang, K. Zheng, H. Tao, L. Zhang, H. Zhang, D. Wang, X. Zhang, H. Li, G. Pan, D. Geng, Bioinspired peptide adhesion on Ti implants alleviates wear particle-induced inflammation and improves interfacial osteogenesis, J. Colloid Interface Sci. 605 (2022) 410–424.
[242] D. Liu, Y. Xi, S. Yu, K. Yang, F. Zhang, Y. Yang, T. Wang, S. He, Y. Zhu, Z. Fan, J. Du, A polypeptide coating for preventing biofilm on implants by inhibiting antibiotic resistance genes, Biomaterials 293 (2023), 121957.
[243] J. Buxadera-Palomero, C. Canal, S. Torrent-Camarero, B. Garrido, F. Javier Gil, D. Rodríguez, Antifouling coatings for dental implants: polyethylene glycol-like coatings on titanium by plasma polymerization, Biointerphases 10 (2) (2015), 029505.
[244] J. Buxadera-Palomero, C. Calvo, S. Torrent-Camarero, F.J. Gil, C. Mas-Moruno, C. Canal, D. Rodríguez, Biofunctional polyethylene glycol coatings on titanium: an in vitro-based comparison of functionalization methods, Colloids Surf. B Biointerfaces 152 (2017) 367–375.
[245] P.H. Mutin, V. Lafond, A.F. Popa, M. Granier, L. Markey, A. Dereux, Selective surface modification of SiO2−TiO2 supports with phosphonic acids, Chem. Mater. 16 (26) (2004) 5670–5675.
[246] A. Córdoba, M. Hierro-Oliva, M.Á. Pacha-Olivenza, M.C. Fernández-Calderón, J. Perelló, B. Isern, M.L. González-Martín, M. Monjo, J.M. Ramis, Direct covalent grafting of phytate to titanium surfaces through Ti–O–P bonding shows bone stimulating surface properties and decreased bacterial adhesion, ACS Appl. Mater. Interfaces 8 (18) (2016) 11326–11335.
[247] E.S. Bronze-Uhle, L.F.G. Dias, L.D. Trino, A.A. Matos, R.C. de Oliveira, P. N. Lisboa-Filho, Physicochemical bisphosphonate immobilization on titanium dioxide thin films surface by UV radiation for bio-application, Surf. Coating. Technol. 357 (2019) 36–47.
[248] X. Cui, T. Murakami, Y. Tamura, K. Aoki, Y. Hoshino, Y. Miura, Bacterial inhibition and osteoblast adhesion on Ti alloy surfaces modified by poly(PEGMA-r-phosmer) coating, ACS Appl. Mater. Interfaces 10 (28) (2018) 23674–23681.
[249] X. Cui, Y. Hoshino, Y. Miura, Fibronectin coating on implant material surface attracted both osteoblasts and bacteria, Chem. Lett. 48 (8) (2019) 764–767.
[250] J. Park, S. Bauer, A. Pittrof, M.S. Killian, P. Schmuki, K. von der Mark, Synergistic control of mesenchymal stem cell differentiation by nanoscale surface geometry and immobilized growth factors on TiO2 nanotubes, Small 8 (1) (2012) 98–107.
[251] P.W. Kämmerer, A.M. Pabst, M. Dau, H. Staedt, B. Al-Nawas, M. Heller, Immobilization of BMP-2, BMP-7 and alendronic acid on titanium surfaces: adhesion, proliferation and differentiation of bone marrow-derived stem cells, J. Biomed. Mater. Res. 108 (2) (2020) 212–220.
[252] M. Godoy-Gallardo, J. Guillem-Marti, P. Sevilla, J.M. Manero, F.J. Gil, D. Rodriguez, Anhydride-functional silane immobilized onto titanium surfaces induces osteoblast cell differentiation and reduces bacterial adhesion and biofilm formation, Mater. Sci. Eng. C 59 (2016) 524–532.
[253] R.R. Costa, J.F. Mano, Polyelectrolyte multilayered assemblies in biomedical technologies, Chem. Soc. Rev. 43 (10) (2014) 3453–3479.
[254] J.J. Richardson, J. Cui, M. Björnmalm, J.A. Braunger, H. Ejima, F. Caruso, Innovation in layer-by-layer assembly, Chem. Rev. 116 (23) (2016) 14828–14867.
[255] J.J. Richardson, M. Björnmalm, F. Caruso, Technology-driven layer-by-layer assembly of nanofilms, Science 348 (6233) (2015).
[256] P.-H. Chua, K.-G. Neoh, E.-T. Kang, W. Wang, Surface functionalization of titanium with hyaluronic acid/chitosan polyelectrolyte multilayers and RGD for promoting osteoblast functions and inhibiting bacterial adhesion, Biomaterials 29 (10) (2008) 1412–1421.
[257] W. Chen, G. Xie, Y. Lu, J. Wang, B. Feng, Q. Wang, K. Xu, J. Bao, An improved osseointegration of metal implants by pitavastatin loaded multilayer films with osteogenic and angiogenic properties, Biomaterials 280 (2022), 121260.
[258] W. Chen, X. Shen, Y. Hu, K. Xu, Q. Ran, Y. Yu, L. Dai, Z. Yuan, L. Huang, T. Shen, K. Cai, Surface functionalization of titanium implants with chitosan-catechol conjugate for suppression of ROS-induced cells damage and improvement of osteogenesis, Biomaterials 114 (2017) 82–96.
[259] X. Shen, K. Hii Ru Yie, X. Wu, Z. Zhou, A. Sun, A.M. Al-bishari, K. Fang, M.A. Al-Baadani, Z. Deng, P. Ma, J. Liu, Improvement of aqueous stability and anti-osteoporosis properties of Zn-MOF coatings on titanium implants by hydrophobic raloxifene, Chem. Eng. J. 430 (2022), 133094.
[260] Y. Hu, K. Cai, Z. Luo, K.D. Jandt, Layer-by-layer assembly of β-estradiol loaded mesoporous silica nanoparticles on titanium substrates and its implication for bone homeostasis, Adv. Mater. 22 (37) (2010) 4146–4150.
[261] H. Xing, X. Wang, G. Xiao, Z. Zhao, S. Zou, M. Li, J.J. Richardson, B.L. Tardy, L. Xie, S. Komasa, J. Okazaki, Q. Jiang, G. Yang, J. Guo, Hierarchical assembly of nanostructured coating for siRNA-based dual therapy of bone regeneration and revascularization, Biomaterials 235 (2020), 119784.
[262] J. Ran, H. Zeng, J. Cai, P. Jiang, P. Yan, L. Zheng, Y. Bai, X. Shen, B. Shi, H. Tong, Rational design of a stable, effective, and sustained dexamethasone delivery platform on a titanium implant: an innovative application of metal organic frameworks in bone implants, Chem. Eng. J. 333 (2018) 20–33.
[263] H. Ao, S. Yang, B.e. Nie, Q. Fan, Q. Zhang, J. Zong, S. Guo, X. Zheng, T. Tang, Improved antibacterial properties of collagen I/hyaluronic acid/quaternized chitosan multilayer modified titanium coatings with both contact-killing and release-killing functions, J. Mater. Chem. B 7 (11) (2019) 1951–1961.
[264] B. Tao, W. Zhao, C. Lin, Z. Yuan, Y. He, L. Lu, M. Chen, Y. Ding, Y. Yang, Z. Xia, K. Cai, Surface modification of titanium implants by ZIF-8@Levo/LBL coating for inhibition of bacterial-associated infection and enhancement of in vivo osseointegration, Chem. Eng. J. 390 (2020), 124621.
[265] Y. Hu, K. Cai, Z. Luo, D. Xu, D. Xie, Y. Huang, W. Yang, P. Liu, TiO2 nanotubes as drug nanoreservoirs for the regulation of mobility and differentiation of mesenchymal stem cells, Acta Biomater. 8 (1) (2012) 439–448.
[266] Q. Ran, Y. Yu, W. Chen, X. Shen, C. Mu, Z. Yuan, B. Tao, Y. Hu, W. Yang, K. Cai, Deferoxamine loaded titania nanotubes substrates regulate osteogenic and angiogenic differentiation of MSCs via activation of HIF-1α signaling, Mater. Sci. Eng. C 91 (2018) 44–54.
[267] L. Zhao, S. Mei, P.K. Chu, Y. Zhang, Z. Wu, The influence of hierarchical hybrid micro/nano-textured titanium surface with titania nanotubes on osteoblast functions, Biomaterials 31 (19) (2010) 5072–5082.
[268] Y. Xie, H. Ao, S. Xin, X. Zheng, C. Ding, Enhanced cellular responses to titanium coating with hierarchical hybrid structure, Mater. Sci. Eng. C 38 (2014) 272–277.
[269] K. Kubo, N. Tsukimura, F. Iwasa, T. Ueno, L. Saruwatari, H. Aita, W.-A. Chiou, T. Ogawa, Cellular behavior on TiO2 nanonodular structures in a micro-to-nanoscale hierarchy model, Biomaterials 30 (29) (2009) 5319–5329.

[270] T. Ueno, N. Tsukimura, M. Yamada, T. Ogawa, Enhanced bone-integration capability of alkali- and heat-treated nanopolymorphic titanium in micro-to-nanoscale hierarchy, Biomaterials 32 (30) (2011) 7297–7308.
[271] R.A. Gittens, T. McLachlan, R. Olivares-Navarrete, Y. Cai, S. Berner, R. Tannenbaum, Z. Schwartz, K.H. Sandhage, B.D. Boyan, The effects of combined micron-/submicron-scale surface roughness and nanoscale features on cell proliferation and differentiation, Biomaterials 32 (13) (2011) 3395–3403.
[272] P. Jiang, J. Liang, C. Lin, Construction of micro–nano network structure on titanium surface for improving bioactivity, Appl. Surf. Sci. 280 (2013) 373–380, 0.
[273] P. Jiang, L. Lin, F. Zhang, X. Dong, L. Ren, C. Lin, Electrochemical construction of micro–nano spongelike structure on titanium substrate for enhancing corrosion resistance and bioactivity, Electrochim. Acta 107 (2013) 16–25.
[274] Y. Zhang, X. Wang, Y. Li, J. Liang, P. Jiang, Q. Huang, Y. Yang, H. Duan, X. Dong, G. Rui, C. Lin, Cell osteogenic bioactivity mediated precisely by varying scaled micro-pits on ordered micro/nano hierarchical structures of titanium, Regenerative Biomaterials 9 (2022), rbac046.
[275] L. Bai, P. Chen, Y. Zhao, R. Hang, X. Yao, B. Tang, C. Liu, Y. Xiao, R. Hang, A micro/nano-biomimetic coating on titanium orchestrates osteo/angio-genesis and osteoimmunomodulation for advanced osseointegration, Biomaterials 278 (2021), 121162.
[276] X. Dai, Y. Bai, B.C. Heng, Y. Li, Z. Tang, C. Lin, O. Liu, Y. He, X. Zhang, X. Deng, Biomimetic hierarchical implant surfaces promote early osseointegration in osteoporotic rats by suppressing macrophage activation and osteoclastogenesis, J. Mater. Chem. B 10 (11) (2022) 1875–1885.
[277] P. Ma, Y. Yu, K.H.R. Yie, K. Fang, Z. Zhou, X. Pan, Z. Deng, X. Shen, J. Liu, Effects of titanium with different micro/nano structures on the ability of osteoblasts to resist oxidative stress, Mater. Sci. Eng. C 123 (2021), 111969.
[278] J. Li, W. Zhang, Y. Qiao, H. Zhu, X. Jiang, X. Liu, C. Ding, Chemically regulated bioactive ion delivery platform on a titanium surface for sustained controlled release, J. Mater. Chem. B 2 (3) (2014) 283–294.
[279] Z. Yuan, P. Liu, Y. Liang, B. Tao, Y. He, Y. Hao, W. Yang, Y. Hu, K. Cai, Investigation of osteogenic responses of Fe-incorporated micro/nano-hierarchical structures on titanium surfaces, J. Mater. Chem. B 6 (9) (2018) 1359–1372.
[280] W. Lu, C. Zhou, Y. Ma, J. Li, J. Jiang, Y. Chen, L. Dong, F. He, Improved osseointegration of strontium-modified titanium implants by regulating angiogenesis and macrophage polarization, Biomater. Sci. 10 (9) (2022) 2198–2214.
[281] B. Li, J. Ma, D. Wang, X. Liu, H. Li, L. Zhou, C. Liang, H. Wang, Self-adjusting antibacterial properties of Ag-incorporated nanotubes on micro-nanostructured Ti surfaces, Biomater. Sci. 7 (10) (2019) 4075–4087.
[282] P. Jiang, J. Liang, R. Song, Y. Zhang, L. Ren, L. Zhang, P. Tang, C. Lin, Effect of octacalcium-phosphate-modified micro/nanostructured titania surfaces on osteoblast response, ACS Appl. Mater. Interfaces 7 (26) (2015) 14384–14396.
[283] P. Jiang, Y. Zhang, R. Hu, X. Wang, Y. Lai, G. Rui, C. Lin, Hydroxyapatite-modified micro/nanostructured titania surfaces with different crystalline phases for osteoblast regulation, Bioact. Mater. 6 (4) (2021) 1118–1129.
[284] Z. Geng, Z. Li, Z. Cui, J. Wang, X. Yang, C. Liu, Novel bionic topography with MiR-21 coating for improving bone-implant integration through regulating cell adhesion and angiogenesis, Nano Lett. 20 (10) (2020) 7716–7721.
[285] B.D. Boyan, Z. Schwartz, C.H. Lohmann, V.L. Sylvia, D.L. Cochran, D.D. Dean, J. E. Puzas, Pretreatment of bone with osteoclasts affects phenotypic expression of osteoblast-like cells, J. Orthop. Res. 21 (4) (2003) 638–647.
[286] S.L. Teitelbaum, F.P. Ross, Genetic regulation of osteoclast development and function, Nat. Rev. Genet. 4 (8) (2003) 638–649.
[287] T. Sasaki, Recent advances in the ultrastructural assessment of osteoclastic resorptive functions, Microsc. Res. Tech. 33 (2) (1996) 182–191.
[288] B.D. Boyan, E.M. Lotz, Z. Schwartz, Roughness and hydrophilicity as osteogenic biomimetic surface properties, Tissue Eng. 23 (23–24) (2017) 1479–1489.
[289] M.T.K. Mulari, Q. Qu, P.L. Härkönen, H.K. Väänänen, Osteoblast-like cells complete osteoclastic bone resorption and form new mineralized bone matrix in vitro, Calcif. Tissue Int. 75 (3) (2004) 253–261.
[290] N. Reznikov, R. Shahar, S. Weiner, Bone hierarchical structure in three dimensions, Acta Biomater. 10 (9) (2014) 3815–3826.
[291] L.J. Raggatt, N.C. Partridge, Cellular and molecular mechanisms of bone remodeling, J. Biol. Chem. 285 (33) (2010) 25103–25108.
[292] M.W. Tibbitt, C.B. Rodell, J.A. Burdick, K.S. Anseth, Progress in material design for biomedical applications, Proc. Natl. Acad. Sci. USA 112 (47) (2015) 14444–14451.
[293] M. Bril, S. Fredrich, N.A. Kurniawan, Stimuli-responsive materials: a smart way to study dynamic cell responses, Smart Materials in Medicine 3 (2022) 257–273.
[294] J. Zarubova, M.M. Hasani-Sadrabadi, R. Ardehali, S. Li, Immunoengineering strategies to enhance vascularization and tissue regeneration, Adv. Drug Deliv. Rev. 184 (2022), 114233.
[295] B.A. Badeau, C.A. DeForest, Programming stimuli-responsive behavior into biomaterials, Annu. Rev. Biomed. Eng. 21 (1) (2019) 241–265.
[296] Y. Lu, A.A. Aimetti, R. Langer, Z. Gu, Bioresponsive materials, Nat. Rev. Mater. 1 (2016), 16075.
[297] C. Tian, J. Zhang, J. Gu, W. Li, Y. Cao, Light controlled biomaterials for regulating cell migration and differentiation, Smart Materials in Medicine 3 (2022) 209–216.
[298] Y.Y. Song, F. Schmidt-Stein, S. Bauer, P. Schmuki, Amphiphilic TiO2 nanotube arrays: an actively controllable drug delivery system, J. Am. Chem. Soc. 131 (12) (2009) 4230–+.
[299] J. Xu, X. Zhou, Z. Gao, Y.-Y. Song, P. Schmuki, Visible-light-triggered drug release from TiO2 nanotube arrays: a controllable antibacterial platform, Angew. Chem. Int. Ed. 55 (2) (2016) 593–597.
[300] J. Zhao, J. Xu, X. Jian, J. Xu, Z. Gao, Y.-Y. Song, NIR light-driven photocatalysis on amphiphilic TiO2 nanotubes for controllable drug release, ACS Appl. Mater. Interfaces 12 (20) (2020) 23606–23616.
[301] X. Xie, C. Mao, X. Liu, Y. Zhang, Z. Cui, X. Yang, K.W.K. Yeung, H. Pan, P.K. Chu, S. Wu, Synergistic bacteria killing through photodynamic and physical actions of graphene oxide/Ag/collagen coating, ACS Appl. Mater. Interfaces 9 (31) (2017) 26417–26428.
[302] Z. Xu, X. Wang, X. Liu, Z. Cui, X. Yang, K.W.K. Yeung, J.C. Chung, P.K. Chu, S. Wu, Tannic acid/Fe3+/Ag nanofilm exhibiting superior photodynamic and physical antibacterial activity, ACS Appl. Mater. Interfaces 9 (45) (2017) 39657–39671.
[303] Y. Jia, S. Zhan, S. Ma, Q. Zhou, Fabrication of TiO2–Bi2WO6 binanosheet for enhanced solar photocatalytic disinfection of E. coli: insights on the mechanism, ACS Appl. Mater. Interfaces 8 (11) (2016) 6841–6851.
[304] B. Wu, Y. Li, K. Su, L. Tan, X. Liu, Z. Cui, X. Yang, Y. Liang, Z. Li, S. Zhu, K.W. K. Yeung, S. Wu, The enhanced photocatalytic properties of MnO2/g-C3N4 heterostructure for rapid sterilization under visible light, J. Hazard Mater. 377 (2019) 227–236.
[305] X. Rao, L. Du, J.J. Zhao, X.D. Tan, Y.X. Fang, L.Q. Xu, Y.P. Zhang, Hybrid TiO2/AgNPs/g-C3N4 nanocomposite coatings on TC4 titanium alloy for enhanced synergistic antibacterial effect under full spectrum light, J. Mater. Sci. Technol. 118 (2022) 35–43.
[306] X. Deng, Z. Shao, Y. Zhao, Solutions to the drawbacks of photothermal and photodynamic cancer therapy, Adv. Sci. 8 (3) (2021), 2002504.
[307] L. Hong, X. Liu, L. Tan, Z. Cui, X. Yang, Y. Liang, Z. Li, S. Zhu, Y. Zheng, K.W. K. Yeung, D. Jing, D. Zheng, X. Wang, S. Wu, Rapid biofilm elimination on bone implants using near-infrared-activated inorganic semiconductor heterostructures, Advanced Healthcare Materials 8 (19) (2019), 1900835.
[308] J. Li, X. Liu, L. Tan, Y. Liang, Z. Cui, X. Yang, S. Zhu, Z. Li, Y. Zheng, K.W. K. Yeung, X. Wang, S. Wu, Light-activated rapid disinfection by accelerated charge transfer in red phosphorus/ZnO heterointerface, Small Methods 3 (3) (2019), 1900048.
[309] M. Zhu, X. Liu, L. Tan, Z. Cui, Y. Liang, Z. Li, K.W. Kwok Yeung, S. Wu, Photo-responsive chitosan/Ag/MoS2 for rapid bacteria-killing, J. Hazard Mater. 383 (2020), 121122.
[310] Z. Yuan, B. Tao, Y. He, C. Mu, G. Liu, J. Zhang, Q. Liao, P. Liu, K. Cai, Remote eradication of biofilm on titanium implant via near-infrared light triggered photothermal/photodynamic therapy strategy, Biomaterials 223 (2019), 119479.
[311] L. Tan, J. Li, X. Liu, Z. Cui, X. Yang, S. Zhu, Z. Li, X. Yuan, Y. Zheng, K.W. K. Yeung, H. Pan, X. Wang, S. Wu, Rapid biofilm eradication on bone implants using red phosphorus and near-infrared light, Adv. Mater. 30 (31) (2018), 1801808.
[312] M. Li, L. Li, K. Su, X. Liu, T. Zhang, Y. Liang, D. Jing, X. Yang, D. Zheng, Z. Cui, Z. Li, S. Zhu, K.W.K. Yeung, Y. Zheng, X. Wang, S. Wu, Highly effective and noninvasive near-infrared eradication of a Staphylococcus aureus biofilm on implants by a photoresponsive coating within 20 min, Adv. Sci. 6 (17) (2019), 1900599.
[313] Y. Li, X. Liu, B. Li, Y. Zheng, Y. Han, D.-f. Chen, K.W.K. Yeung, Z. Cui, Y. Liang, Z. Li, S. Zhu, X. Wang, S. Wu, Near-infrared light triggered phototherapy and immunotherapy for elimination of methicillin-resistant Staphylococcus aureus biofilm infection on bone implant, ACS Nano 14 (7) (2020) 8157–8170.
[314] Z. Yuan, J. Wu, Z. Fu, S. Meng, L. Dai, K. Cai, Polydopamine-mediated interfacial functionalization of implants for accelerating infected bone repair through light-activatable antibiosis and carbon monoxide gas regulated macrophage polarization, Adv. Funct. Mater. 32 (27) (2022), 2200374.
[315] J. Fu, X. Liu, L. Tan, Z. Cui, Y. Zheng, Y. Liang, Z. Li, S. Zhu, K.W.K. Yeung, X. Feng, X. Wang, S. Wu, Photoelectric-responsive extracellular matrix for bone engineering, ACS Nano 13 (11) (2019) 13581–13594.
[316] Z. Yan, K. Li, D. Shao, Q. Shen, Y. Ding, S. Huang, Y. Xie, X. Zheng, Visible-light-responsive reduced graphene oxide/g-C3N4/TiO2 composite nanocoating for photoelectric stimulation of neuronal and osteoblastic differentiation, RSC Adv. 12 (15) (2022) 8878–8888.
[317] Y. Li, X. Xu, X. Liu, B. Li, Y. Han, Y. Zheng, D.-f. Chen, K.W.K. Yeung, Z. Cui, Z. Li, Y. Liang, S. Zhu, X. Wang, S. Wu, Photoelectrons mediating angiogenesis and immunotherapy through heterojunction film for noninvasive disinfection, Adv. Sci. 7 (17) (2020), 2000023.
[318] X. Ying, N.J. Barlow, A. Tatiparthi, Chapter 63 - micro-CT and volumetric imaging in developmental toxicology, in: R.C. Gupta (Ed.), Reproductive and Developmental Toxicology, third ed., Academic Press, 2022, pp. 1261–1285.
[319] Z. Hong, Z. Chen, Q. Chen, H. Yang, Advancing X-ray luminescence for imaging, biosensing, and theragnostics, Acc. Chem. Res. 56 (1) (2023) 37–51.
[320] L. Karim, S. Judex, Low level irradiation in mice can lead to enhanced trabecular bone morphology, J. Bone Miner. Metabol. 32 (5) (2014) 476–483.
[321] X.Z. Zhou, G. Zhang, Q.R. Dong, C.W. Chan, C.F. Liu, L. Qin, Low-dose X-irradiation promotes mineralization of fracture callus in a rat model, Arch. Orthop. Trauma Surg. 129 (1) (2009) 125–132.
[322] C. She, G.-L. Shi, W. Xu, X.-Z. Zhou, J. Li, Y. Tian, J. Li, W.-H. Li, Q.-R. Dong, P.-G. Ren, Effect of low-dose X-ray irradiation and Ti particles on the osseointegration of prosthetic, J. Orthop. Res. 34 (10) (2016) 1688–1696.
[323] F. Schmidt-Stein, R. Hahn, J.-F. Gnichwitz, Y.Y. Song, N.K. Shrestha, A. Hirsch, P. Schmuki, X-ray induced photocatalysis on TiO2 and TiO2 nanotubes: degradation of organics and drug release, Electrochem. Commun. 11 (11) (2009) 2077–2080.
[324] S.B. Behbahani, S.D. Kiridena, U.N. Wijayaratna, C. Taylor, J.N. Anker, T.-R. J. Tzeng, pH variation in medical implant biofilms: causes, measurements, and its implications for antibiotic resistance, Front. Microbiol. (2022) 13.

[325] U. Uzair, D. Benza, C.J. Behrend, J.N. Anker, Noninvasively imaging pH at the surface of implanted orthopedic devices with X-ray excited luminescence chemical imaging, ACS Sens. 4 (9) (2019) 2367–2374.
[326] U. Uzair, C. Johnson, S. Beladi-Behbahani, A.C. Rajamanthrilage, Y.S. Raval, D. Benza, M. Ranasinghe, G. Schober, T.-R.J. Tzeng, J.N. Anker, Conformal coating of orthopedic plates with X-ray scintillators and pH indicators for X-ray excited luminescence chemical imaging through tissue, ACS Appl. Mater. Interfaces 12 (47) (2020) 52343–52353.
[327] X. Wang, Y. Li, H.H.Y. Tong, P. Yuan, K.-L. Wong, Y. Yang, A noninvasive precise treatment strategy for implant-related infections based on X-ray-induced luminescent/photodynamic therapeutic multilayered device surface materials, J. Lumin. 222 (2020), 117108.
[328] A. Casella, A. Panitch, J.K. Leach, Endogenous electric signaling as a blueprint for conductive materials in tissue engineering, Bioelectricity 3 (1) (2021) 27–41.
[329] B. Ercan, T.J. Webster, The effect of biphasic electrical stimulation on osteoblast function at anodized nanotubular titanium surfaces, Biomaterials 31 (13) (2010) 3684–3693.
[330] J. Park, A. Mazare, H. Schneider, K. von der Mark, M.J.M. Fischer, P. Schmuki, Electric field-induced osteogenic differentiation on TiO2 nanotubular layer, Tissue Eng. C Methods 22 (8) (2016) 809–821.
[331] A. Mazare, J. Park, S. Simons, S. Mohajernia, I. Hwang, J.E. Yoo, H. Schneider, M. J. Fischer, P. Schmuki, Black TiO2 nanotubes: efficient electrodes for triggering electric field-induced stimulation of stem cell growth, Acta Biomater. 97 (2019) 681–688.
[332] J. Liao, Y. Zhu, Z. Zhou, J. Chen, G. Tan, C. Ning, C. Mao, Reversibly controlling preferential protein adsorption on bone implants by using an applied weak potential as a switch, Angew. Chem. Int. Ed. 53 (48) (2014) 13068–13072.
[333] J. Liao, W. Chen, M. Yang, J. Zhou, Z. Wang, Y. Zhou, C. Ning, H. Yuan, Conducting photopolymers on orthopeadic implants having a switch of priority between promoting osteogenic and antibacterial activity, Mater. Horiz. 5 (3) (2018) 545–552.
[334] G. Tan, Y. Liu, Y. Wu, K. Ouyang, L. Zhou, P. Yu, J. Liao, C. Ning, Electrically reversible redox-switchable polydopamine films for regulating cell behavior, Electrochim. Acta 228 (2017) 343–350.
[335] C. Xie, P. Li, L. Han, Z. Wang, T. Zhou, W. Deng, K. Wang, X. Lu, Electroresponsive and cell-affinitive polydopamine/polypyrrole composite microcapsules with a dual-function of on-demand drug delivery and cell stimulation for electrical therapy, NPG Asia Mater. 9 (3) (2017) e358-e358.
[336] C. Wu, X. He, Y. Zhu, W. Weng, K. Cheng, D. Wang, Z. Chen, Electrochemical deposition of Ppy/Dex/ECM coatings and their regulation on cellular responses through electrical controlled drug release, Colloids Surf. B Biointerfaces 222 (2023), 113016.
[337] K. Kapat, Q.T.H. Shubhra, M. Zhou, S. Leeuwenburgh, Piezoelectric nano-biomaterials for biomedicine and tissue regeneration, Adv. Funct. Mater. 30 (44) (2020), 1909045.
[338] C. Ning, Z. Zhou, G. Tan, Y. Zhu, C. Mao, Electroactive polymers for tissue regeneration: developments and perspectives, Prog. Polym. Sci. 81 (2018) 144–162.
[339] A.C. Ahn, A.J. Grodzinsky, Relevance of collagen piezoelectricity to "Wolff's Law": a critical review, Med. Eng. Phys. 31 (7) (2009) 733–741.
[340] L. Mao, L. Bai, X. Wang, X. Chen, D. Zhang, F. Chen, C. Liu, Enhanced cell osteogenesis and osteoimmunology regulated by piezoelectric biomaterials with controllable surface potential and charges, ACS Appl. Mater. Interfaces 14 (39) (2022) 44111–44124.
[341] Z. Liu, X. Wan, Z.L. Wang, L. Li, Electroactive biomaterials and systems for cell fate determination and tissue regeneration: design and applications, Adv. Mater. 33 (32) (2021), 2007429.
[342] B. Tandon, J.J. Blaker, S.H. Cartmell, Piezoelectric materials as stimulatory biomedical materials and scaffolds for bone repair, Acta Biomater. 73 (2018) 1–20.
[343] W. Liu, X. Li, Y. Jiao, C. Wu, S. Guo, X. Xiao, X. Wei, J. Wu, P. Gao, N. Wang, Y. Lu, Z. Tang, Q. Zhao, J. Zhang, Y. Tang, L. Shi, Z. Guo, Biological effects of a three-dimensionally printed Ti6Al4V scaffold coated with piezoelectric BaTiO3 nanoparticles on bone formation, ACS Appl. Mater. Interfaces 12 (46) (2020) 51885–51903.
[344] H. Wu, H. Dong, Z. Tang, Y. Chen, Y. Liu, M. Wang, X. Wei, N. Wang, S. Bao, D. Yu, Z. Wu, Z. Yang, X. Li, Z. Guo, L. Shi, Electrical stimulation of piezoelectric BaTiO3 coated Ti6Al4V scaffolds promotes anti-inflammatory polarization of macrophages and bone repair via MAPK/JNK inhibition and OXPHOS activation, Biomaterials 293 (2023), 121990.
[345] K. Cai, Y. Jiao, Q. Quan, Y. Hao, J. Liu, L. Wu, Improved activity of MC3T3-E1 cells by the exciting piezoelectric BaTiO3/TC4 using low-intensity pulsed ultrasound, Bioact. Mater. 6 (11) (2021) 4073–4082.
[346] J. Chen, S. Li, Y. Jiao, J. Li, Y. Li, Y.-l. Hao, Y. Zuo, Vitro study on the piezodynamic therapy with a BaTiO3-coating titanium scaffold under low-intensity pulsed ultrasound stimulation, ACS Appl. Mater. Interfaces 13 (41) (2021) 49542–49555.
[347] B. Fan, Z. Guo, X. Li, S. Li, P. Gao, X. Xiao, J. Wu, C. Shen, Y. Jiao, W. Hou, Electroactive barium titanate coated titanium scaffold improves osteogenesis and osseointegration with low-intensity pulsed ultrasound for large segmental bone defects, Bioact. Mater. 5 (4) (2020) 1087–1101.
[348] C. Xiao, L. Fan, S. Zhou, X. Kang, P. Guan, R. Fu, C. Li, J. Ren, Z. Wang, P. Yu, Y. Wang, C. Deng, L. Zhou, C. Ning, One-dimensional ferroelectric nanoarrays with wireless switchable static and dynamic electrical stimulation for selective regulating osteogenesis and antiosteosarcoma, ACS Nano 16 (12) (2022) 20770–20785.
[349] B. Tang, J. Zhuang, L. Wang, B. Zhang, S. Lin, F. Jia, L. Dong, Q. Wang, K. Cheng, W. Weng, Harnessing cell dynamic responses on magnetoelectric nanocomposite films to promote osteogenic differentiation, ACS Appl. Mater. Interfaces 10 (9) (2018) 7841–7851.
[350] F. Jia, S. Lin, X. He, J. Zhang, S. Shen, Z. Wang, B. Tang, C. Li, Y. Wu, L. Dong, K. Cheng, W. Weng, Comprehensive evaluation of surface potential characteristics on mesenchymal stem cells' osteogenic differentiation, ACS Appl. Mater. Interfaces 11 (25) (2019) 22218–22227.
[351] H. Qi, Q. Ke, Q. Tang, L. Yin, L. Yang, C. Ning, J. Su, L. Fang, Magnetic field regulation of mouse bone marrow mesenchymal stem cell behaviours on TiO2 nanotubes via surface potential mediated by Terfenol-D/P(VDF-TrFE) film, Biosurface and Biotribology 8 (3) (2022) 254–265.
[352] C. Liang, X. Liu, Y. Yan, R. Sun, J. Li, W. Geng, Effectiveness and mechanisms of low-intensity pulsed ultrasound on osseointegration of dental implants and biological functions of bone marrow mesenchymal stem cells, Stem Cell. Int. 2022 (2022), 7397335.
[353] J. Chen, J. Li, F. Hu, Q. Zou, Q. Mei, S. Li, Y. Hao, W. Hou, J. Li, Y. Li, Y. Zuo, Effect of microarc oxidation-treated Ti6Al4V scaffold following low-intensity pulsed ultrasound stimulation on osteogenic cells in vitro, ACS Biomater. Sci. Eng. 5 (2) (2019) 572–581.
[354] M.S. Aw, D. Losic, Ultrasound enhanced release of therapeutics from drug-releasing implants based on titania nanotube arrays, Int. J. Pharm. 443 (1–2) (2013) 154–162.
[355] J. Zhou, M.A. Frank, Y. Yang, A.R. Boccaccini, S. Virtanen, A novel local drug delivery system: superhydrophobic titanium oxide nanotube arrays serve as the drug reservoir and ultrasonication functions as the drug release trigger, Materials Science & Engineering C-Materials for Biological Applications 82 (2018) 277–283.
[356] X. Wang, X. Zhong, F. Gong, Y. Chao, L. Cheng, Newly developed strategies for improving sonodynamic therapy, Mater. Horiz. 7 (8) (2020) 2028–2046.
[357] W. Guan, L. Tan, X. Liu, Z. Cui, Y. Zheng, K.W.K. Yeung, D. Zheng, Y. Liang, Z. Li, S. Zhu, X. Wang, S. Wu, Ultrasonic interfacial engineering of red phosphorous–metal for eradicating MRSA infection effectively, Adv. Mater. 33 (5) (2021), 2006047.
[358] A. Jayasree, S. Ivanovski, K. Gulati, ON or OFF: triggered therapies from anodized nano-engineered titanium implants, J. Contr. Release 333 (2021) 521–535.
[359] M.S. Aw, J. Addai-Mensah, D. Losic, Magnetic-responsive delivery of drug-carriers using titania nanotube arrays, J. Mater. Chem. 22 (14) (2012) 6561–6563.
[360] L. Fassina, E. Saino, L. Visai, G. Silvani, M.G. Cusella De Angelis, G. Mazzini, F. Benazzo, G. Magenes, Electromagnetic enhancement of a culture of human SAOS-2 osteoblasts seeded onto titanium fiber-mesh scaffolds, J. Biomed. Mater. Res. 87A (3) (2008) 750–759.
[361] L. Fassina, E. Saino, M.S. Sbarra, L. Visai, M.G. Cusella De Angelis, G. Mazzini, F. Benazzo, G. Magenes, Ultrasonic and electromagnetic enhancement of a culture of human SAOS-2 osteoblasts seeded onto a titanium plasma-spray surface, Tissue Eng. C Methods 15 (2) (2009) 233–242.
[362] J. Wang, Y. An, F. Li, D. Li, D. Jing, T. Guo, E. Luo, C. Ma, The effects of pulsed electromagnetic field on the functions of osteoblasts on implant surfaces with different topographies, Acta Biomater. 10 (2) (2014) 975–985.
[363] D. Jing, M. Zhai, S. Tong, F. Xu, J. Cai, G. Shen, Y. Wu, X. Li, K. Xie, J. Liu, Q. Xu, E. Luo, Pulsed electromagnetic fields promote osteogenesis and osseointegration of porous titanium implants in bone defect repair through a Wnt/β-catenin signaling-associated mechanism, Sci. Rep. 6 (1) (2016), 32045.
[364] J. Cai, W. Li, T. Sun, X. Li, E. Luo, D. Jing, Pulsed electromagnetic fields preserve bone architecture and mechanical properties and stimulate porous implant osseointegration by promoting bone anabolism in type 1 diabetic rabbits, Osteoporos. Int. 29 (5) (2018) 1177–1191.
[365] J. Cai, X. Shao, Q. Yang, Y. Yang, Z. Yan, E. Luo, X. Feng, D. Jing, Pulsed electromagnetic fields modify the adverse effects of glucocorticoids on bone architecture, bone strength and porous implant osseointegration by rescuing bone-anabolic actions, Bone 133 (2020), 115266.
[366] S. Lin, J. Li, J. Shao, J. Zhang, X. He, D. Huang, L. Dong, J. Lin, W. Weng, K. Cheng, Anisotropic magneto-mechanical stimulation on collagen coatings to accelerate osteogenesis, Colloids Surf. B Biointerfaces 210 (2022), 112227.
[367] X. Lv, J. Zhang, D. Yang, J. Shao, W. Wang, Q. Zhang, X. Dong, Recent advances in pH-responsive nanomaterials for anti-infective therapy, J. Mater. Chem. B 8 (47) (2020) 10700–10711.
[368] W. Zhou, Z. Jia, P. Xiong, J. Yan, M. Li, Y. Cheng, Y. Zheng, Novel pH-responsive tobramycin-embedded micelles in nanostructured multilayer-coatings of chitosan/heparin with efficient and sustained antibacterial properties, Mater. Sci. Eng. C 90 (2018) 693–705.
[369] C. Ning, J. Jiajia, L. Meng, Q. Hongfei, W. Xianglong, L. Tingli, Electrophoretic deposition of GHK-Cu loaded MSN-chitosan coatings with pH-responsive release of copper and its bioactivity, Mater. Sci. Eng. C 104 (2019), 109746.
[370] W. Zhou, Y. Li, J. Yan, P. Xiong, Q. Li, Y. Cheng, Y. Zheng, Construction of self-defensive antibacterial and osteogenic AgNPs/gentamicin coatings with chitosan as nanovalves for controlled release, Sci. Rep. 8 (1) (2018), 13432.
[371] A.J. Parnell, S.J. Martin, C.C. Dang, M. Geoghegan, R.A.L. Jones, C.J. Crook, J. R. Howse, A.J. Ryan, Synthesis, characterization and swelling behaviour of poly (methacrylic acid) brushes synthesized using atom transfer radical polymerization, Polymer 50 (4) (2009) 1005–1014.
[372] J. Chen, X. Shi, Y. Zhu, Y. Chen, M. Gao, H. Gao, L. Liu, L. Wang, C. Mao, Y. Wang, On-demand storage and release of antimicrobial peptides using Pandora's box-like nanotubes gated with a bacterial infection-responsive polymer, Theranostics 10 (1) (2020) 109–122.

[373] T. Wang, X. Liu, Y. Zhu, Z.D. Cui, X.J. Yang, H. Pan, K.W.K. Yeung, S. Wu, Metal ion coordination polymer-capped pH-triggered drug release system on titania nanotubes for enhancing self-antibacterial capability of Ti implants, ACS Biomater. Sci. Eng. 3 (5) (2017) 816–825.
[374] B.L. Tao, Y.M. Deng, L.Y. Song, W.W. Ma, Y. Qian, C.C. Lin, Z. Yuan, L. Lu, M. W. Chen, X. Yang, K.Y. Cai, BMP2-loaded titania nanotubes coating with pH-responsive multilayers for bacterial infections inhibition and osteogenic activity improvement, Colloids Surf. B Biointerfaces 177 (2019) 242–252.
[375] Y. Xiang, X. Liu, C. Mao, X. Liu, Z. Cui, X. Yang, K.W.K. Yeung, Y. Zheng, S. Wu, Infection-prevention on Ti implants by controlled drug release from folic acid/ZnO quantum dots sealed titania nanotubes, Mater. Sci. Eng. C 85 (2018) 214–224.
[376] Y. Yang, B. Tao, Y. Gong, R. Chen, W. Yang, C. Lin, M. Chen, L. Qin, Y. Jia, K. Cai, Functionalization of Ti substrate with pH-responsive naringin-ZnO nanoparticles for the reconstruction of large bony after osteosarcoma resection, J. Biomed. Mater. Res. 108 (11) (2020) 2190–2205.
[377] S. Zhang, Q. Chai, Z. Man, C. Tang, Z. Li, J. Zhang, H. Xu, X. Xu, C. Chen, Y. Liu, F. Guo, M. Abdalla, G. Yu, K. Zhao, B. Shi, W. Li, X. Jiang, Bioinspired nano-painting on orthopedic implants orchestrates periprosthetic anti-infection and osseointegration in a rat model of arthroplasty, Chem. Eng. J. 435 (2022), 134848.
[378] Z. Yuan, S. Huang, S. Lan, H. Xiong, B. Tao, Y. Ding, Y. Liu, P. Liu, K. Cai, Surface engineering of titanium implants with enzyme-triggered antibacterial properties and enhanced osseointegration in vivo, J. Mater. Chem. B 6 (48) (2018) 8090–8104.
[379] L. Sutrisno, Y. Hu, X. Shen, M. Li, Z. Luo, L. Dai, S. Wang, J.L. Zhong, K. Cai, Fabrication of hyaluronidase-responsive biocompatible multilayers on BMP2 loaded titanium nanotube for the bacterial infection prevention, Materials Science & Engineering C-Materials for Biological Applications 89 (2018) 95–105.
[380] Y. Yu, Q. Ran, X. Shen, H. Zheng, K. Cai, Enzyme responsive titanium substrates with antibacterial property and osteo/angio-genic differentiation potentials, Colloids Surf. B Biointerfaces 185 (2020), 110592.
[381] A. Ghimire, J.D. Skelly, J. Song, Micrococcal-nuclease-triggered on-demand release of vancomycin from intramedullary implant coating eradicates Staphylococcus aureus infection in mouse femoral canals, ACS Cent. Sci. 5 (12) (2019) 1929–1936.
[382] P. Jiang, S. Li, J. Lai, H. Zheng, C. Lin, P. Shi, Y. Wang, Nanoparticle-programmed surface for drug release and cell regulation via reversible hybridization reaction, ACS Appl. Mater. Interfaces 9 (5) (2017) 4467–4474.
[383] Y. Zhang, K. Hu, X. Xing, J. Zhang, M.-R. Zhang, X. Ma, R. Shi, L. Zhang, Smart titanium coating composed of antibiotic conjugated peptides as an infection-responsive antibacterial agent, Macromol. Biosci. 21 (1) (2021), 2000194.
[384] Z. Wang, Y. Niu, X. Tian, N. Yu, X. Yin, Z. Xing, Y. Li, L. Dong, C. Wang, Switching on and off macrophages by a "bridge-burning" coating improves bone-implant integration under osteoporosis, Adv. Funct. Mater. 31 (7) (2021), 2007408.
[385] Y. Okazaki, E. Gotoh, Comparison of metal release from various metallic biomaterials in vitro, Biomaterials 26 (1) (2005) 11–21.
[386] T. Majumdar, N. Eisenstein, J.E. Frith, S.C. Cox, N. Birbilis, Additive manufacturing of titanium alloys for orthopedic applications: a materials science viewpoint, Adv. Eng. Mater. 20 (9) (2018), 1800172.
[387] Q. Chen, G.A. Thouas, Metallic implant biomaterials, Mater. Sci. Eng. R Rep. 87 (2015) 1–57.
[388] E. Zhang, X. Zhao, J. Hu, R. Wang, S. Fu, G. Qin, Antibacterial metals and alloys for potential biomedical implants, Bioact. Mater. 6 (8) (2021) 2569–2612.
[389] S. Ferraris, S. Spriano, Antibacterial titanium surfaces for medical implants, Mater. Sci. Eng. C 61 (2016) 965–978.
[390] C. Xin, N. Wang, Y. Chen, B. He, Q. Zhao, L. Chen, Y. Tang, B. Luo, Y. Zhao, X. Yang, Biological corrosion behaviour and antibacterial properties of Ti-Cu alloy with different Ti2Cu morphologies for dental applications, Mater. Des. 215 (2022), 110540.
[391] D. Cai, X. Zhao, L. Yang, R. Wang, G. Qin, D.-f. Chen, E. Zhang, A novel biomedical titanium alloy with high antibacterial property and low elastic modulus, J. Mater. Sci. Technol. 81 (2021) 13–25.
[392] S. Fu, X. Zhao, L. Yang, G. Qin, E. Zhang, A novel Ti-Au alloy with strong antibacterial properties and excellent biocompatibility for biomedical application, Biomaterials Advances 133 (2022), 112653.
[393] S. Gomes, I.B. Leonor, J.F. Mano, R.L. Reis, D.L. Kaplan, Natural and genetically engineered proteins for tissue engineering, Prog. Polym. Sci. 37 (1) (2012) 1–17.
[394] K. Hosoyama, C. Lazurko, M. Muñoz, C.D. McTiernan, E.I. Alarcon, Peptide-based functional biomaterials for soft-tissue repair, Front. Bioeng. Biotechnol. 7 (205) (2019).
[395] J. Zhou, J. Rossi, Aptamers as targeted therapeutics: current potential and challenges, Nat. Rev. Drug Discov. 16 (3) (2017) 181–202.
[396] S. Ni, Z. Zhuo, Y. Pan, Y. Yu, F. Li, J. Liu, L. Wang, X. Wu, D. Li, Y. Wan, L. Zhang, Z. Yang, B.-T. Zhang, A. Lu, G. Zhang, Recent progress in aptamer discoveries and modifications for therapeutic applications, ACS Appl. Mater. Interfaces 13 (8) (2021) 9500–9519.
[397] D.W. Drolet, L.S. Green, L. Gold, N. Janjic, Fit for the eye: aptamers in ocular disorders, Nucleic Acid Therapeut. 26 (3) (2016) 127–146.
[398] Y. Wei, M. Chen, M. Li, D. Wang, K. Cai, Z. Luo, Y. Hu, Aptamer/hydroxyapatite-functionalized titanium substrate promotes implant osseointegration via recruiting mesenchymal stem cells, ACS Appl. Mater. Interfaces 14 (38) (2022) 42915–42930.
[399] Y. Shi, L. Wang, Y. Niu, N. Yu, P. Xing, L. Dong, C. Wang, Fungal component coating enhances titanium implant-bone integration, Adv. Funct. Mater. 28 (46) (2018), 1804483.
[400] M.E. Scarritt, R. Londono, S.F. Badylak, Host response to implanted materials and devices: an overview, in: B. Corradetti (Ed.), The Immune Response to Implanted Materials and Devices: the Impact of the Immune System on the Success of an Implant, Springer International Publishing, Cham, 2017, pp. 1–14.
[401] Z. Chen, T. Klein, R.Z. Murray, R. Crawford, J. Chang, C. Wu, Y. Xiao, Osteoimmunomodulation for the development of advanced bone biomaterials, Mater. Today 19 (6) (2016) 304–321.
[402] S. Shirazi, S. Ravindran, L.F. Cooper, Topography-mediated immunomodulation in osseointegration; ally or enemy, Biomaterials 291 (2022), 121903.
[403] J. Lee, H. Byun, S.K. Madhurakkat Perikamana, S. Lee, H. Shin, Current advances in immunomodulatory biomaterials for bone regeneration, Advanced Healthcare Materials 8 (4) (2019), 1801106.
[404] B.N. Brown, R. Londono, S. Tottey, L. Zhang, K.A. Kukla, M.T. Wolf, K.A. Daly, J. E. Reing, S.F. Badylak, Macrophage phenotype as a predictor of constructive remodeling following the implantation of biologically derived surgical mesh materials, Acta Biomater. 8 (3) (2012) 978–987.
[405] J.R. Alhamdi, T. Peng, I.M. Al-Naggar, K.L. Hawley, K.L. Spiller, L.T. Kuhn, Controlled M1-to-M2 transition of aged macrophages by calcium phosphate coatings, Biomaterials 196 (2019) 90–99.
[406] K.M. Hotchkiss, G.B. Reddy, S.L. Hyzy, Z. Schwartz, B.D. Boyan, R. Olivares-Navarrete, Titanium surface characteristics, including topography and wettability, alter macrophage activation, Acta Biomater. 31 (2016) 425–434.
[407] J.O. Abaricia, N. Farzad, T.J. Heath, J. Simmons, L. Morandini, R. Olivares-Navarrete, Control of innate immune response by biomaterial surface topography, energy, and stiffness, Acta Biomater. 133 (2021) 58–73.
[408] J. Li, X. Jiang, H. Li, M. Gelinsky, Z. Gu, Tailoring materials for modulation of macrophage fate, Adv. Mater. 33 (12) (2021), 2004172.
[409] J. Li, J. Wen, B. Li, W. Li, W. Qiao, J. Shen, W. Jin, X. Jiang, K.W.K. Yeung, P. K. Chu, Valence state manipulation of cerium oxide nanoparticles on a titanium surface for modulating cell fate and bone formation, Adv. Sci. 5 (2) (2018), 1700678.
[410] Y. Zhu, H. Liang, X. Liu, J. Wu, C. Yang, T.M. Wong, K.Y.H. Kwan, K.M.C. Cheung, S. Wu, K.W.K. Yeung, Regulation of macrophage polarization through surface topography design to facilitate implant-to-bone osteointegration, Sci. Adv. 7 (14) (2021), eabf6654.
[411] R. Hang, Y. Zhao, Y. Zhang, R. Yao, X. Yao, Y. Sun, D. Huang, R. Hang, The role of nanopores constructed on the micropitted titanium surface in the immune responses of macrophages and the potential mechanisms, J. Mater. Chem. B 10 (38) (2022) 7732–7743.
[412] Z. Fu, Y. Hou, H.J. Haugen, X. Chen, K. Tang, L. Fang, Y. Liu, S. Zhang, Q. Ma, L. Chen, TiO2 nanostructured implant surface-mediated M2c polarization of inflammatory monocyte requiring intact cytoskeleton rearrangement, J. Nanobiotechnol. 21 (1) (2023) 1.
[413] R.S.B. Lee, S.M. Hamlet, H.-J. Moon, S. Ivanovski, Re-establishment of macrophage homeostasis by titanium surface modification in type II diabetes promotes osseous healing, Biomaterials 267 (2021), 120464.
[414] N. Su, C. Villicana, F. Yang, Immunomodulatory strategies for bone regeneration: a review from the perspective of disease types, Biomaterials 286 (2022), 121604.